MAGNETIC FIELD RECONNECTION THEORY AND THE SOLAR WIND – MAGNETOSPHERE INTERACTION: A REVIEW

M. I. PUDOVKIN and V. S. SEMENOV

Institute of Physics, State University, Leningrad, 199164, U.S.S.R.

(Received 17 February, 1985)

Abstract. This review considers the theory of the magnetic field line reconnection and its application to the problem of the interaction between the solar wind and the Earth's magnetosphere. In particular, we discuss the reconnection models by Sonnerup and by Petschek (for both incompressible and compressible plasmas, for the asymmetric and nonsteady-state cases), the magnetic field annihilation model by Parker; Syrovatsky's model of the current sheet; and Birn's and Schindler's solution for the plasma sheet structure. A review of laboratory and numerical modelling experiments is given.

Results concerning the field line reconnection, combined with the peculiarities of the MHD flow, were used in investigating the solar wind flow around the magnetosphere. We found that in the presence of a frozen-in magnetic field, the flow differs significantly from that in a pure gas dynamic case; in particular, at the subsolar. part of the magnetopause a 'stagnation' line appears (i.e., a line along which the stream lines are branching) instead of a stagnation point. The length and location of the stagnation line determine the character of the interaction of the solar wind with the Earth's magnetosphere. We have developed the theory of that interaction for a steady-state case, and compare the results of the calculations with the experimental data.

In the last section of the review, we propose a qualitative model of the solar wind – the Earth's magnetosphere interaction in the nonsteady-state case on the basis of the solution of the problem of the spontaneous magnetic field line reconnection.

1. Introduction

The interaction of the solar wind with the Earth's magnetosphere causes a series of phenomena, the character and intensity of which change significantly with the solar wind parameters. The most intensive and peculiar phenomena, such as the plasma convection, the acceleration of charged particles and their precipitation into the ionosphere, and the generation of global current systems, are associated with the existence of large-scale electric fields in the magnetosphere. The appearance of these fields is most often assumed to be due to the process of reconnection of magnetic fields and to transformation of the magnetic energy into the kinetic energy of charged particles in the vicinity of neutral lines at the magnetopause and in the magnetotail.

However, magnetic field line reconnection is only a part of the whole process of the interaction of the solar wind with the Earth's magnetosphere, and peculiarities of the flow of the solar wind around the magnetosphere may greatly affect the development and the course of that process.

In this connection, it has to be noted that beginning with the classic model by Dungey (1961), many models of the interaction of the solar wind with the geomagnetic field have been semiqualitative, and in some aspects they contradict each other. For example, the flow of the solar wind around the magnetosphere is considered in the MHD approxima-

Space Science Reviews **41** (1985) 1–89. 0038–6308/85.15.

tion with the magnetic field assumed to be weak, while the reconnection theories are based on the opposite assumption that the magnetic field is strong.

Besides, some models are based not on a solution of the corresponding MHD equations but on some geometrical consideration and on ideas about the motion of frozen-in magnetic field lines. This concept of magnetic field line motion has often led to some confusion; because of that, some models based on that concept were accurately criticized by Alfvén (1976, 1977). We also believe that physical models cannot be based on the qualitative and to some degree speculative ideas on magnetic field line motion (the more so because in some regions the frozen-in conditions are surely violated); physical models must be constructed on the basis of meaningful solutions of the problems of magnetic hydrodynamics (or even better, kinetics). Because of that belief, in the following analysis we shall first pay attention to solutions of that very kind, and only when the solution is obtained shall we use the concept of the field line motion in the physical interpretation of that solution.

Unfortunately, the number of such solutions is rather small and is insufficient for the construction of consistent models. Because of that we shall briefly consider some other methods of investigating the reconnection problem: numerical modelling and laboratory experiments which have been successfully developed over the last few years.

As will be shown further on (Section 3), for the reconnection process to begin and then proceed on to a steady-state mode, it is necessary that: (1) the magnetic field in the vicinity of the reconnection region is sufficiently intensive and (2) there exists at the magnetopause a quasi-stationary tangential electric field maintaining electric currents in the diffusion region and the plasma convection in the reconnection region.

The first condition surely is not realized within the undisturbed solar wind (the Alfvénic Mach number in the solar wind is equal on the average to 10). Because of that it seems to be of great importance that in the course of the solar wind flow around the magnetosphere, the intensity of the magnetic field increases towards the magnetopause. However, the value to which the solar wind magnetic field intensity may increase is not quiet clear. In the case of the gas dynamic flow with an isolated stagnation point as usually supposed, the value of B/ρ has to tend to infinity at the magnetopause. Both variants leading to this result: $B = \infty, \rho \neq 0$, and $B \neq \infty, \rho = 0$, seem to be unlikely from the physical point of view (Section 6), which raises doubts about the validity of the usual conception of the pure gas dynamic topology of the flow.

The second condition, $E_t \neq 0$ in the case of the gas dynamic flow with an isolated stagnation point, is not fulfilled either, which contradicts not only the hypothesis about the magnetic field reconnection, but also the experimental data for the electric field at the magnetopause (see Section 6).

All the points stated above force one to reject the attempts to solve the problem within the framework of the traditional pure gas-dynamic model of the solar wind flow around the magnetosphere and instead to seek first a topology of the flow adequate to the problem. We believe that the flow with a stagnation line meets these demands. Indeed, the existence of such a stagnation line limits the value of B/ρ for the greater part of the magnetopause and provides for the existence of the tangential electric field along that

line. Besides, the topology of the magnetic field in the vicinity of the stagnation line proves to be favorable for the development of the magnetic field reconnection. In its turn, the field line reconnection maintains the flow with the stagnation line, which makes the whole process self-consistent. The first preliminary estimates of the plasma parameters, and of the magnetic and electric fields in the magnetosheath, obtained on the assumption that the stagnation line exists, seem to be rather reassuring, as we shall see below.

At the same time we must note that the steady-state reconnection of the interplanetary magnetic field (IMF) and the geomagnetic field may be realized only as an average over time. In reality the reconnection must have a spontaneous and impulsive charatcer, so the structure of the flow and of the magnetic field at any given moment may be very complicated.

The idea on the spontaneous reconnection may also be of use in explaining the change of the flow from a pure gas-dynamic one in the absence of the IMF to a flow with the stagnation line in the case of the nonzero IMF. Thus, the spontaneous reconnection concept allows one to look at the whole problem of the solar wind flow around the magnetosphere from a single viewpoint (see Sections 4 and 7).

In this review we shall first consider the magnetic energy storing phase (Section 2) and discuss solutions concerning the steady-state (Section 3) and spontaneous (Section 4) reconnection. To illustrate the physical meaning of the phenomena under consideration, we tried to choose the most obvious models involving mostly incompressible media. Results of more complicated solutions are given briefly for reference.

In order to avoid overloading the text with mathematical formulae, most of them are given in the Appendix. The latter may be of some independent interest, for in it there is given a consistent description of the techniques of the frozen-in coordinate system which may be useful in a series of various problems of ideal magnetic hydrodynamics.

In Section 5 the results of numerical and laboratory experiments are considered, and Section 6 is devoted to the analysis of the steady-state flow of the solar wind with a frozen-in magnetic field of arbitrary direction around the magnetosphere. The same problem under nonsteady-state conditions is considered in Section 7.

The Reconnection Process and the Development of the Current Sheet

2.1. Qualitative description of the reconnection process

Magnetic field line reconnection is believed to be the source of many explosive phenomena in which the energy of the magnetic field is converted into the kinetic and internal energy of the plasma. At first the magnetic energy is stored near the current sheet; for its rapid release it is necessary to destroy the current sheet as quickly as possible. There are two main possibilities to do this: (i) Joule dissipation, or the magnetic field line annihilation as this process is traditionally called, and (ii) the current sheet disruption.

The first process may be illustrated by the following simple consideration (Yeh and Axford, 1970). Let us assume that an incompressible plasma with the conductivity σ

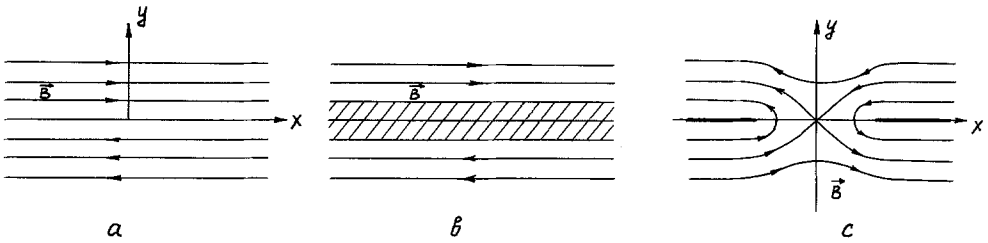

Fig. 2.1. Configuration of the magnetic field lines near the current sheet (a) at an initial moment, and at some later time in the case of (b) field line annihilation, after Yeh and Axford (1970), and (c) current sheet disruption, after Bulanov and Sasorov (1978).

occupies the region $Y \gtrless 0$ and is permeated by uniform magnetic field $(\pm B_0; 0)$; thus, initially there is a current sheet at $Y = 0$ (see Figure 2.1a). The subsequent evolution of the magnetic field is described by the diffusion equation, which in the case under consideration has the solution:

$$B_x(y, t) = \pm 2\pi^{-1/2} B_0 \operatorname{erf}(\pi\sigma y^2/c^2 t)^{1/2},$$

where $\operatorname{erf}(x)$ is the error function. It can be seen that the width of the transition layer with a weak magnetic field is of the order of $Y_D = (c^2 t/\pi\sigma)^{1/2}$, and it increases with time (see Figure 2.1b). The energy of the annihilated magnetic field is directly converted into heat. However, the diffusion velocity $V_D = (c^2/4\pi\sigma t)^{1/2}$ decreases with time, and the annihilation process fades quickly. To provide a release of a considerable amount of the energy, an instability is triggered to reduce the conductivity of the current sheet plasma. It should be emphasized that this instability must be triggered throughout the whole current sheet simultaneously, which seems to be unlikely from the physical point of view. If the instability develops locally, a disruption of the current sheet should arise.

In the latter case, an X-line appears, the magnetic field lines reconnect in the diffusion region in the vicinity of the X-line, and then, while shortening, they sweep the current sheet plasma away from the X-line (see Figure 2.1c). This is the so-called 'catapult' model which was very popular earlier. Unfortunately, it led often to some confusion; mainly because of the basic concepts such as 'reconnection', 'moving field lines', 'diffusion region', and so on were not defined correctly. Only recently some progress has been achieved due to extensive analytical (see Section 2 and 3), laboratory and numerical (Section 5) investigations. The analysis of the available results allowed a quantitative model of the reconnection process to be developed.

The following remark should be made before the model is described. The main shortcoming of the catapult model is that the role of the MHD-waves is neglected in this approach. In fact, a local decrease of the plasma conductivity and the appearance of an X-line are accompanied by the generation of the MHD-waves which may propagate, interfere and essentially affect the whole plasma flow and magnetic field pattern. Taking into consideration the MHD-waves reduces the model of the current sheet disruption to the well-known Petschek's (1964) reconnection model.

Let us consider now the disruption of the current sheet in more detail (Semenov *et al.*, 1984). As before, let the plasma conductivity and, hence, the current intensity decrease locally in a part of the current sheet. It means that a current I_1 directed against the initial sheet current I_0 appears in the region of the conductivity decrease (see Figure 2.2a). The appearance of the current I_1 leads to the generation of MHD-waves in the plasma medium. Among them the Alfvén wave is of great importance, since it produces currents which close the circuit. We denote this current system as I_A; it consists of the current I_1 in the diffusion region, the field-aligned currents I_2 and polarization currents I_3 at the fronts of the Alfvén waves.

Initially, the current sheet is a tangential discontinuity. However, after the current system I_A of the Alfvén wave has been generated, the regions of the current sheet passed

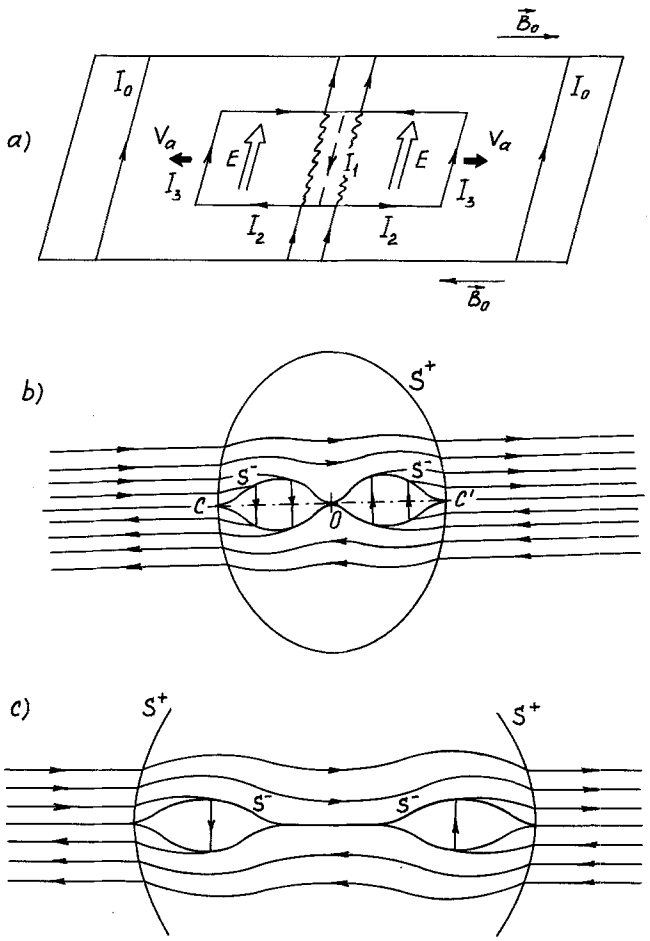

Fig. 2.2. A qualitative model of the field line reconnection. (a) Propagation of the Alfvén wave along the magnetic field lines. (b) Breakup of the current sheet and appearance of Petchek's slow shocks S^-. (c) Propagation of the FR-regions along the current sheet after the switch-off of the electric field in the diffusion region.

by the disturbance cease to be a tangential discontinuity. Instead, a component of the magnetic field normal to the current sheet as well as a tangential component of electric field appear in these regions. As a result, both the energy flux and the mass flux exhibit a jump there. A discontinuity at which the conservation laws are not satisfied is unstable; it breaks down immediately into a system of a fast and slow shocks, expansion fans, and tangential or contact discontinuities (Akhiezer *et al.*, 1975). In the simplest case, when the plasma and field parameters are symmetric, the discontinuity breaks down into two fast shocks and two slow shocks, as illustrated in Figure 2.2b.

Thus, the initial breakup of the current sheet and appearance of Petschek's slow shocks take place. The subsequent influence of the diffusion region on the reconnection process proceeds by means of the same mechanism. For example, let the current I_1 increase (that is, let the total current $I_0 + I_1$ decrease) in the diffusion region. Then Alfvén waves arise and propagate along the field lines which permeate the diffusion region. The conservation laws are violated in those parts of the slow shocks which this new disturbance has reached. These parts of slow shocks have to break down, but in contrast to the initial breakup of the current sheet, this breakup seems to reduce to a deformation of the slow shocks. By this mechanism the slow shocks adjust themselves to the new reconnection rate: if the current I_1 grows, then the inclination of the slow shock with respect to the initial magnetic field increases. As a result, the plasma flow and magnetic field pattern also adjusted to the new reconnection rate. The process is self-consistent, it is initiated and controlled by the behavior of the plasma in the diffusion region.

In the course of time, the Alfvén wave propagates along the field lines and makes a new parts of the current sheet to break down. The whole process has an explosive nature with a characteristic velocity of the order of the Alfvén speed.

Two slow shocks confine the field reversal region (FR-region) in which the plasma is heated and accelerated up to the Alfvén velocity, and the magnetic field is reconnected. The leading fronts of the slow shocks (marked as C and C' in Figure 2.2b) propagate with the Alfvén velocity. Once the reconnection process is complete, the FR-regions run along the current sheet as a solitary wave (Figure 2.2c). The part of the current sheet is recovered behind them, but the magnetic field intensity near the origin (where the diffusion region was initially located) is smaller than its initial intensity, B_0. Deficit of magnetic energy is carried out by the moving FR-regions.

In the general case, a reconnection line can move along the current sheet with a velocity U. If the neutral line moves to the right (see Figure 2.3), the right hand FR-region inflates, the reconnected magnetic field and the electric field are enhanced here. At the left hand side the configuration evolves in the opposite direction: the FR-region flattens and the magnetic field magnitude decreases.

Several requirements have to be satisfied for the reconnection process to start. First of all, there must exist a current sheet I_0. The reconnection is not possible at all in the case of a current-free magnetic field. It is the energy of the current sheet magnetic field that is converted into the plasma energy; the magnetic field from distant sources affects the reconnection only in an indirect way.

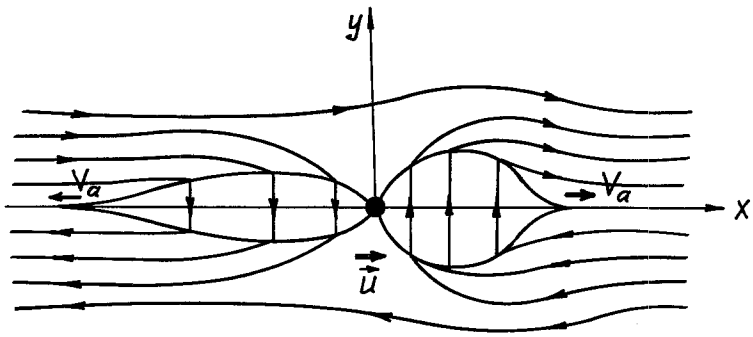

Fig. 2.3. Effect of the reconnection line motion, U being the velocity of the reconnection line.

It is necessary also that the current system of the Alfvén wave be generated by some causes. Most often it seems to arise owing to the development of the anomalous resistivity in a part of the current sheet. Besides, the tearing mode instability may lead to the necessary redistribution of the electric currents in the current sheet and thereby to initiate the reconnection in the case of a sufficiently long-wave mode.

The generation of the current system I_A may be caused also by external sources. For example, if the Alfvén wave with the appropriate polarization falls upon the current sheet, the currents at the front of the Alfvén wave may initiate the reconnection (see Section 3).

2.2. Development of the Current Sheet

As we have seen above, the reconnection (in the framework of Petschek's mechanism for the generation of shocks) cannot develop in the current-free (i.e., rot $\mathbf{B} = 0$) magnetic field. Some currents have to flow in the reconnection region; their energy is the source for all the other kinds of energy gained by the plasma in the course of the reconnection, including the kinetic and thermal ones. For the energy to accumulate, some time as well as certain conditions are needed. At present only the simplest regimes have been investigated: (a) when the total amount of energy entering the system is accumulated as free energy, and (b) when all the energy is spent for Joule heating of the plasma.

We shall start with the first case. Thus, assume there exists a magnetic field with a neutral X-line of the vacuum type in a perfectly conducting plasma, and let the electric field be switched on along that line at a certain moment. Just after that moment a fast magneto-acoustic cylindrical wave appears (Syrovatsky, 1979b, 1981), propagating towards the line. Before the wave front the medium is not disturbed, while behind it the convection is set up which compresses the magnetic field along the Y-axis and stretches it along the X-axis (Figure 2.4a).

The main features of the process of the magnetic energy accumulation may be obtained from the following rather simple consideration (Figure 2.4b) (see also Priest, 1981). The plasma convection caused by the electric field is carrying the magnetic field lines to the X-line. In a perfectly conducting plasma the field lines cannot tear and,

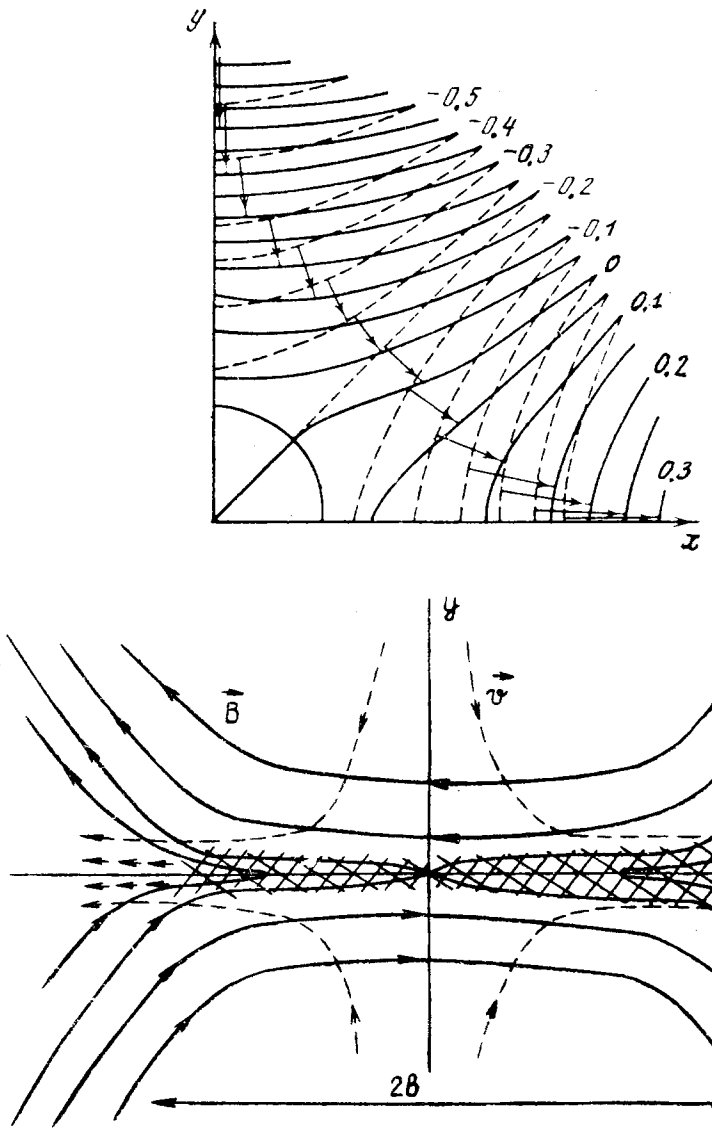

Fig. 2.4. Development of a current sheet at the site of the X-point of the magnetic field. (a) Distortion of the magnetic field by a converging cylindrical wave. Circle with a small radius represent the wave front; solid lines represent the magnetic field lines, and dotted lines show their initial configuration; the arrows show the displacement of the plasma. The picture is symmetric with respect to the coordinate axes. The figures at the curves show the values of the vector potential. (b) The structure of the plasma flow and of the magnetic field in the vicinity of a developed current sheet; 'b' is the half-width of the sheet.

hence, they are accumulated. At the X-line the field lines stop moving (otherwise, they would be torn) and, therefore, the electric field intensity has to be zero there.

The compensation of the electric field is accomplished in the following way. As we have just seen, the magnetic field intensity increases in the vicinity of the current sheet.

According to Lenz's rule, the induction electric field E_r is directed against the initial field E_0. Thus the electric field at the current sheet equals $E_{NS} = E_0 - E_r \ll E_0$, and $(\mathbf{E}_{NS} \cdot \mathbf{I}_{NS}) \ll (\mathbf{E}_0 \cdot \mathbf{I}_{NS})$. According to the Poynting theorem, in such a case most of the energy entering the system is stored as magnetic energy.

Certainly, this qualitative and very rough consideration has to be confirmed by more rigorous calculations. As often occurs in magnetic hydrodynamics, the solution of the problem does not exist in the general case, and some simplifications are usually introduced; in particular, in a more complicated case we have to restrict ourselves by a simpler geometry.

To begin with, let us consider some more or less general and, as a consequence, rather rough models of that kind.

(1) Syrovatsky's approximation (Syrovatsky, 1971, 1979a, b, 1981). In that approximation, magnetic pressure is supposed to be much greater than both the thermal and the dynamic plasma pressures: $\beta = 8\pi p_0/B_0^2 \ll 1$; $Ma = V_0/V_a \ll 1$. Then in the zero-order (with respect to β and Ma) approximation the magnetic field is self-balanced ($\mathbf{j} \times \mathbf{B} = 0$). Besides, in studies of the systems with current sheets, magnetic field may be considered as not only force-free but also as current-free (rot $\mathbf{B} = 0$) everywhere except for the current sheets, which, in their turn, can be considered as infinitely thin.

Such an approach appears to be remarkably fruitful, as it allows one to introduce such powerful mathematical tools as functions of complex variables.

To illustrate the method, we shall discuss in detail the problem considered qualitatively at the beginning of this section. So, let there exist at some initial instant a hyperbolic magnetic field with a vacuum-type X-line, and at that very instant let there be switched on an electric field $E_0(t)$ parallel to the X-line. It is obvious that the electric field cannot penetrate into the plasma instantly. It exists initially only outside the plasma volume; let us consider the latter to be enveloped by a cylindrical surface with radius R and the axis along the X-line. After the converging cylindrical magneto-acoustic wave has approached the X-line, a current sheet arises there (Figure 2.5). The complex

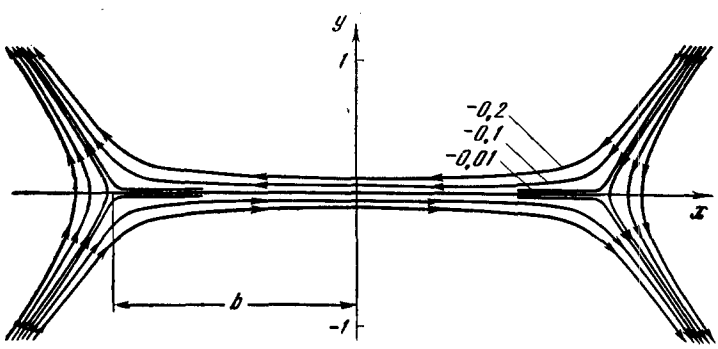

Fig. 2.5. The neutral sheet developed at the site of an X-line of the first order; 'b' is the half-width of the sheet. The figures at the curves show the values of the vectors potential $A(x, y, t)$.

potential corresponding to that solution is

$$F(z, t) = \frac{h_0}{2} z(z^2 - b^2)^{1/2} - \frac{h_0 b^2}{2} \ln \frac{z + (z^2 - b^2)^{1/2}}{b}, \tag{2.1}$$

where h_0 is the ghradient of the initial magnetic field in the vicinity of the neutral line and b is the halfwidth of the current sheet. The Z-component of the vector potential may be obtained from F as $A(x, y, t) = \mathrm{Re}\, F(z, t)$. The components of the magnetic and of the electric fields are expressed by formulae:

$$\frac{\mathrm{d}F}{\mathrm{d}z} = -B_y - iB_x = (z^2 - b^2)^{1/2}, \tag{2.2}$$

$$E_z = -\frac{1}{c} \frac{\partial A}{\partial t}. \tag{2.3}$$

One can see from (2.3) that the electric field is greatly inhomogeneous; it vanishes at the current sheet and reaches the maximum value E_0 at the boundaries of the region under consideration.

The current sheet evolution is described by the function $b(t)$ which may be obtained by equaling the tangential components of the electric field at the boundaries:

$$\frac{h_0^2}{2} b^2(t) \left(1 - \ln \frac{b(t)}{2R}\right) = -\int_0^t E_0(t')\, \mathrm{d}t'. \tag{2.4}$$

It follows from (2.4) that when $E_0(t)$ does not change sign, the current sheet is widening with time. The free energy of the magnetic field per unit length of the neutral line is estimated as

$$\Delta W = \frac{1}{32} h_0^2 b^2 \left(\ln \frac{4R^2}{b^2} - \frac{1}{2}\right) \tag{2.5}$$

and ΔW increases rapidly as $b(t)$ increases.

The total current in the current sheet is

$$J = \frac{c h_0 b^2}{4}. \tag{2.6}$$

An important conclusion may be drawn from the results obtained above: the free energy is the more effectively accumulated, the more intense the electric field E_0 is, the nearer to the X-line it is applied, and the greater the gradient of the initial magnetic field is.

Syrovatsky's method is good for calculation of the magnetic and electric field intensities (Somov and Syrovatsky, 1974; Priest and Raadu, 1975; Tur and Priest, 1976). However, it is difficult to obtain gas dynamic parameters of the flow in that approximation. Because of that, in seeking for an accurate solution of the problem, we

have to restrict ourselves to considering only incompressible plasma in the immediate vicinity of the current sheet.

In a dimensionless form, the solution may be written as:

$$B_x = t; \qquad B_y = 0; \qquad V_x = x/t; \qquad V_y = -y/t; \qquad P = P_0 - y^2/t^2. \quad (2.7)$$

Here P is the total pressure. It is seen from (2.7) that when the magnetic field increases with time, the velocity of the plasma motion is decreasing. Such a decrease of the plasma velocity is caused by the requirement that the field lines cannot break and are accumulated in a perfectly conducting plasma.

According to Syrovatsky (1979b, 1981), who has calculated the flow parameters for a compressible plasma, the plasma density also decreases with time in the vicinity of the current sheet, and may drop to a very small value. As will be shown below (see Section 4, formula (4.27)), this promotes especially effective energy release (the latter being proportional to ρ^{-1}) at the reconnection phase.

Syrovatsky's model permits one to calculate the magnetic field and the plasma flow outside the current sheet, as well as the amount of free energy accumulated in the system. However, that model cannot provide any information on the internal structure of the current sheet and, hence, on the development of instabilities causing the reconnection. To investigate the structure of the current sheet, quite another technique is necessary, in particular, the technique developed by Birn and Schindler.

(2) Birn–Schindler's approximation (Birn *et al.*, 1977; Birn, 1979; Schindler, 1979; Schindler and Birn, 1982).

It is supposed that the Ampère force in the current sheet is balanced by the plasma pressure gradient

$$-\nabla p = \frac{1}{c}\mathbf{j} \times \mathbf{B}. \quad (2.8)$$

Calculating the dot product of (2.8) by **B**, one obtains: $(\mathbf{B}\nabla)p = 0$, i.e. plasma pressure is constant along the magnetic field lines and, hence, may be specified at some initial surface. Then, having expressed the magnetic field by means of Euler potentials: $\mathbf{B} = \nabla\alpha \times \nabla\beta$, Equation (2.8) may be reduced to equations in terms of variables α and β. In the above-referenced papers a method of solving these equations is developed for the case in which the gradients across the current sheet are much greater than those along it. The method allows one to calculate the magnetic field and the plasma pressure within the current sheet, with the proper boundary conditions.

Thus, Birn–Schindler's method is local and is applicable only to the inner part of the current sheet where significant gradient exist. It would be of great interest to match the solutions of the models by Syrovatsky and by Birn and Schindler, because such a matching could provide the boundary condition for the pressure, which has been imposed by Birn and Schindler rather arbitrarily.

So far we have considered stationary current sheets. To deal with dynamic problems, the time-dependent boundary conditions for the pressure have to be assumed. Then, as earlier, the magnetic field is calculated and from that the electric field, the plasma density

and the velocity may be obtained. Such an approach permits one to find out some fine details of the energy accumulation process.

In one of their first papers of that kind Schindler and Birn (1982) obtained a family of analytical solutions for the evolution of the current sheet in the magnetosphere's tail, under a variety of imposed boundary conditions. The regime under consideration was chosen in such a way that no neutral line could arise there. The main results obtained in that study are as follows (Figure 2.6):

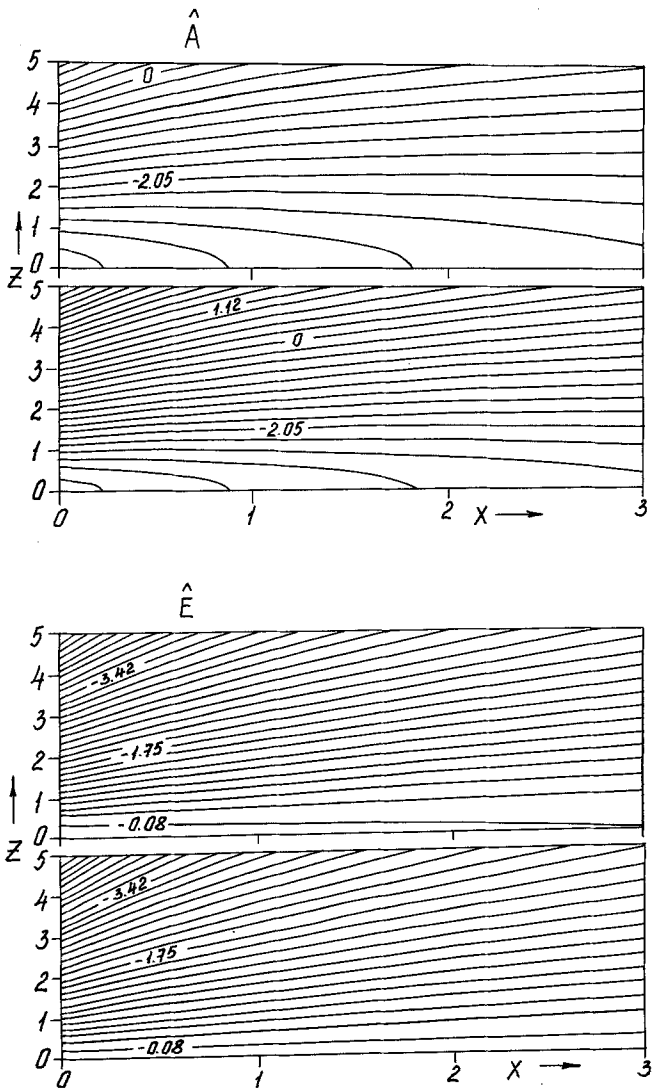

Fig. 2.6. Evolution of the magnetic field and of the electric field in the magnetotail according to Schindler and Birn (1982). Figures at the curves show the values of the vector potential $A(x, z, t)$ – (a), or of the electric field intensity $E(x, z, t)$ – (b). The bottom figure corresponds to a later moment.

(1) The stationary convection in the magnetotail is possible only in a rather special case with the polytropic exponent $\gamma < 1$; in the opposite case the balance of forces is impossible.

(2) Typically, the magnetospheric convection is nonstationary. Convection may be caused by the following conditions at the boundary: (a) by the electric field, (b) by the increase of the magnetic field intensity in the magnetotail lobes; (c) by the increase of the total pressure ($P = p + B^2/8\pi$).

(3) Electric field intensity rapidly decreases with distance from the boundary, and drops to very small values near the current sheet, where it can even change its sign.

(4) Intensity of the currents within the plasma sheet, as well as the magnetic field energy in the magnetotail lobes, increase with time, while the magnetic field component normal to the current sheet decreases; thereupon the threshold of the tearing instability (or that of anomalous resistivity) is achieved. Thus, the current sheet evolves in the process of energy accumulation to an unstable state.

These results, combined with the conclusion by Syrovatsky on the decrease of the plasma density in the vicinity of the current sheet at the phase of energy accumulation, provide a sufficiently complete picture of that phase.

2.3. Parker's Model

By now we have considered plasma as a perfectly conducting medium. In reality the plasma has a finite conductivity and, hence, a part of the energy entering the system or even all of it may dissipate as Joule heat. In particular, there was obtained (Parker, 1973; Sonnerup and Priest, 1975; Priest and Sonnerup, 1975) a simple and nevertheless exact solution of a special problem in which the magnetic field energy converts completely into heat (the so-called process of the magnetic field annihilation).

Let us consider the flow of a incompressible plasma in the vicinity of the stagnation point (see Figure 6.3 in Section 6):

$$V_x = -k_1 x, \qquad V_y = k_2 y, \qquad V_z = (k_1 - k_2) z. \tag{2.9}$$

Magnetic field lines are supposed to be straight ones and parallel to the Z-axis: $B_x = B_y = 0$; $B_z = B(x)$. Then the pressure may be obtained from the equation of motion:

$$p = \text{const.} - \tfrac{1}{2}\rho V^2 - \frac{1}{8\pi} B^2 \tag{2.10}$$

and $B(x)$ is determined by the equation:

$$\text{rot}\,[\mathbf{V} \times \mathbf{B}] + \frac{c^2}{4\pi\sigma} \nabla^2 \mathbf{B} = 0 \tag{2.11}$$

which is reduced in the case under consideration to:

$$\frac{1}{\text{Re}_m} \frac{\mathrm{d}^2 B}{\mathrm{d}x^2} + x \frac{\mathrm{d}B}{\mathrm{d}x} + \alpha B = 0, \tag{2.12}$$

where Re_m is the magnetic Reynolds number, and $\alpha = (k_1 - k_2)/k_1$. The solution of (2.12) may be expressed in parabolic cylinder functions and is characterized by the following peculiarities. When $\mathrm{Re}_m \gg 1$, there appears a magnetic boundary layer with a width of the order of $L/(\mathrm{Re}_m)^{1/2}$. Beyond that layer the magnetic field intensity increases as $B \sim x^{-\alpha}$ while approaching $x = 0$. The most rapid increase takes place when $\alpha = 1$ which corresponds to the stagnation line being perpendicular to the magnetic field. In the case of a longitudinal stagnation line (i.e. parallel to B) $\alpha = 0$, and the magnetic field intensity does not increase (Figure 2.7); the axially symmetric flow corresponds to $\alpha = \frac{1}{2}$.

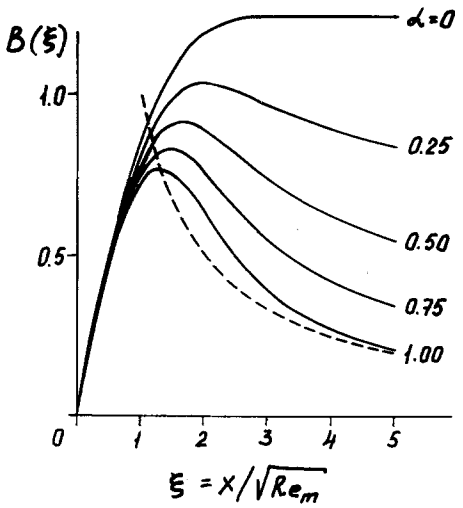

Fig. 2.7. Distribution of the magnetic field intensity in Parker's model of the magnetic field merging. The dotted line corresponds to the case of the infinite conductivity and $\alpha = 1$.

It is of interest to compare the behavior of the magnetic field intensity in Parker's model ($B \sim 1/x$) with that corresponding to the nonsteady-state solution (2.7). In both cases the flow structure is the same, and the field lines are equally stretched in the two cases. However, in Parker's model this stretching corresponds to the plasma (and field line) motion in an inhomogeneous magnetic field with $B \to \infty$ at $x \to 0$, while, according to (2.7), this stretching is associated with the increase in time ($B \sim t$) of a homogeneous magnetic field; thus, in the latter case the singularity in B at the point $x = 0$ disappears.

Let us now discuss basic similarities and differences between the process of the magnetic field annihilation (Parker's solution) and of the magnetic field line reconnection (Petschek's solution). As we have seen, when considered locally within the diffusion region, both processes are indistinguishable. However, with the plasma flow and magnetic field configuration being taken into account, the two processes are quite different. The main differences are as follows.

(1) In the reconnection process, the magnetic energy transforms at the shocks into kinetic and thermal energy, and the energy dissipation is necessary only locally in the

diffusion region, for the magnetic field lines could break there. In the case of the magnetic field annihilation, the energy is transformed into Joule heat, and for this process to proceed effectively, the plasma conductivity has to be sufficiently low in a significant part of the current sheet.

(2) In the process of reconnection the shock waves are generated which drastically modify the configuration of the magnetic field and of the plasma flow, turning it into quasi-two-dimensional one. This effect is especially important in the case of a three-dimensional flow of a highly conducting plasma around a blunt body (e.g. the magnetosphere) (see Section 6). In the case of the magnetic field annihilation, the structure of the flow is similar to that in the purely gas-dynamic flow.

Of great importance is the question of which state – stationary or impulsive reconnection, or annihilation of the magnetic field lines – the system is evolving to, and what determines this final state. However, this problem is far from being solved as yet, and we have to restrict ourselves to a qualitative consideration. For example, we shall consider the problem formulated at the beginning of this section, the plasma conductivity now assumed to be finite and equal to σ_0 (or σ_{cr} if the current density exceeds some critical value j_{cr} corresponding to the threshold of some plasma instability development).

First of all, it is necessary to ascertain if the system can evolve to the state of field line annihilation. As stated above, the width of the magnetic boundary layer equals $h = L/\sqrt{\mathrm{Re}_m}$, and the magnetic field frozen into the plasma increases towards the boundary up to the value

$$B = B_0(\mathrm{Re}_m)^{1/2}, \tag{2.13}$$

where B_0 is the magnetic field intensity at the boundaries of the region under consideration; we set here $\alpha = 1$ for the sake of simplicity. Then the mean current density in the boundary layer is:

$$\langle j \rangle = \frac{c}{4\pi}\frac{\Delta B}{h} = \frac{c}{2\pi}\frac{B_0}{L}\mathrm{Re}_m. \tag{2.14}$$

If the plasma conductivity σ_0 is low, so that $\langle j \rangle < j_{cr}$, the anomalous resistivity does not develop, and it seems that the system evolves to the state of magnetic field annihilation. When $\langle j \rangle > j_{cr}$, the anomalous resistivity starts to develop, at first locally, and at that very region the field line reconnection begins. The greater is the anomalous resistivity, the more effective is the process of the field line reconnection.

Thus, both processes are associated with a low plasma conductivity. However, in the case of the field line annihilation the plasma conductivity has to be low everywhere from the very beginning of the process, while in the case of the field line reconnection, the plasma conductivity has to be sufficiently high at the initial stage (that is necessary for the free energy accumulation). Later on it drops off; this decrease of the plasma conductivity develops only locally.

A similar consideration can be applied to the case of the field line reconnection triggered by the tearing-mode instability.

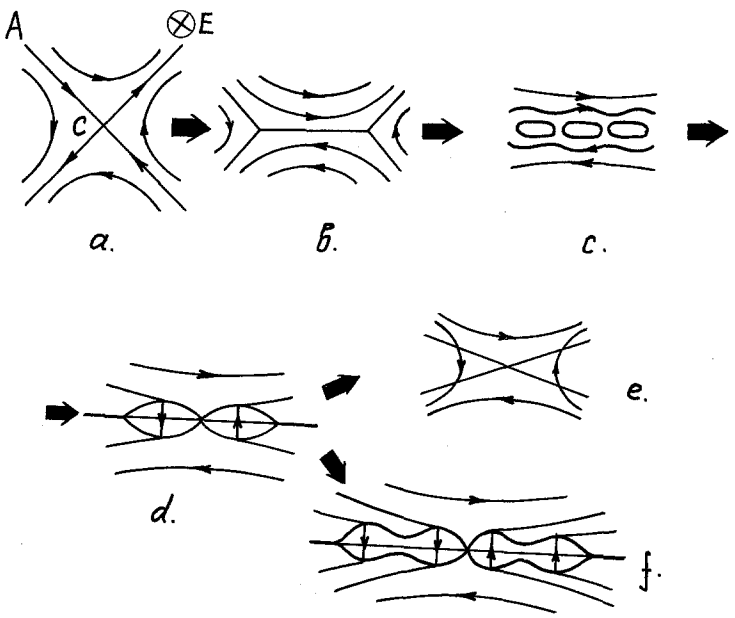

Fig. 2.8. Sequence of events leading to the magnetic field line reconnection. (a) Hyperbolic magnetic field in the vicinity of an X-line. (b) Development of a current sheet at the site of the X-line. (c) Development of a plasma instability (tearing mode or anomalous resistivity) in the current sheet. (d) Beginning of the time-dependent magnetic field line reconnection. (e) Steady-state reconnection. (f) Impulsive reconnection.

On the role, the sequence of events constituting the field reconnection may be illustrated by the following scheme (Figure 2.8). An electric field applied along the neutral line (Figure 2.8a) leads to its development into the current sheet (Figure 2.8b), and free magnetic energy is stored. During the process of energy accumulation, the current sheet evolves to an unstable state (Figure 2.8c). On having approached the instability threshold, a spontaneous reconnection starts to develop (Figure 2.8d). If there exists a stationary electric field, and the boundary conditions are favorable, the system may proceed to the steady-state reconnection (Figure 2.8e). In the opposite case, the reconnection seems to have a spontaneous and impulsive character (Figure 2.8f).

3. Steady-State Reconnection of the Magnetic Field Lines

As we have seen in the preceding section, the reconnection process is responsible for the drastic change of the magnetic field structure and the release of the magnetic energy. Thus, the process is essentially nonstationary and, logically, a stationary reconnection would be described as a particular case of the general time-dependent reconnection problem. However, from a mathematical point of view it is convenient to choose another, quite different way: first we shall consider the most simple Sonnerup's model, then Petschek's stationary model and finally the time-dependent reconnection problem. Mathematically, all these problems are successive ones: each problem will be solved on

the basis of the previous simpler one. For simplicity we shall restrict our consideration to the case of incompressible plasma. The solutions of all problems mentioned above will be obtained by means of the method of the frozen-in coordinates (see Appendix 2). The system of MHD equations in frozen-in coordinates (t, α) is:

$$\varepsilon^2 x_{tt} - x_{\alpha\alpha} = -P_t y_\alpha + P_\alpha y_t, \tag{3.1}$$

$$\varepsilon^2 y_{tt} - y_{\alpha\alpha} = -P_\alpha x_t + P_t x_\alpha, \tag{3.2}$$

$$x_t y_\alpha - x_\alpha y_t = 1, \tag{3.3}$$

where $\varepsilon = V_0/V_a$ is the Alfvénic–Mach number (the symbol ε is used here instead of the standard symbol *Ma* to emphasize that this ratio is playing the role of a small parameter in the problem of reconnection), and P is the total pressure. The dimensionless form of the system of Equations (3.1)–(3.3) is obtained by normalizing to the characteristic values for velocity V_0, magnetic field B_0 and length (which will be detailed later). Formally, the slow shock is degenerated in an Alfvén discontinuity in the case of incompressible plasma; all the relations at the shock may be described in frozen-in coordinates (t, α) by (A35) and the equation of the shock front reduces (as shown in Appendix 2) to

$$\pm \varepsilon\alpha = t. \tag{3.4}$$

The frozen-in coordinate system is a double-Lagrangian one: both the parameter along the stream flow line (time t) and the parameter along the magnetic line α are Lagrangian ones. As usual, while using the Lagrangian approach (see for example Sedov, 1973), the dependence of the Cartesian coordinates on Lagrangian ones (frozen-in ones in this case) should be found first:

$$x = x(t, \alpha); \qquad y = y(t, \alpha) \tag{3.5}$$

and then the flow velocity and magnetic field intensity are obtained:

$$B_x = x_\alpha(t, \alpha); \qquad B_y = y_\alpha(t, \alpha); \qquad V_x = x_t(t, \alpha); \qquad V_y = y_t(t, \alpha). \tag{3.6}$$

Thus, formulas (3.5) and (3.6) give a solution in a parametric way. From a mathematical point of view, the functions given in (3.5) map the physical space onto parameter space. The structure of that space is nontrivial in the reconnection problems, so according to Semenov and Pudovkin (1978) the space of the frozen-in coordinates onto which physical space is mapped is called F-manifold. For the convenience of the reader we shall list the results in the Cartesian coordinates as well.

3.1. SONNERUP'S MODEL (Sonnerup, 1970)

We start with a two-dimensional case. Let two constant magnetic fields B_1 and B_2 exist in two different hemiplanes (x, y) and a constant electric field be applied along the z-axis. Then plasma convection appears and both conditions $\{V_n\} = 0$, $\{B_n\} = 0$ are not fulfilled at the x-axis (see Figure 3.1), except for the trivial case $B_1 = B_2$. A system of shocks must arise that deflects the flow and magnetic field in such a way that conditions

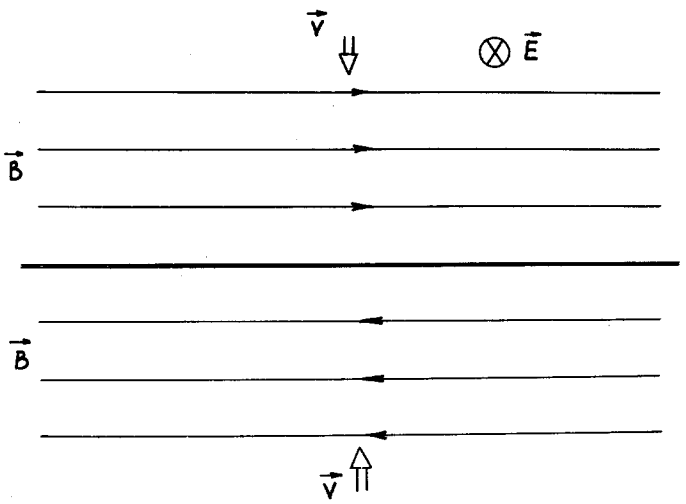

Fig. 3.1. Initial state (the zeroth approximation) of the system in the problem on the steady-state reconnection of the magnetic field lines.

$\{V_n\} = \{B_n\} = 0$ can be satisfied. In Sonnerup's model an additional assumption is introduced according to which the solution consists of the homogeneous flow and magnetic field in newly created sectors between shocks also.

As there is only one free parameter on a shock and there should be four parameters (two components of the flow and two of the magnetic field) in agreement, it is clear that eight discontinuities (four in each of the left and right hemiplanes) must develop in Sonnerup's model.

For constant **V** and **B** the differential equations are satisfied automatically and the problem is reduced to algebraic relations on shocks. The symmetric solution corresponding to initial data

$$\mathbf{B}_1 = (1, 0); \quad \mathbf{V}_1 = (0, -1); \quad \mathbf{B}_2 = (-1, 0); \quad \mathbf{V}_2 = (0, 1)$$

(see Figure 3.2a) in the *I* quadrant is:

Region 1:

$$x = \alpha; \quad y = -t; \quad \mathbf{B} = (0, -1); \quad \mathbf{B} = (1, 0),$$

discontinuity

$$t = -\varepsilon\alpha; \quad y = \varepsilon x.$$

Region 2:

$$x = \frac{f}{\sqrt{2}}\alpha + \frac{t}{\varepsilon\sqrt{2}} = \frac{f}{\sqrt{2}}\alpha + \frac{1}{\sqrt{2}}t', \qquad \mathbf{V} = \left(\frac{1}{\varepsilon\sqrt{2}}; -\frac{1}{f\sqrt{2}}\right),$$

$$y = \frac{\varepsilon}{\sqrt{2}}\alpha - \frac{t}{f\sqrt{2}} = \varepsilon\left(\frac{1}{\sqrt{2}}\alpha - \frac{1}{f\sqrt{2}}t'\right), \qquad \mathbf{B} = \left(\frac{f}{\sqrt{2}}, \frac{\varepsilon}{\sqrt{2}}\right),$$

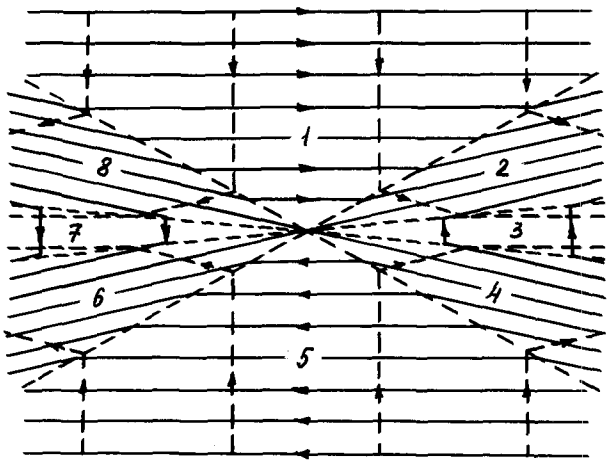

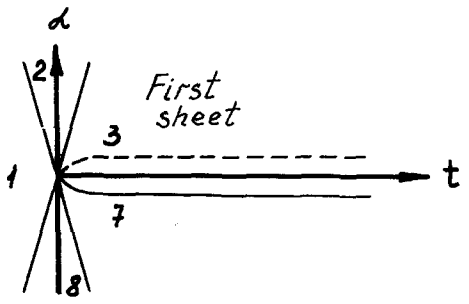

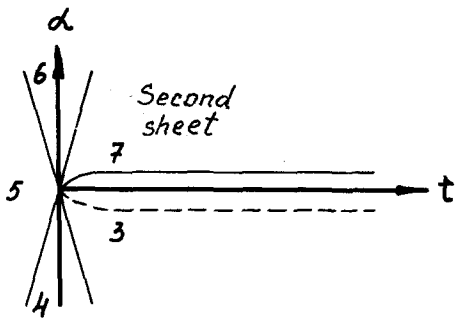

Fig. 3.2. The field line reconnection in Sonnerup's model. (a) Configuration of the magnetic field lines (the solid lines) and of the stream lines (dotted lines with arrows) in the physical space. The dotted lines passing the origin of the coordinate system represent the shock waves. (b) *F*-manifold consisting of two sheets. The figures show correspondence of various regions within the physical and parametric spaces.

discontinuity

$$t = \varepsilon\alpha, \qquad y = \frac{\varepsilon}{f^2}x.$$

Region 3:

$$x = \frac{f}{\varepsilon}t = ft', \qquad \mathbf{V} = (f/\varepsilon, 0),$$

$$y = \frac{\varepsilon}{f}\alpha = \varepsilon\left(\frac{\alpha}{f}\right), \qquad \mathbf{B} = (0, \varepsilon/f), \tag{3.7}$$

where

$$f = 1 + \sqrt{2}, \qquad t' = t/\varepsilon, \qquad \varepsilon = V_0/V_a.$$

On the left-hand side the solution is presented in frozen-in coordinates; on the right-hand side it is given in Cartesian coordinates.

Let us consider the physical sense of the results obtained. Having accepted that the structure of the magnetic field and flow shown in Figure 3.1 is the initial state, and the configuration shown in Figure 3.2a is the final state to which the system has evolved, then the following conclusions can be deduced. First of all, one may see that the magnetic field structure reconstructs itself, i.e., two hemispaces which did not interact at the initial instant turn out to be connected by the magnetic field lines. Second, from (3.7) it follows that the plasma is accelerated up to the velocity of the order of Alfvén speed while the magnetic field weakens in region 3. Though the magnetic field increases slightly in region 2, on the whole the magnetic energy is transformed to kinetic energy.

As we have said above, Sonnerup's model assumes the flow and the magnetic field to be homogeneous in all the four sectors shown in Figure 3.2. To meet these demands, the model contains four discontinuities produced by external causes, so-called incoming discontinuities. Indeed, information in an incompressible plasma is propagated with the velocity $\mathbf{V} \pm \mathbf{V}_a$, and the same vector defines the inclination of the Alfvén discontinuity.

In the *I* quadrant, the vector $\mathbf{V} + \mathbf{V}_a$ is parallel to the internal .(between regions 2 and 3) discontinuity while $\mathbf{V} - \mathbf{V}_a$ is parallel to the external (between regions 1 and 2) discontinuity, with vector $\mathbf{V} + \mathbf{V}_a$ directing along the shock front from the origin and $\mathbf{V} - \mathbf{V}_a$ to the origin. This means that the internal discontinuities are produced by the causes at the origin whereas the external ones are generated by the sources at infinity. Physically, since field lines are reconnected exactly at the origin, the solution must contain only the outgoing shocks. Besides, as Landau and Lifshitz (1959a) have pointed out, the intersection of three or more incoming shocks along a single line would be an improbable coincidence (see also Vasyliunas, 1975). For all these reasons, Sonnerup's model is unlikely to describe real physical conditions.

However, Sonnerup's model can be useful because many of its important features are conserved in the more realistic model devised by Petschek, as described below. In addition, Sonnerup's model is sufficiently simple so that up until now it is the only one investigated completely (Sonnerup, 1970; Yeh andDryer, 1973; Cowley, 1974a, b;

Vasyliunas, 1975; Yang and Sonnerup, 1976; Mitchell and Kan, 1978; Semenov and Kubyshkin, 1981). It should be emphasized that almost all our knowledge about three-dimensional reconnection is based on Sonnerup's model.

Let us now list the features of the reconnection process following from Sonnerup's model which may be preserved to some extent in other reconnection models that do not deal with incoming shocks.

(1) Three-dimensional solutions turn out to be, in fact, quasi-two-dimensional. Any of them may be obtained from the two-dimensional case by adding the **V** and **B** components (which are different in different sectors) parallel to the reconnection line. This permits one to describe a three-dimensional reconnection based on the more simple two-dimensional problems.

(2) For the reconnection to take place, the reconnection line should be located within the smaller angle between the magnetic field projections on the current layer (Figure 3.3). In other words, the magnetic field projections on the normal to the reconnection line should be antiparallel.

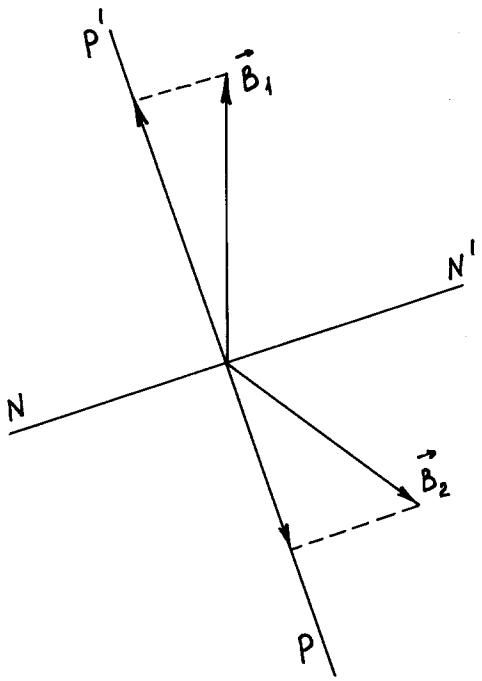

Fig. 3.3. A scheme to illustrate conditions necessary for the reconnection to proceed in Sonnerup's model. NN' is the merging line; PP' is perpendicular to NN'. Projections of the reconnected fields on PP' have to be orthogonal to each other.

The location of the reconnection line may be determined uniquely provided the position of the current layer is known and the electric field is given on opposite sides of the current layer.

If the electric field is not given on one side of the current layer (as occurs in the solar wind interaction with the magnetosphere) the position of the reconnection line is not determined by the geometry of the reconnected magnetic field. The only requirement, as in the previous case, is that the reconnection line falls within the smaller angle between the magnetic field projections. In this case the electric field penetrating through the current layer is not determined by the magnetic field geometry either, and its intensity may vary from zero to some maximum value.

(3) Formally, beside the magnetic field line reconnection, in the Sonnerup model the stream line reconnection is also possible (Figure 3.4). A solution corresponding to the stream line reconnection may be derived from the solution for the magnetic field reconnection by a simple change: $\sqrt{4\pi\rho}\,\mathbf{V} \Rightarrow \mathbf{B}$; $\mathbf{B} \Rightarrow -\sqrt{4\pi\rho}\,\mathbf{V}$; $\varepsilon \Rightarrow \varepsilon^{-1}$. However, as yet it is not quite clear whether such a solution is realized physically. Indeed, no solution concerning the stream line reconnection which would contain only outward propagating shocks is yet known. If such a solution were found it might be used for describing the solar wind – magnetosphere interaction in the case of the northward IMF.

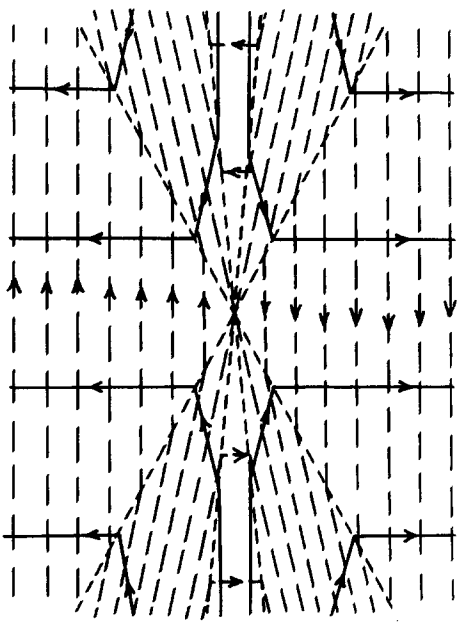

Fig. 3.4. The stream line reconnection. The solid lines are the magnetic field lines; the dotted lines with arrows are the stream lines; the dotted lines passing the origin of the coordinate system represent the shock waves.

(4) Sonnerup's model is useful also in investigating the structure of the *F*-manifold. Using a symmetry considerations, the expressions (3.7) may be extended from quadrant *I* to the whole plane. Formulas extended in such a way permit one to map the physical plane onto an *F*-manifold consisting of two sheets (planes) in the (t, α)-space (see

Figure 3.2b); the cut is made along the t-axis from 0 to ∞. Thus, from the topological point of view, the existence of the field-line reconstruction caused by the reconnection manifests itself as a two-sheet structure (a many-sheet structure in the general case) mapping the physical space onto the F-manifold. (One may say that the two-sheet structure is the topological feature of the reconnection process.)

(5) When the Alfvénic Mach number is small, i.e. when the magnetic field is strong, the inclination angles of discontinuities to the x-axis are of order ε (see Equation (3.7)). Consequently, when $\varepsilon \to 0$ the width of the region in which the magnetic field varies rapidly and plasma is accelerated tends to zero as well. Such a behavior of the solution is typical for the boundary layer phenomena, which arise when the main derivative is multiplied by a small parameter (ε in our case). As will be seen below, the appearance of a boundary layer in the problem of reconnection is essential. Following Vasyliunas (1975), we shall call the boundary layer in the reconnection problem the FR-region (field reversal region).

3.2. Petschek's reconnection model (Petschek, 1964)

The principal defect of Sonnerup's model is the presence of the incoming discontinuities. Now we shall construct a solution with outgoing discontinuities only (Semenov *et al.*, 1983a).

The stationary reconnection problem may be formulated as follows. In a zero-order approximation with respect to the Alfvénic Mach number $\varepsilon = V_0/V_a \ll 1$, there are given homogeneous magnetic fields and flows $\mathbf{B} = (1, 0)$; $\mathbf{V} = (0, -1)$ in the upper hemiplane and $\mathbf{B} = (-1, 0)$; $\mathbf{V} = (0, 1)$ in the low hemiplane respectively. Evidently, the condition $\{V_n\} = 0$ is not satisfied on the neutral sheet ($y = 0$). Then a system of shocks is assumed to arise to deflect the flow in such a way that a stationary state can exist. It is necessary to find the shape of the shocks as well as the flow, magnetic field and pressure. The problem will be treated over an area which is a square with a unit side.

The F-manifold is believed (and as follows from the results) to contain two sheets, as it does in Sonnerup's model. In contrast to that model, Petchek's solution suggests the existence of the outgoing shocks only; the assumption that the magnetic field and the plasma flow are homogeneous in the regions between the shocks is rejected (see Figure 3.5). Clearly it is sufficient to consider only the I quadrant of the physical space, which is mapped onto the upper hemiplane of the first sheet of the F-manifold.

Following Petschek (1964), we shall try to find an asymptotic solution in the inflow region (sectors 1, 3 in Figure 3.5a) in the following form:

$$\mathbf{r}(t, \alpha) = \mathbf{r}^{(0)}(t, \alpha) + \varepsilon \mathbf{r}^{(1)}(t, \alpha) + \cdots,$$
$$P(t, \alpha) = P^{(0)}(t, \alpha) + \varepsilon P^{(1)}(t, \alpha) + \cdots, \tag{3.8}$$

where $\mathbf{r}^{(0)} = (\alpha, -t)$, $P^{(0)} = \text{const.}$ in the upper hemiplane of the physical space while $\mathbf{r}^{(0)} = (-\alpha, t)$, $P^{(0)} = \text{const.}$ in the lower hemiplane, which corresponds to a homogeneous magnetic field and flow that are opposite in direction.

Inserting (3.8) into (3.1)–(3.3) we obtain the equations of the first-order approxima-

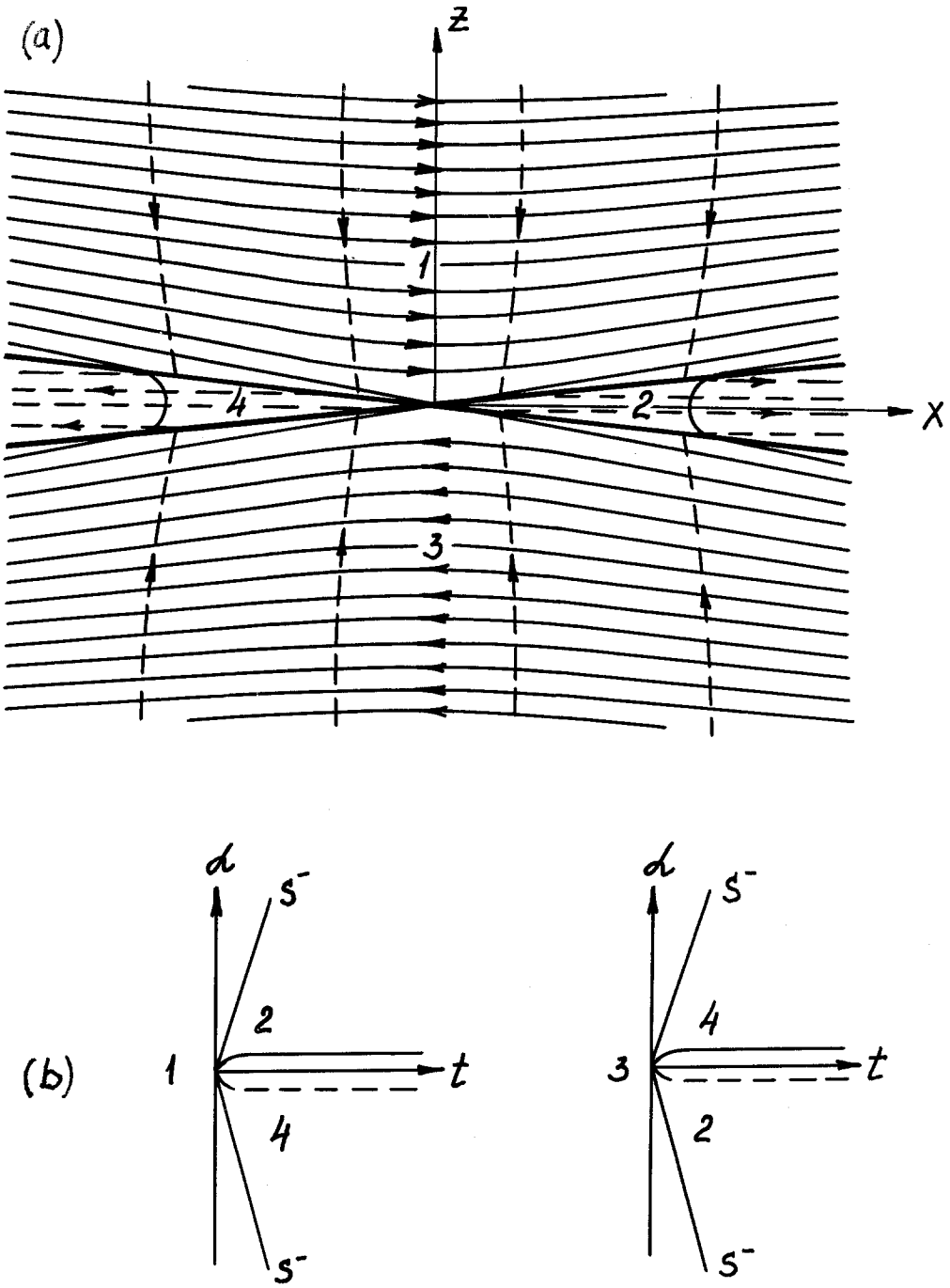

Fig. 3.5. The field line reconnection in Petschek's model. (a) Physical space; (b) *F*-manifold. Designations are the same as in Figure 3.2.

tion:

$$x_{\alpha\alpha}^{(1)} = P_{\alpha}^{(1)}; \qquad -y_{\alpha\alpha}^{(1)} = P_{t}^{(1)}; \qquad y_{t}^{(1)} = x_{\alpha}^{(1)}, \tag{3.9}$$

which results in:

$$\Delta y^{(1)} = j^{(1)}(t). \tag{3.10}$$

It can be proved that the function $j^{(1)}(t)$ on the right-hand side of (3.10) is the first-order approximation of the electrical current. This function is determined by the conditions at the boundary of the region considered. We assume $j^{(1)}(t) = 0$. Thus, in the zero-order approximation as well as in the first-order approximation there are no currents in the inflow region (Vasyliunas, 1975). Then (3.10) may be rewritten in the form:

$$\Delta y^{(1)}(t, \alpha) = 0. \tag{3.11}$$

Some points must be noted. When $\varepsilon \neq 0$ the total system in Equations (3.1)–(3.3) is of the elliptic-hyperbolic type because the speed of sound is infinite, while Alfvénic speed is finite. The degenerated system (corresponding to $\varepsilon = 0$) is elliptical; the limit $\varepsilon \to 0$ corresponds to $V_a \to \infty$. As a consequence of the degeneration of Equations (3.1)–(3.3), a boundary layer appears, which in the case under consideration is the FR-region.

Since the pioneer paper by Prandtl (1904), it has been clear that the key to any problem involving the boundary layer is the appropriate choice of variables inside the layer. It is of no use to look for the solution in the FR-region in the form given in Equation (3.8), corresponding to the regular perturbation theory, because of the rapid variation of the magnetic field and flow at the shocks. For this reason all the variables should be changed to new ones in the FR-region. Unfortunately, a formal mathematical theory giving the methods to find these new variables is not yet worked out, and this lack is the main difficulty in any concrete problem with the boundary layer.

In the case under consideration, the question about new variables in the FR-region is solved on the basis of Sonnerup's model. It may be seen from (3.7) that the new variables must be the following: $x = x(t'; \alpha)$; $y = \varepsilon \bar{y}(t', \alpha)$; $t' = t/\varepsilon$. Now it is possible to apply the regular perturbation theory:

$$\begin{aligned} x(t', \alpha) &= \bar{x}^{(0)}(t', \alpha) + \varepsilon \bar{x}^{(1)}(t', \alpha) + \cdots, \\ y(t', \alpha) &= \varepsilon[\bar{y}^{(0)}(t', \alpha) + \varepsilon \bar{y}^{(1)}(t', \alpha) + \cdots], \\ P(t', \alpha) &= \bar{P}^{(0)}(t', \alpha) + \varepsilon \bar{P}^{(1)}(t', \alpha) + \cdots. \end{aligned} \tag{3.12}$$

The steps to find the unknowns are:

$$(x^{(0)}, y^{(0)}) \Rightarrow \bar{x}^{(0)} \Rightarrow \bar{y}^{(0)} \Rightarrow x^{(1)} \Rightarrow y^{(1)} \Rightarrow \bar{x}^{(1)} \Rightarrow \bar{y}^{(1)} \Rightarrow \ldots. \tag{3.13}$$

In accordance with this scheme we start with finding $\bar{x}^{(0)}$.

The problem considered here is rather simple, hence one may find $\bar{x}^{(0)}$ in the form: $\bar{x}^{(0)} = at'$. The unknown constant is determined from the discontinuity relation $\{x\} = 0$ (see (A35)). In the upper hemiplane this relation combined with the shock equation $t' = \alpha$ gives: $x^{(0)} = \alpha = \bar{x}^{(0)} = at'|_{t'=\alpha} = a\alpha$. It results in $a = 1$. Then $\bar{y}^{(0)}$ is obtained

from Equation (3.3) and condition $V_y(y = 0) = \bar{y}_{t'}(\alpha = 0) = 0$: $\bar{y}^{(0)} = \alpha$. The pressure relation $\{P\} = 0$ yields: $\bar{P}^{(0)} = P^{(0)} = \text{const}$. Thus, the zero order approximation in the FR-region gives:

$$\bar{x}^{(0)} = t'; \qquad \bar{y}^{(0)} = \alpha; \qquad \bar{P}^{(0)} = P^{(0)} = \text{const}. \tag{3.14}$$

Now it is necessary to obtain the function $y^{(1)}(t, \alpha)$ from (3.11). The boundary condition for $y^{(1)}$ follows from the relation valid at the discontinuity $\{y\} = 0$:

$$y^{(0)}(0, \alpha) + \varepsilon(y_t^{(0)}(0, \alpha)\,\alpha + y^{(1)}(0, \alpha)) = \varepsilon\bar{y}^{(0)}(\alpha, \alpha).$$

This results in

$$y^{(1)}(0, \alpha) = 2\,|\alpha|. \tag{3.15}$$

For $\alpha < 0$, Equation (3.15) follows from the symmetric condition. For solving the Laplace equation (3.11), it is necessary to specify the solution at the whole boundary of the reconnection region. In principle this could be done, e.g., as described in Vasyliunas (1975), but as we are basically interested in the reconnection process in the vicinity of the origin of the coordinate system, we can confine ourselves to $\alpha \ll 1$, $t \ll 1$, and use the Poisson formula for the determination of $y^{(1)}$:

$$y^{(1)}(t, \alpha) = -\frac{4}{\pi}\left(\alpha\,\mathrm{tg}^{-1}\frac{\alpha}{t} + t\ln\frac{1}{\sqrt{\alpha^2 + t^2}}\right). \tag{3.16}$$

Then (see Equation (3.13)), $P^{(1)}$ and $x^1(t, \alpha)$ are obtained from (3.9) with the boundary condition $x(t, 0) = 0$, which implies that $V_x(x = 0) = 0$:

$$x^{(1)}(t, \alpha) = \frac{4}{\pi}\left(t\,\mathrm{tg}^{-1}\frac{\alpha}{t} - \alpha\ln\frac{1}{\sqrt{\alpha^2 + t^2}}\right), \tag{3.17}$$

$$P^{(1)}(t, \alpha) = -\frac{4}{\pi}\ln\frac{1}{\sqrt{\alpha^2 + t^2}}. \tag{3.18}$$

The next step consists of finding $\bar{x}^{(1)}$ and $\bar{y}^{(1)}$. Inserting (3.12) into (3.1)–(3.3) we get the first order equations in the FR-region:

$$\bar{x}^{(1)}_{t't'} - \bar{x}^{(1)}_{\alpha\alpha} = -\bar{P}^{(1)}_{t'}, \tag{3.19}$$

$$\bar{P}^{(1)}_{\alpha} = 0, \tag{3.20}$$

$$\bar{y}^{(1)}_{\alpha} + \bar{x}^{(1)}_{t'} = 0. \tag{3.21}$$

From (3.20) it follows that $\bar{P}^{(1)} = \bar{P}^{(1)}(t')$ and then from the pressure relation $\{P\} = 0$ may be obtained:

$$\bar{P}^{(1)}(t') = \frac{4}{\pi}\ln t'. \tag{3.22}$$

The boundary condition for $\bar{x}^{(1)}(t', \alpha)$ may be obtained in the case: when $\alpha = 0$ from

the condition $B_x(y = 0) = 0$, which implies $\bar{x}^{(1)}_{\alpha}(t', 0) = 0$; and when $\alpha = t'$ (at the shock), from the discontinuity relation $\{x\} = 0$, which implies

$$\bar{x}^{(1)}(\alpha, \alpha) = x^{(1)}(0, \alpha) = \frac{4}{\pi}\alpha \ln \alpha.$$

The integration of Equation (3.19) leads to the solution:

$$\bar{x}^{(1)}(t', \alpha) = \frac{4}{\pi}\{(t' + \alpha)\ln(t' + \alpha) + (t' - \alpha)\ln(t' - \alpha) - t' \ln 4t'\}. \quad (3.23)$$

Finally, $\bar{y}^{(1)}(t', \alpha)$ is calculated from (3.21) for the boundary condition $\bar{y}^{(1)}(t', 0) = 0$:

$$\bar{y}^{(1)}(t', \alpha) = \frac{4}{\pi}\{(t' + \alpha)\ln(t' + \alpha) + (t' - \alpha)\ln(t' - \alpha) - \alpha \ln 4t' - \alpha\}. \quad (3.24)$$

Formulas (3.14), (3.16)–(3.18), and (3.22)–(3.24) completely describe the solution in the zero- and first-order approximation; flow and magnetic field are obtained with the formulas given in (3.6). Taking into account the symmetry of the problem under consideration, we shall present formulas for the upper hemiplane and the right-hand FR-region only. The results will be listed in Cartesian coordinates also, using the fact that in the inflow region $\alpha = x$, $t = -y$, while in the FR-region $\alpha = y/\varepsilon$, $t' = x$, in the zero-order approximation:

Inflow region:

$$V_x = -\frac{4}{\pi} V_0 \varepsilon \operatorname{tg}^{-1}\frac{x}{y}, \quad (3.25a)$$

$$B_x = B_0 - \frac{4\varepsilon}{\pi} B_0 \left(\ln \frac{L}{\sqrt{x^2 + y^2}} - 1\right), \quad (3.25b)$$

$$V_y = -V_0 - \frac{4\varepsilon}{\pi} V_0 \left(\ln \frac{L}{\sqrt{x^2 + y^2}} - 1\right), \quad (3.25c)$$

$$B_y = \frac{4\varepsilon}{\pi} B_0 \operatorname{tg}^{-1}\frac{x}{y}, \quad (3.25d)$$

$$P = P^{(0)} - \frac{4\varepsilon}{\pi}\rho V_0^2 \ln \frac{L}{\sqrt{x^2 + y^2}}, \quad (3.25e)$$

FR-region:

$$V_x = V_a + \frac{4}{\pi} V_0 \left(\ln \frac{x^2 - \bar{y}^2}{4Lx} + 1\right), \quad (3.26a)$$

$$B_x = \frac{4\varepsilon}{\pi} B_0 \ln \frac{x + \bar{y}}{x - \bar{y}}, \quad (3.26b)$$

$$V_y = -\frac{4}{\pi} V_0 \left(\ln \frac{x + \bar{y}}{x - \bar{y}} + \frac{\bar{y}}{x} \right), \tag{3.26c}$$

$$B_y = \varepsilon B_0 - \frac{4\varepsilon^2}{\pi} \left(\ln \frac{x^2 - \bar{y}^2}{4Lx} + 1 \right), \tag{3.26d}$$

$$P = P^{(0)} - \frac{4\varepsilon}{\pi} \rho V_0^2 \ln \frac{L}{x}. \tag{3.26e}$$

Shock equation

$$y = \varepsilon |x|, \tag{3.27}$$

where $V_0 = cE_0/B_0$; $\varepsilon = V_0/V_a$; L is characteristic length, $\bar{y} = y/\varepsilon$.

The magnetic field line configuration as well as the flow structure are shown in Figure 3.5a. Unlike Sonnerup's model, there are only outgoing shocks in Petschek's model, hence Petschek's model has its own special features. But for the main properties of the reconnection process, both models are quite similar. As one may see from comparison of Figure 3.1 and 3.5a, the reconstruction of the magnetic field structure takes place in both cases. From Equation (3.25a) it follows that plasma in the FR-region is accelerated at the shocks up to the Alfvén velocity, i.e., the transformation of the magnetic energy to kinetic energy takes place.

Petschek (1964) was the first to solve the reconnection problem in the formulation described above. He found the zero- and the first-order approximation in the inflow region but only the zero-order approximation in the FR-region. These results were extended and improved by Vasyliunas (1975). A first-order approximation in the FR-region has been obtained by Soward and Priest (1977), who used a different technique based on the generalization of similarity solutions.

Unlike Yeh and Axford (1970) and Yeh and Dryer (1973), who looked for a similarity solution in the form

$$\psi = rg(v); \qquad A = rf(v),$$

where ψ is a stream function, A is the vector potential, and (r, v) are polar coordinates, Soward and Priest searched for a solution in a form containing a weak (logarithmic) dependence on r:

$$\psi = rg(R, v); \qquad A = rf(R, v); \qquad R = \ln (r/l) + R_0,$$

where R_0 is a constant. Solutions for f and g in the inflow region were assumed as follows:

$$f = R^{1/2} f_0(v) + R^{-1/2}(f_{11}(v) \ln R + f_1(v)),$$

$$g = R^{-1/2} g_0(v) + R^{-3/2}(g_{11}(v) \ln R + g_1(v)).$$

In the FR-region they changed the variable from v to $\xi = v/\theta(R)$, where equation $v = \theta(R)$ defines the discontinuity.

Recently, by use of an analogous technique, Soward and Priest (1982) have obtained the solution of the reconnection problem for the case of compressible plasma. In spite of that, in Soward and Priest's model the Alfvénic Mach number slowly (logarithmically) varies with distance; their results may be compared with those obtained by means of the frozen-in coordinates method (Semenov *et al.*, 1983a). With the exception of some details, the results proved to be the same.

The plasma acceleration in Petschek's model is, in fact, a cumulative effect. Gathered from a big area under the action of the electric field, plasma is then focused by the shocks into narrow jets. The more intensive the initial magnetic field is, the higher is the velocity up to which the plasma is accelerated. Physically the acceleration is accomplished by the Ampère's force on the shock front or, in other words, by the work of the electric field: $(\mathbf{E} \cdot \mathbf{j}) > 0$. This principal idea by Petschek is valid also for all more complicated cases: compressible plasma, asymmetric and nonstationary flow, etc. The investigation of these cases is of great importance for practical applications because the solution obtained by Petschek in frames of the incompressible plasma model is oversimplified.

The qualitative consideration of the problem is given below.

In the case of compressible plasma (Soward and Priest, 1982; Soward, 1982; Semenov *et al.*, 1983a, b) the picture is qualitatively similar to that in Petschek's solution. In a wide sector, plasma flows slowly to the current layer with its density remaining constant up to terms of the second order. Plasma acceleration and density change takes place on the slow shocks S^-. In the zero-order approximation, the plasma velocity in the FR-region is equal to the Alfvénic one while the pressure and density increase as:

$$\rho = \rho_0 \frac{\gamma(\beta + 1)}{\gamma(\beta + 1) - 1}; \qquad p = \frac{B_0^2}{8\pi} + p_0, \tag{3.28}$$

where γ is the ratio of specific heats, $\beta = 8\pi p_0 / B_0^2$. The density increases insignificantly (approximately by two times) while the pressure in plasma with $\beta \ll 1$ amounts to the magnetic field pressure in front of the shock. This means that in the low-pressure plasma intense heating takes place in addition to its acceleration. The incompressible case is attained in the limit $\beta \to \infty$.

The structure of the FR-region is much more complicated in the nonsymmetrical case, i.e. when the plasma parameters are different on the opposite sides of the current layer (Levy *et al.*, 1964; Yang and Sonnerup, 1977; Semenov *et al.*, 1983b). Depending on the parameter relations, the following four cases may take place: AS^-CS^-, AR^-CS^-, S^-CS^-A, and S^-CR^-A; here S^-, A, C, and R^- are slow shock, Alfvénic discontinuity, contact discontinuity and slow expansion fan, respectively.

The flow structure and magnetic field configuration for the case AS^-CS^- are shown in Figure 3.6.

As is shown by Semenov *et al.* (1983b), only one possible sequence of discontinuities exists for any concrete set of parameters satisfying the pressure balance equation (Figure 3.7).

The parametrical space ($\mu = B_1/B_2 = V_2/v_1$; $\nu = \rho_2/\rho_1$) may be divided into four fields with a single solution in any of them. At the boundaries of these fields one of the

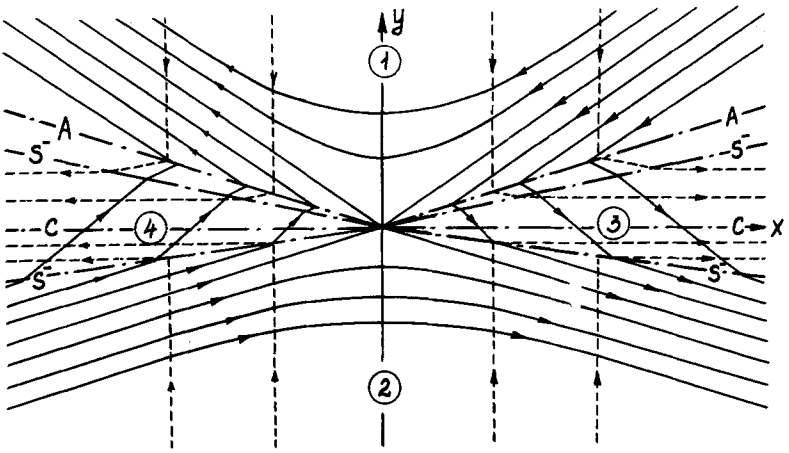

Fig. 3.6. The scheme of the flow and of the magnetic field lines in the case of asymmetric flow for the $AS^{-}CS^{-}$ version.

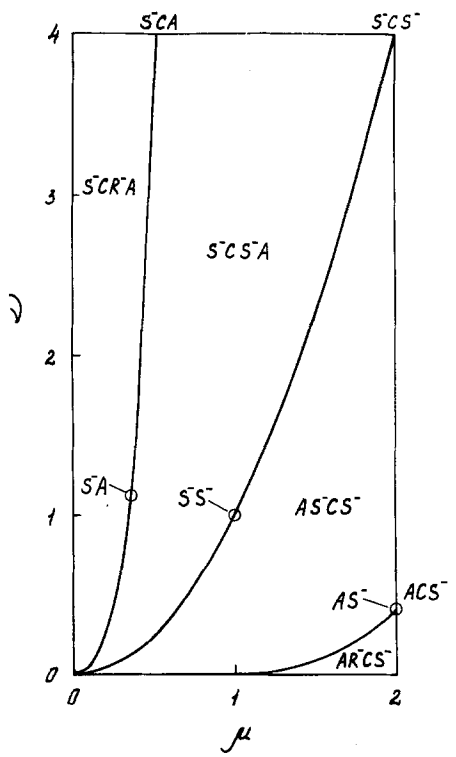

Fig. 3.7. The regions of existence of various solutions of the problem on the field line reconnection in the space of parameters $\nu = \rho_2/\rho_1$, $\mu = B_2/B_1$, in the case of an asymmetric flow. Indices 1 and 2 correspond to the hemiplanes above and beneath the current sheet.

waves degenerates. In addition, there are points at the boundaries where two waves degenerate. The typical solutions AR^-CS^- ($\beta_1 = 8\pi p_1/B_1^2 = 2.3$; $\beta_2 = 8\pi p_2/B_1^2 = 0.3$; $\mu = B_2/B_1 = 1.7$; $\nu = \rho_2/\rho_1 = 0.5$) and AS^-CS^- ($\beta_2 = 3$; $\beta_2 = 1$; $\mu = 1.7$; $\nu = 0.5$) are shown in Figure 3.8a, b. As the Alfvénic discontinuity is the first (or the outermost) one, the velocity reaches the value of $2V_a$ just behind it. Then, in version AR^-CS^- the plasma is accelerated some more in the expansion fan while in the version AS^-CS^- it is slowed down behind the first slow shock. Thus, plasma acceleration in the non-symmetrical case is more effective than in the symmetrical one. The more asymmetry, the more intense is the plasma acceleration. In the case AS^-CS^- the velocity lies within the limits $V_a \leqslant V \leqslant 2V_a$ while in the case AR^-CS^- $2V_a \leqslant V \leqslant 2(\sqrt{\beta_1} + 1)V_a$. So the plasma acceleration (up to V_a) in the symmetrical case considered by Petschek is the smallest of all the possible ones.

As is shown in Figure 3.7, the solution AS^-CS^- describes the case of weak asymmetry whereas AR^-CS^- corresponds to the strong one.

3.3. Mixed reconnection models

Now we consider reconnection models with an arbitrary number of incoming discontinuities (Semenov and Kubyshkin, 1984). These models have the features of both Petschek's solution and Sonnerup's one. For simplicity we shall restrict our considerations to the cases of two and four incoming discontinuities.

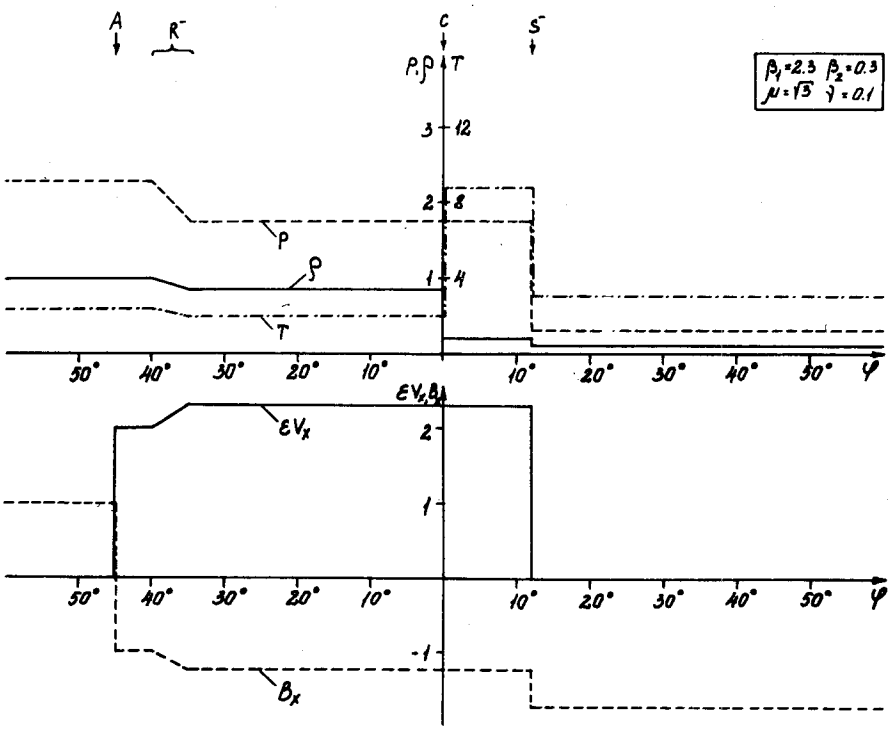

Fig. 3.8a.

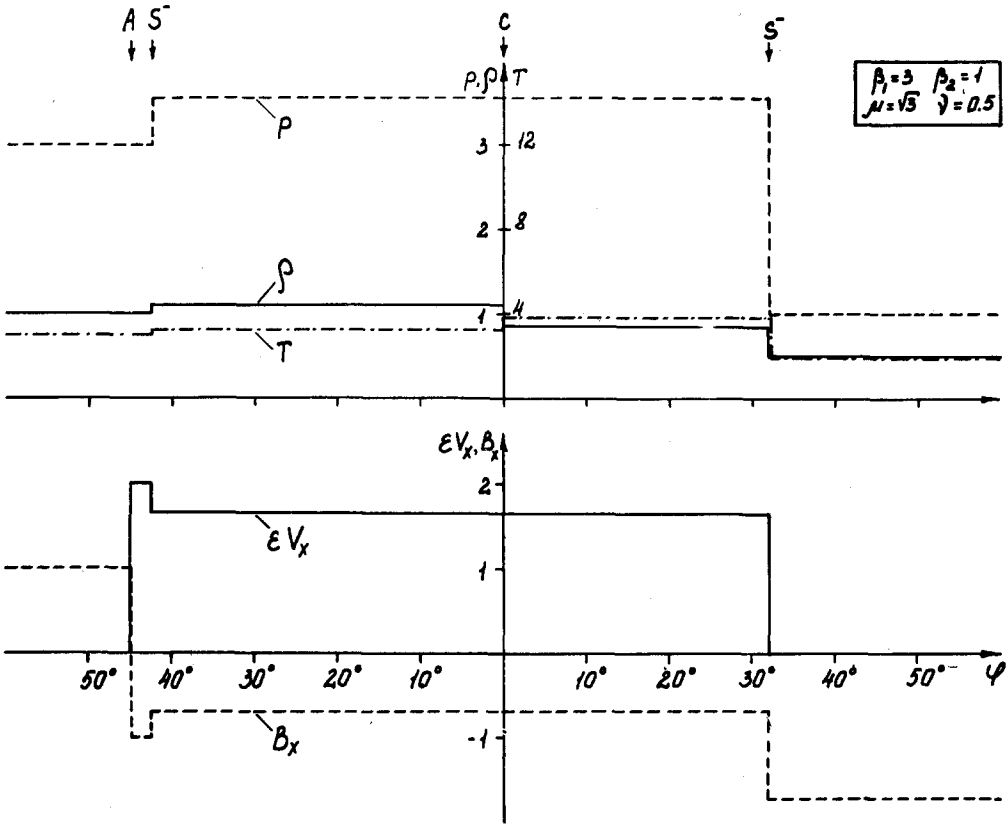

Fig. 3.8b.

Fig. 3.8a–b. Typical solutions $AR^{-}CS^{-}$ (a), and $AS^{-}CS^{-}$ (b). The variations of the density, temperature and of the X-component of the velocity and of the magnetic field are shown; φ is the polar angle in the frozen-in space $(t/\varepsilon, \alpha)$; this angle is related to the polar angle in the physical space by approximately linear dependence.

We start with the first case of two incoming discontinuities (see Figure 3.9). The magnetic field and flow are believed to be homogeneous and known in the zero-order approximation in the inflow regions 1 and 5: $x_1^{(0)} = \alpha$; $y_1^{(0)} = -t$; $x_5^{(0)} = -\alpha$; $y_5^{(0)} = t$. Two incoming discontinuities are assumed to be of the same intensity, the electric current I on the discontinuities is known in the zero-order approximation:

$$(x_2^{(0)})_\alpha - (x_1^{(0)})_\alpha = (x_4^{(0)})_\alpha - (x_5^{(0)})_\alpha = I. \tag{3.29}$$

If $I < 0$ ($I > 0$), the current on the discontinuity is parallel (antiparallel) to the current in the current sheet. The incoming discontinuity will be called the discontinuity with parallel ($I < 0$) or antiparallel ($I > 0$) current polarization.

In the outflow regions 2, 3, 4, and 6 we look for a solution with a constant velocity and magnetic field in the zero-order approximation:

$$x_i^{(0)} = a_i\alpha + b_i t'; \qquad \bar{y}_i^{(0)} = c_i\alpha + d_i t', \tag{3.30}$$

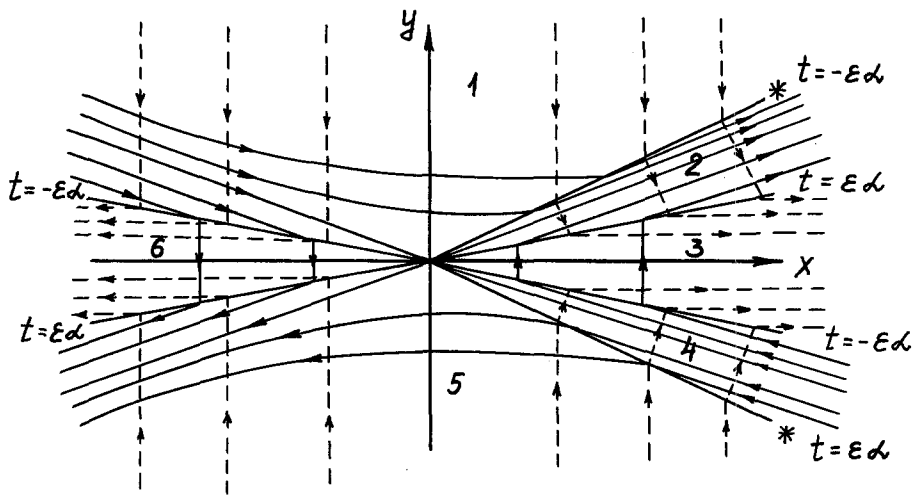

Fig. 3.9. Mixed reconnection model in the case of two incoming discontinuities, shown by asterisks. Designation are the same as in Figure 3.2.

where i is the region number, $t' = t/\varepsilon$, $y = \bar{y}/\varepsilon$. The constants a_i and b_i are determined by the jump relation $\{x\} = 0$ and the Equation (3.29). Taking into account that $d_3 = d_6 = 0$ (e.g., $V_y(y = 0) = 0$ in regions 3 and 6) the constants c_i and d_i are determined by the jump relation $\{y\} = 0$ on the discontinuities $2 \to 3$ and $3 \to 4$ and Equation (3.3). The solution in the upper hemiplane is:

$$
\begin{aligned}
x_1^{(0)} &= \alpha, & y_1^{(0)} &= -t, \\
x_2^{(0)} &= (I+1)\alpha + It', & \bar{y}_2^{(0)} &= ((3I+2)\alpha - (I+1)t')/(2I+1)^2, \\
x_3^{(0)} &= (2I+1)t', & \bar{y}_3^{(0)} &= \alpha/(2I+1), \\
x_6^{(0)} &= -t', & \bar{y}_6^{(0)} &= -\alpha.
\end{aligned} \tag{3.31}
$$

Now from $\{y\} = 0$ across the discontinuities $1 \to 2$ and $1 \to 6$ we obtain the boundary condition for the first-order approximation $y^{(1)}(t, \alpha)$ in the inflow region 1:

$$
y_1^{(1)}(0, \alpha) = \begin{cases} 2(1-2I^2)\alpha/(2I+1)^2, & \alpha \geqslant 0, \\ -2\alpha & \alpha < 0. \end{cases} \tag{3.32}
$$

Solving the Laplace equation (3.11) we find:

$$
y_1^{(1)}(t, \alpha) = -k\left(\alpha \operatorname{tg}^{-1}\frac{\alpha}{t} - t \ln\sqrt{(\alpha^2 + t^2)}\right) + p\alpha, \tag{3.33}
$$

$$
x_1^{(1)}(t, \alpha) = k\left(t \operatorname{tg}^{-1}\frac{\alpha}{t} + \alpha \ln\sqrt{(\alpha^2 + t^2)}\right), \tag{3.34}
$$

where

$$k = \frac{4}{\pi} \frac{(1+I)^2}{(1+2I)^2}; \qquad P = -\frac{2I(3I+2)}{(2I+1)^2}. \tag{3.35}$$

It may be seen from the solution obtained that the incoming discontinuities with antiparallel current polarization ($I > 0$) stimulate the reconnection process, since the plasma is accelerated in outflow region 3 more effectively that in Petschek's model ($I = 0$). Rather, the incoming discontinuities with parallel current polarization ($I < 0$) decrease the intensity of the reconnection process. It is worth noting that when $I \leqslant -\frac{1}{2}$, the reconnection is not possible at all. From a physical point of view, this phenomenon can be explained as follows. As we have seen in Section 2, the reconnection process is due to the development of the current system I_1. The incoming discontinuity with antiparallel current polarization increases current I_1 in the diffusion region and therefore stimulates the reconnection process. On the other hand, the incoming discontinuity with parallel current polarization weakens the current system I_1, and when $I \leqslant -\frac{1}{2}$ it forbids the reconnection.

The solution with four incoming discontinuities is constructed analogously. It is given by the same formulas (3.31) and (3.32) in the I quadrant, but with new constants k and p:

$$k = \frac{4}{\pi} \frac{(1-2I^2)}{(1+2I)^2}, \qquad p = 0. \tag{3.36}$$

The solution presented in (3.31), (3.32), and (3.36) is of particular interest as a generalization of Petchek's and Sonnerup's solutions. Actually, the solution obtained is reduced to Petschek's solution when $I = 0$ and to Sonnerup's solution (3.7) when $I = 1/\sqrt{2}$. In this latter case the solution becomes strict rather than asymptotic.

4. Time-Dependent Field Line Reconnection

4.1. Asymptotic solution of the time-dependent reconnection problem

Let us now consider the formal method of obtaining the solution of the time-dependent reconnection problem (Semenov *et al.*, 1983c). Just as in Section 3, we restrict our consideration to the case of an incompressible plasma. Then the MHD system (A27)–(A31) in frozen-in coordinates (τ, α, ζ) will be:

$$\varepsilon^2 x_{\tau\tau} - x_{\alpha\alpha} = -P_\zeta y_\alpha + P_\alpha y_\zeta, \tag{4.1}$$

$$\varepsilon^2 y_{\tau\tau} - y_{\alpha\alpha} = -P_\alpha x_\zeta + P_\zeta x_\alpha, \tag{4.2}$$

$$x_\zeta y_\alpha - x_\alpha y_\zeta = 1. \tag{4.3}$$

The dimensionless form is obtained by normalizing to the initial magnetic field B_0, velocity $V_0 = (4\pi\rho_0)^{-1/2} b_{\text{dim}}$, where ρ_0 is the plasma density, and b_{dim} is the reconnected

magnetic field. $\varepsilon = V_0/V_a$ is the Alfvén Mach number. We suppose that $\varepsilon \ll 1$ or $b_{\text{dim}}/B_0 \ll 1$, that is, the reconnection process is expected to be weak.

MHD system (4.1)–(4.3) is similar to the stationary system (3.1)–(3.3), hence the method of the previous section can be used here again. It must be borne in mind that in an incompressible plasma the sound velocity is infinite and the fast shock instantly goes up to infinity. Similarly to the stationary case, the asymptotic solution in the inflow region is given by:

$$\begin{aligned} \mathbf{r}(\tau', \alpha, \zeta) &= \mathbf{r}^{(0)}(\tau', \alpha, \zeta) + \varepsilon \mathbf{r}^{(1)}(\tau', \alpha, \zeta) + \cdots, \\ P(\tau', \alpha, \zeta) &= P^{(0)}(\tau', \alpha, \zeta) + \varepsilon P^{(1)}(\tau', \alpha, \zeta) + \cdots, \end{aligned} \tag{4.4}$$

where $P^{(0)} = \text{const.}$, $\tau' = \tau/\varepsilon$, $\mathbf{r}^{(0)} = (\alpha, -\zeta)$ in the upper hemiplane, $\mathbf{r}^{(0)} = (-\alpha, \zeta)$ in the low hemiplane. The fast τ' time is introduced to take into account fast movement of the FR-regions. In the FR-region it is necessary to change the variables used to $\tau' = \tau/\varepsilon$, $\zeta' = \zeta/\varepsilon$, and $\bar{y} = y/\varepsilon$, and to look for an asymptotic solution of the form:

$$\begin{aligned} x(\tau', \alpha, \zeta') &= \bar{x}^{(0)}(\tau', \alpha, \zeta') + \varepsilon \bar{x}^{(1)}(\tau', \alpha, \zeta') + \cdots, \\ y(\tau', \alpha, \zeta') &= \varepsilon\{\bar{y}^{(0)}(\tau', \alpha, \zeta') + \varepsilon \bar{y}^{(1)}(\tau', \alpha, \zeta') + \cdots\}, \\ P(\tau', \alpha, \zeta') &= \bar{P}^{(0)}(\tau', \alpha, \zeta') + \varepsilon \bar{P}^{(1)}(\tau', \alpha, \zeta') + \cdots. \end{aligned} \tag{4.5}$$

The procedure of obtaining the unknowns is the same as (3.13). The equation of the slow shock in the first quadrant is (see (A34)):

$$\alpha = \tau' - q(\zeta'), \tag{4.6}$$

where $q(\zeta')$ is an arbitrary function.

Now let us determine the unknowns according to the scheme (3.13). The zero-order approximation in the inflow region is known, hence we may start with the zero-order approximation in the FR-region. We are describing the simplest case of reconnection, and thus one might find the function $\bar{x}^{(0)}(\tau', \alpha, \zeta')$ in the form $\bar{x}^{(0)} = \tau' - \tilde{q}(\zeta')$. From the jump relation on the shock $\{x\} = 0$ we get $q = \tilde{q}$. From (4.3), $\bar{y}^{(0)}(\tau', \alpha, \zeta')$ is:

$$\bar{x}^{(0)} = \tau' - q(\zeta'); \qquad \bar{y}^{(0)} = -\frac{\alpha - f(\tau', \zeta')}{q_{\zeta'}}, \tag{4.7}$$

where an arbitrary function $f(\tau', \zeta')$ is defined by the condition $V_y(y = 0) = 0$, that is $\bar{y}^{(0)}_{\tau'}(\alpha = 0)$, which gives $f = f(\zeta')$.

The next step is the determination of the boundary condition for the function $y^{(1)}(\tau', \alpha, \zeta)$ from the relation on the shock $\{y\} = 0$:

$$\begin{aligned} y(\tau', \alpha, \zeta) = y(\tau', \alpha, \varepsilon\zeta') &= y^{(0)}(\tau', \alpha, 0) + \\ &+ \varepsilon[y^{(0)}_{\zeta}(\tau', \alpha, 0)\, \zeta' + y^{(1)}(\tau', \alpha, 0)] = \varepsilon \bar{y}^{(0)}(\tau', \alpha, \zeta'). \end{aligned}$$

For the shock ζ' it can be found from (4.6): $\zeta' = h(\tau' - \alpha)$, where h is the inverse to q

function. It results in:

$$y^{(1)}(\tau', \alpha, 0) = -(|\alpha| - f)h'(\tau' - |\alpha|) + h(\tau' - |\alpha|), \qquad \alpha \in S^-,$$

$$y^{(1)}(\tau', \alpha, 0) = 0, \qquad \alpha \overline{\in} S^-, \qquad . \tag{4.8}$$

where $h'(\tau' - |\alpha|)$ is the first derivative of h with respect to the argument $\tau' - |\alpha|$. Inserting (4.4) into (4.1)–(4.3) one obtains the equations to the first-order approximation in the inflow region:

$$x^{(1)}_{\tau'\tau'} - x^{(1)}_{\alpha\alpha} = -P^{(1)}_{\alpha}, \tag{4.9}$$

$$y^{(1)}_{\tau'\tau'} - y^{(1)}_{\alpha\alpha} = P^{(1)}_{\zeta}, \tag{4.10}$$

$$x^{(1)}_{\alpha} = y^{(1)}_{\zeta}. \tag{4.11}$$

Whence it appears:

$$\left(\frac{\partial^2}{\partial\tau'^2} - \frac{\partial^2}{\partial\alpha^2}\right)\left(\frac{\partial^2}{\partial\alpha^2} + \frac{\partial^2}{\partial\zeta^2}\right) y^{(1)}(\tau', \alpha, \zeta) = 0. \tag{4.12}$$

For $y^{(1)}$ must vanish at the infinity, only the elliptical operator has to be used:

$$y^{(1)}_{\alpha\alpha} + y^{(1)}_{\zeta\zeta} = 0. \tag{4.13}$$

The solution of the Laplace equation (4.13) with the boundary condition (4.8) is obtained by using the Poisson formulas:

$$y^{(1)}(\tau', \alpha, \zeta) = -\frac{\zeta}{\pi} \int_{-\infty}^{\infty} \frac{y^{(1)}(\tau', \eta, 0)\, d\eta}{(\alpha - \eta)^2 + \zeta^2}, \tag{4.14}$$

$$x^{(1)}(\tau', \alpha, \zeta) = \frac{1}{\pi} \int_{-\infty}^{\infty} \frac{(\alpha - \eta) y^{(1)}(\tau', \eta, 0)\, d\eta}{(\alpha - \eta)^2 + \zeta^2}. \tag{4.15}$$

Here $x^{(1)}$ is found from (4.11). The first-order approximation for the pressure can be determined from (4.4) or (4.10).

Let us now find the first-order approximation in the FR-region for the case $f = 0$. Substitution of the series expansions (4.5) into (4.1)–(4.3) yields:

$$\bar{x}^{(1)}_{\tau'\tau'} - \bar{x}^{(1)}_{\alpha\alpha} = -P^{(1)}_{\zeta'} \cdot \bar{y}^{(0)}_{\alpha}, \tag{4.16}$$

$$\bar{P}^{(1)}_{\alpha} = 0, \tag{4.17}$$

$$\bar{x}^{(0)}_{\zeta'} \cdot \bar{y}^{(1)}_{\alpha} + \bar{x}^{(1)}_{\zeta'} \cdot \bar{y}^{(0)}_{\alpha} - \bar{x}^{(1)}_{\alpha} \cdot \bar{y}^{(0)}_{\zeta'} = 0, \tag{4.18}$$

(4.17) implies that the total pressure does not depend on α and can be found from the discontinuity condition $\{P\} = 0$:

$$\bar{P}^{(1)}(\tau', \zeta') = P^{(1)}(\tau', \tau' - q, 0). \tag{4.19}$$

The total pressure in the inflow region is defined by (4.9), hence the equation for $\bar{x}^{(1)}(\tau', \alpha, \zeta')$ will be:

$$\bar{x}^{(1)}_{\tau'\tau'} - \bar{x}^{(1)}_{\alpha\alpha} = x^{(1)}_{\tau'\tau'}(\tau', \tau' - q, 0) - x^{(1)}_{\alpha\alpha}(\tau', \tau' - q, 0). \tag{4.20}$$

Boundary conditions for the Equation (4.20) may be obtained from the discontinuity condition $\{x\} = 0$ as well as from the condition $B_x(y = 0) = 0$:

$$\begin{aligned} &\bar{x}^{(1)}(\tau', \tau' - q, \zeta') = x^{(1)}(\tau', \tau' - q, 0), \\ &\bar{x}^{(1)}_{\alpha}(\tau', 0, \zeta') = 0. \end{aligned} \tag{4.21}$$

The solutions of the Equation (4.20) with the boundary conditions (4.21) can be written as follows:

$$\begin{aligned} \bar{x}^{(1)}(\tau', \alpha, \zeta') = {} & x^{(1)}\left(\frac{\tau' + \alpha + q}{2}; \frac{\tau' + \alpha - q}{2}; 0\right) - \\ & - x^{(1)}\left(\frac{\tau' - \alpha + q}{2}; \frac{\tau' - \alpha - q}{2}; 0\right) - \Phi\left(\frac{\tau' + \alpha + q}{2}; \zeta'\right) - \\ & - \Phi\left(\frac{\tau' - \alpha + q}{2}; \zeta'\right) - \Phi(\tau', \zeta') - \Phi(q, \zeta'), \end{aligned} \tag{4.22}$$

where $x^{(1)}(\tau', \alpha, 0)$ is given by (4.15), and the function Φ is:

$$\Phi(\tau', \zeta') = \int_0^{\tau'} [x^{(1)}_{\tau}(\mu; \mu - q(\zeta'); 0) - x^{(1)}_{\alpha}(\mu, \mu - q(\zeta'), 0)]\, d\mu. \tag{4.23}$$

After $\bar{x}^{(1)}(\tau', \alpha, \zeta')$ has been obtained, the function $\bar{y}^{(1)}(\tau', \alpha, \zeta')$ can be found from equation (4.18).

Formulas (4.6), (4.7), (4.14), (4.15), (4.22) and (4.23) describe the zero- and the first-order approximations of the solution of the time-dependent reconnection problem. This solution depends on the arbitrary functions $q(\zeta')$ (or $h(\tau' - |\alpha|)$ and $f(\zeta')$.

The function $h'(\tau' - |\alpha|)$ has to meet the following conditions. According to the definition, $\zeta' = h(\tau' - |\alpha|)$, hence $h(\mu) < 0$ since $y = -\zeta$; $y > 0$ in the upper hemiplane of the physical space. Besides, $h(\mu)$ is supposed to be monotonous: $h'(\mu) \leqslant 0$.

Let us now investigate the solution obtained. The zero-order approximation for the right-hand FR-region is given by the formulas (4.6) and (4.7) in the parametric manner. If the second arbitrary function f is assumed to be zero, the shock equation, x- and y-components of both **V** and **B**, and z-component of **E** in the Cartesian coordinates can be expressed as follows:

$$y = -\varepsilon x h'(t/\varepsilon - x), \tag{4.24a}$$

$$V_x = 1/\varepsilon; \qquad V_y = 0, \tag{4.24b}$$

$$B_x = 0; \qquad B_y = -\varepsilon h'(t/\varepsilon - x), \tag{4.24c}$$

$$E = h'(t/\varepsilon - x). \tag{4.24d}$$

The leading front of the FR-region (where $h' = 0$, $x \neq 0$, i.e. $x = t/\varepsilon$ – see (4.24a)) is moving with the Alfvén speed (see Figure 2.2b). Within the FR-region the plasma velocity is $V_x = x_\tau = 1/\varepsilon$ (the plasma is accelerated up to the Alfvén speed), and V_y and B_x vanish in this zero-order approximation. Both the electric field and y-component of the magnetic field are inhomogeneous here: they equal zero on the leading front, while $h'(t/\varepsilon) \neq 0$ at the coordinate origin.

It can be seen from (4.24d) that the first arbitrary function $h'(t/\varepsilon)$ is just the electric field in the diffusion region. In that sense the solution obtained is determined by the temporal variation of the electric field at the reconnection line.

The reconnected magnetic flux F_b and the kinetic energy W (kinetic energy density $\frac{1}{2}\varepsilon^2$ multiplied by the volume of the FR-region) can be calculated as follows:

$$F_b = \int_0^{t/\varepsilon} B_y(x, t)\, \mathrm{d}x = -\varepsilon h(t/\varepsilon), \tag{4.25}$$

$$W = -(1/\varepsilon) \int_0^{t/\varepsilon} x h'(t/\varepsilon - x)\, \mathrm{d}x = -\frac{1}{\varepsilon} \int_0^{t/\varepsilon} h(\xi)\, \mathrm{d}\xi = \frac{1}{\varepsilon^2} \int_0^{t/\varepsilon} F_b(\xi)\, \mathrm{d}\xi, \tag{4.26}$$

where the integration by parts is used in the derivation of (4.26). It follows from (4.26) that kinetic energy in the FR-region changes proportionally to the time integral of the reconnected magnetic flux. Roughly, W can be estimated as:

$$W = \frac{\rho V_a^2}{2} L_x L_y L_z = \frac{\rho V_a^2}{2} (V_a t)(\varepsilon V_a t) l = \frac{B_0^3 b t_0^2 l}{32\pi\rho}, \tag{4.27}$$

where $L_x = V_a t$, $L_y = \varepsilon V_a t$, $L_z = 1$ are the characteristic dimensions of the FR-region along the x, y, and z axes, respectively, and t_0 is the characteristic duration of the reconnection process. As is shown in Section 2.2, the magnetic field increases and the plasma density decreases in the vicinity of the current sheet during the initial phase of the current sheet evolution. Both these effects of the initial phase will enhance the energy release in the spontaneous reconnection process.

To illustrate an overall structure of the field and plasma flow we turn now to the Figure 4.1a, b obtained for a particular example of time dependence $E(t)$ (or $h(t)$). Some features, which are common in different types of $E(t)$ time dependence, can be seen from here. In the inflow region the magnetic field strength clearly decreases around the reconnection site, while it is enhanced before the passage of the FR-region leading front. A sign of electric field is, therefore, opposite at these two positions. A jump in the electric field at the slow shocks in Figure 4.1b arises here due to the fast movement of the shocks.

The same formulas (4.24) can be used to describe the situation after the reconnection electric field is turned off in the diffusion region. At this moment the backward

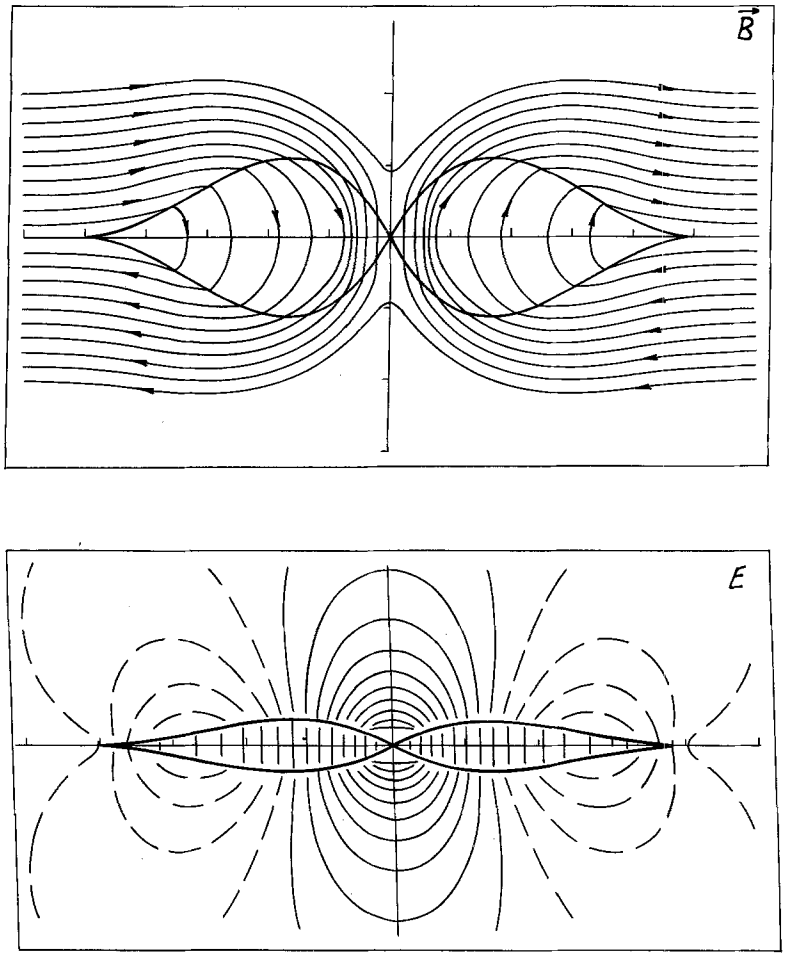

Fig. 4.1. The structure of the magnetic field (a) and of the electric field (b) for the case of the time-dependent reconnection, in which the electric field in the diffusion region is assumed to change as $E(t) = 3t^2$. The equicontours of $E_z < 0$ and $E_z > 0$ are shown by solid and dotted lines, respectively.

boundaries of the FR-regions are formed which move afterwards in both x-directions with the same Alfvén velocities as the leading fronts of the FR-regions (see Figure 2.2c). As a result, each FR-region conserves at this phase both its size along x axis and the reconnected magnetic flux, but its height (4.24a), volume, and the energy release at the shock front (4.26), (4.27) will grow in time.

The importance and meaning of the second arbitrary function $f(\zeta')$ in (4.7) can be clarified by taking into account the movement of the reconnection line. For this purpose let us introduce a new function $x = g(t')$; the speed of the reconnection line is, hence, $U = g_{t'}$. As before, the function $h'(t')$ is the electric field given at the reconnection line. Similarly to (4.24), the equations for the slow shock front and the reconnected magnetic

and electric field within the FR-region are obtained from (4.6), (4.7) in the form:

$$y = -\varepsilon(x - f^+(x + t'))h'_+(x + t'), \tag{4.28a}$$

$$B_y^+ = -\varepsilon h'_+(x + t'), \tag{4.28b}$$

$$E^+ = h'_+(x + t'), \tag{4.28c}$$

$$y = -\varepsilon(x - f^-(x - t'))h'_-(x - t'), \tag{4.29a}$$

$$B_y^- = -\varepsilon h'_-(t' - x), \tag{4.29b}$$

$$E^- = h'_-(t' - x), \tag{4.29c}$$

where signs (+) and (−) correspond to the left-hand and right-hand FR-regions, respectively, and electric fields $E_\pm$ are expressed in the fixed frame of reference. In the frame moving with the neutral line velocity U, a relation between $h'_\pm$ (or $E_\pm$ – see (4.28c) and (4.29c)) and h' is as follows:

$$h'_+(g + t')(1 + u) = h'_-(t' - g)(1 - u) = h'(t'). \tag{4.30}$$

The electric fields $E_\pm$ in both FR-regions can be simply determined from (4.30).

A position of the neutral line in addition to the equation $x = g(t')$ may be specified also by two other equations $x = f^+(x + t')$ and $x = f^-(t' - x)$ (see (4.28a) and (4.29a)). This allows us to express arbitrary functions $f^\pm$, contained in the formal solution (4.7) through the physically meaningful function g.

The effect of the movement of the reconnection line consists mainly in the deformation of the shock fronts and changes of B_y and E amplitudes. So, when the neutral line moves to the right (see Figure 2.3), the right-hand FR-region is inflated and the field magnitudes B_y and E are enhanced by a factor of $(1 + U)/(1 - U)$. At the left-hand side the changes are in opposite direction. We emphasize, however, that both the reconnected magnetic flux and energy release (a volume of the FR-region) are not affected by these effects, so that a function f influences mainly on the configuration and local features of the FR-regions, but not on their global properties.

As follows from this discussion of time-dependent reconnection problem, a solution is completely defined by the two functions which describe the temporal evolution of the electric field at the reconnection line and the movement of this line.

4.2. The Role of the Dissipative Effects

It seems well known (see also Section 2.1) that dissipative processes are of crucial importance in the reconnection phenomenon. However, the solutions considered above are obtained in the framework of the ideal MHD model. Absence of dissipation in our treatment displays itself through the signularities which appear in our formal asymptotic solution. E.g., in the case of an incompressible plasma all the components of **V** and **B** vectors in the FR-regions tend to infinity at the shock fronts (3.2a)–(3.2g). It will be seen below that in the time-dependent case the singularities also take place. In the compressible plasma these singularities disappear on the shocks, but instead of them there

appear singularities in the density and entropy at the x-axis in the FR-region, which corresponds to the generation of an entropy wave (Soward and Priest, 1982).

The appearance of singularities may be considered as evidence for the reconnection to be impossible for infinite conductivity. This means that the very fact of the existence of the logarithmic singularities points to the places where dissipative effects are of particular importance. From the mathematical point of view logarithmic singularities correspond to jumps of the function $y_\alpha^{(1)}(\tau', \eta, 0)$, which may be derived from (4.8):

$$y_\alpha^{(1)}(\tau', \eta, 0) = \operatorname{sign}\eta\,(-2rh' + |\eta|\,h''); \qquad \eta \in S^-,$$
$$y_\alpha^{(1)}(\tau', \eta, 0) = 0; \qquad \eta \overline{\in} S^-, \tag{4.31}$$

where $h = h(\tau - |\eta|)$. The X-component of the magnetic field B_x in the inflow region can be found from (4.15):

$$B_x^{(1)} = \frac{1}{\pi} \int_{-\infty}^{\infty} \frac{(\alpha - \eta) y_\alpha^{(1)}(\tau', \eta, 0)\, \mathrm{d}\eta}{(\alpha - \eta)^2 + \zeta^2}. \tag{4.32}$$

If the function $y_\alpha^{(1)}(\tau', \eta, 0)$ is continuous with respect to η and finite, then B_x together with other functions of the first-order approximation do not have any singularities and vanish at infinity. The jump of $y_\alpha^{(1)}(\tau', \eta, 0)$ produces the logarithmic singularities in the B_x and in some other functions. For example, in the stationary case $y_\alpha^{(1)}(\tau', \eta, 0) = 2 \operatorname{sign}\eta$, the jump of $y_\alpha^{(1)}$ is $\Delta y_\alpha^{(1)} = 4$, and the solution contains the ln-singularity $B_x^{(1)} \sim (4\varepsilon/\pi) \ln(\alpha^2 + t^2)^{-1/2}$. In the time-dependent case the jump of $y_\alpha^{(1)}$ at the origin is $\Delta y_\alpha^{(1)} = -4h'(\tau')$, which results in the ln-singularity in $B_x^{(1)}$:

$$B_x^{(1)} = \frac{2}{\pi} h'(\tau') \ln \frac{\tau'^2}{\alpha^2 + \zeta^2}. \tag{4.33}$$

At the leading front at point C $\Delta y_\alpha^{(1)} = \tau' h''(0)$. If the reconnection starts gradually, $h''(0) = 0$, then the FR-region should propagate without dissipation, with the outer surface of the FR-region having a characteristic nose at point C (see (4.17) and Figure 2.3).

Let us now consider the role of the dissipation in more detail. In the stationary case, the only one treated by many authors (Sweet, 1958; Parker, 1963; Petschek, 1964; Cowley, 1975; Vasyliunas, 1975; Soward and Priest, 1977, 1982), the main question is what the plasma conductivity should be to provide the reconnection, or, in other words, what the relation between the basic parameters of the problem should be (i.e. the Alfvén Mach number ε and the magnetic Reynolds number Re_m) to make the reconnection possible.

It is in principle clear how to find such a relation between ε and Re_m. The solution of the MHD-equations including the dissipative effects should be constructed in the vicinity of the singular points and lines, and then it should be joined with the solution of the ideal magnetohydrodynamics. Unfortunately, in such a formulation the problem is not solved, and only some estimates of the sought relation are available so far. We

consider briefly the estimations obtained by Petschek (1964) and by Vasyliunas (1975), which can be generalized for the time-dependent case. The main idea of their approach is the following. The first-order approximation perturbation of the magnetic field $B_x^{(1)}$ (3.25b) is opposite in direction to the initial field B_0 and increases when moving to the origin of coordinates. Thus, the summary field equals zero on the y-axis at some distance l from the origin. If the size of the diffusion region estimated by L/Re_m is less than l, a zero magnetic point appears there, and, in addition, the electric current in the diffusion region is opposite to the electric field applied, which may be easily proved by the circulation theorem. Because the current in the diffusion region should be parallel to E_0, so l is the minimum size of the diffusion region. Equating l and L/Re_m, one obtains the relation between the reconnection rate (as traditionally the Alfvén Mach number is called) and the magnetic Reynolds number Re_m. To improve the estimation, it is necessary to estimate the size of the diffusion region and the magnetic field on its boundary as exactly as possible. Thus, the following estimation has been obtained:

$$1 \geqslant k\varepsilon \ln \varepsilon \, \mathrm{Re}_m, \tag{4.34}$$

where $k = 8/\pi$ (Petschek, 1964; Vasyliunas, 1975). In the compressible plasma $k = \pi\gamma/4(2\gamma - 1)$ when $\beta \ll 1$, $M \ll 1$, and $k = \pi\gamma/3(2\gamma - 1)$ when $\beta \gg 1$, $M \gg 1$; where γ is the ratio of specific heats, $\beta = 8\pi p_0/B_0^2$ is the pressure ratio, and M is the Mach number (Soward and Priest, 1982).

A different approach to this problem is possible on the basis of the following consideration. A reconnection process can be decomposed into two parts. First of all, an electric field must be created someway in the diffusion region, this field will control all the properties of the reconnection phenomena (see Section 4.1). At the next stage this electric field must be transferred into the surrounding medium by the Alfvén wave, which is fed by the field-aligned currents (Figure 2.2a). A maximum intensity of these currents (and, hence, of the transferred electric field) can be obtained in case all the current flowing within the diffusion region is deflected via field-aligned currents of the Alfvén wave. This limiting value of total current available is clearly related to the size of the diffusion region.

A linear current density in the diffusion region J is given by

$$\tfrac{1}{2}J(\tau') = 1 + \varepsilon B_x^{(1)}(\tau', 0, 0), \tag{4.35}$$

where $B_x^{(1)}$ is the first-order approximation of the x-component of the magnetic field in the inflow region. Following Petschek (1964), let B_y to change linearly with the scale x_d in the diffusion region. This results also in smooth behavior of both $y_\alpha^{(1)}$ (see (4.31)) and $B_x^{(1)}$ (see (4.32)). Physically, J may change between 2 (no reconnection yet possible) and 0 (all current is deflected into the Alfvén wave current system). From this we can obtain an estimation of maximum possible reconnection rate versus the scale of the diffusion region x_d. By using (4.31), (4.32) and (4.35) we have:

$$1 + \frac{\varepsilon}{\pi} \int_{-\tau'}^{\tau'} \frac{(\alpha - \eta) y_\alpha^{(1)}(\tau', \eta, 0)\, \mathrm{d}\eta}{(\alpha - \eta)^2 + \zeta^2} \geqslant 0. \tag{4.36}$$

From here, by neglecting the quantities of the order of $\max\{\varepsilon; (x_d/\tau')\ln(x_d/\tau')\}$, a limiting value of the electric field transferred by the Alfvén wave is

$$|h'(t')| \leqslant \pi/4 \ln(\tau'/x_d), \tag{4.37}$$

or, in the dimensional form:

$$E^*(t) \leqslant \frac{\pi B_0^2}{4c(4\pi\rho_0)^{1/2} \ln(V_a t/x_d)}, \tag{4.38}$$

$$B_y(t) \leqslant \pi B_0/4 \ln(V_a t/x_d), \tag{4.39}$$

where $B_y(t)$ is the reconnected magnetic field at the boundary of the diffusion region.

In a stationary case x_d must be replaced by $L/\varepsilon\,\mathrm{Re}_m$ and $V_a t$ by the characteristic scale L. Then (4.39) yields the Petschek condition (4.34) with $k = 4/\pi$.

In the stationary case both main parameters ε and Re_m are given; then it follows from (4.32) that the stationary reconnection may take place only when (a) the electric field applied is small enough, (b) the initial magnetic field is strong, and (c) the plasma conductivity is low. If the Petschek condition is not fulfilled, the system stays in a non-stationary state (see Vasyliunas, 1975). That state, as we have seen in Section 2, is characterized by magnetic energy accumulation. In such conditions, the magnetic field increases, ε decreases, and at some instant the Petschek criterion (4.32) is satisfied. Thus, the Petschek condition determines the steady-state reconnection threshold.

It is interesting to discuss the mixed solutions obtained in Section 2 from this point of view. The constant k given by formulas (3.35) and (3.36) for the cases of two and four incoming discontinuities respectively can be shown to determine the reconnection threshold. It may be seen from (3.35) and (3.36) that incoming discontinuities with the antiparallel polarization ($I > 0$) cause the thresholds to decrease in comparison with the Petschek model ($I = 0$), and therefore they stimulate the reconnection process. On the contrary, in the case of parallel polarization ($I < 0$), the threshold increases and becomes infinite when $I = -\frac{1}{2}$. The solution obtained by Sonnerup is the only one which gives $k = 0$ when $I = 2^{-1/2}$, i.e. the threshold equals zero; the reconnection is caused in that case by incoming discontinuity only without any dissipation.

It is worth now comparing the main features of the time-dependent and the stationary reconnection processes. In contrast to the stationary case, the spontaneous reconnection is a local process. Until the fast shock reaches the boundaries, reflects and returns back, the reconnection is completely determined by plasma properties in the diffusion region. For the stationary reconnection to take place, at least three conditions should be fulfilled:

(a) During the initial phase the magnetic field intensity has to amount to the value which is necessary to satisfy the Petschek condition (4.34).

(b) In the diffusion region, the steady-state conditions ($E(t) = \text{const.}$) have to exist for sufficiently long time.

(c) The boundary conditions correspond to the stationary state.

In reality the simultaneous realization of all these requirements seems to be unlikely.

That is why the reconnection proceeds in most cases as a nonstationary impulsive process.

5. Laboratory and Numerical Experiments

For the last several years the reconnection process has been investigated not only theoretically but also using the laboratory and numerical experiments.

Before giving an account of the main results of these investigations, we have to make the following remark: unfortunately, it is impossible to simulate an event precisely in its whole complexity in laboratory conditions. Therefore, the principle of limited simulation (Podgorny and Sagdeev, 1969), which allows a certain group of conditions to be simulated, is most often used. This means that an experiment has to be carried out in such a way that only those dimensionless parameters should be preserved which are of the order of unity in the real space phenomena, whereas for the parameters much smaller or much greater than unity only the signs of inequalities should remain the same. Thus, the laboratory simulation experiment is not a precise copy of the real phenomenon; rather, it is merely similar to it, to some extent. Because of that, a complex approach including theoretical, laboratory and numerical methods should be developed, for each way has its own merits and disadvantages. Only after having combined these methods can one produce a comprehensive description of the reconnection process.

Now, with that remark in mind, let us consider the laboratory results on the reconnection problem. First of all, the current sheet appears to develop if an electric field is applied along the neutral X-line of the magnetic field (Ohyabu and Kawashima, 1972; Baum and Bratenahl, 1974a, b, 1977; Frank, 1974; Kirii *et al.*, 1979; Bogdanov *et al.*, 1980; Stenzel and Gekelman, 1981; Gekelman and Stenzel, 1981). The accumulation of magnetic energy in the vicinity of the current sheet has been shown to depend on the following parameters: (a) The magnetic Reynolds number Re_m. If the conductivity of the plasma is low, no significant amount of the free energy can be stored. (b) The Alfvénic–Mach number Ma; this quantity has to be suitably small. If Ma exceeds a certain limiting value, an intermediate plasma configuration develops, instead of the current sheet (with respect to current sheet and cylindrical z-pinch) (Kirii *et al.*, 1979). (c) Ratio of the gas to magnetic pressure β; β has to be relatively small as well. For example, in experiments by Stenzel and Gekelman (1981) and Gekelman and Stenzel (1981) with a plasma having $\beta \sim 1$, the current sheet formed. However, no more that 20% of the energy which entered the system could be accumulated as free energy; the rest of the energy was spent in heating the plasma, mainly electrons (Stenzel *et al.*, 1982).

Thus, the laboratory experiments confirm as a whole the theoretical conclusions: to accumulate effectively the free magnetic energy in the vicinity of the current sheet, the following conditions are to be met: $\mathrm{Re}_m \gg 1$, $\beta < 1$, $\mathrm{Ma} < 1$. Free energy is accumulated the more effectively, the greater magnetic Reynolds number, the smaller the ratio of the gas to magnetic pressure and the greater the Alfvénic–Mach number are, though, as has been mentioned above, the latter has an upper limit value. All three conditions have a simple physical meaning. A greater Re_m corresponds to a smaller energy spent on the

Joule heating; the smaller β is, the easier can the magnetic field affect the plasma; and, finally, the greater Ma is, the greater is the rate of the energy input to the system.

As to the process of reconnection associated with the fast reconstruction of the magnetic field structure and magnetic energy release, it has been investigated in less detail, mainly because the process turned out to be highly time-dependent.

In the experiments by Baum and Bratenahl (1974a, b, 1977) on the double inverse pinch, the magnetic field was maintained by two parallel currents I flowing along two metal rods, and by a return current $2I$ flowing in the plasma along the outer envelope (see Figure 5.1a). At the beginning, during the first 7 ms a current sheet had developed at the X-line of the magnetic field, and then reconnection took place, which was observed as fast reconstruction of the magnetic field structure. Therefore this phenomenon was called an 'impulsive flux transfer event' (IFTE). The time scale of IFTE is shorter than that of the change of currents in the rods. On the other hand, when averaged in time, the distribution of the current density was similar to that in Petschek's model with the slow shocks (see Figure 5.1b).

The oscillograms of the magnetic field component normal to the current sheet (H_y) obtained for different points x along the sheet are shown in Figure 5.2 (experiments by Bogdanov *et al.*, 1980, with the quadrupole magnetic field). At the initial phase of the process the H_y-component decreased which correspond to the development of the current sheet. At some instant a fast increase of the H_y-component in the center of the current sheet was observed and then the disturbance moved out of the origin along the sheet with a velocity of the order of 6×10^6 cm s^{-1}, which approximately coincided with the Alfvén velocity $V_a = 6.5 \times 10^6$ cm s^{-1} calculated for the region above (but not inside) the current sheet. This behavior of the H_y-component is very similar to the time-dependent reconnection considered in Section 3.

Bogdanov *et al.* (1980) and Kirii *et al.* (1979) have pointed out that the time-dependent reconnection process takes place only when a sufficient amount of free magnetic energy is stored in the system. Just before the beginning of the reconnection, a drop of the plasma density has been observed, and, of great importance, a local increase of the plasma resisitivity near the neutral line has been detected. Baum and Bratenahl (1974b), who observed the local increase of plasma resistivity, ascribed this phenomenon to the development of the ion sound turbulence. Thus, according to these experiments the reconnection process seems to be due to the development of anomalous resistivity rather than to tearing instability.

It should be noticed that in the laboratory experiments the reconnection process is highly time-dependent, with a time scale of order of $t_0 = L/V_a$, where L the length of current sheet, due to the presence of device walls, impulsive regime and other reasons. For the majority of devices used $t_0 < 0.5$ ms and, hence, it is very difficult to investigate the reconnection expermentally. On the whole, the process observed by Baum and Bratenahl (1977) and Bogdanov *et al.* (1980) seems to be similar to the one described in Section 3; nevertheless, additional evidence is quite essential.

Now we shall discuss the results of numerical simulation. In contrast to laboratory experiments, stationary (or quasi-stationary) reconnection with standing slow shocks

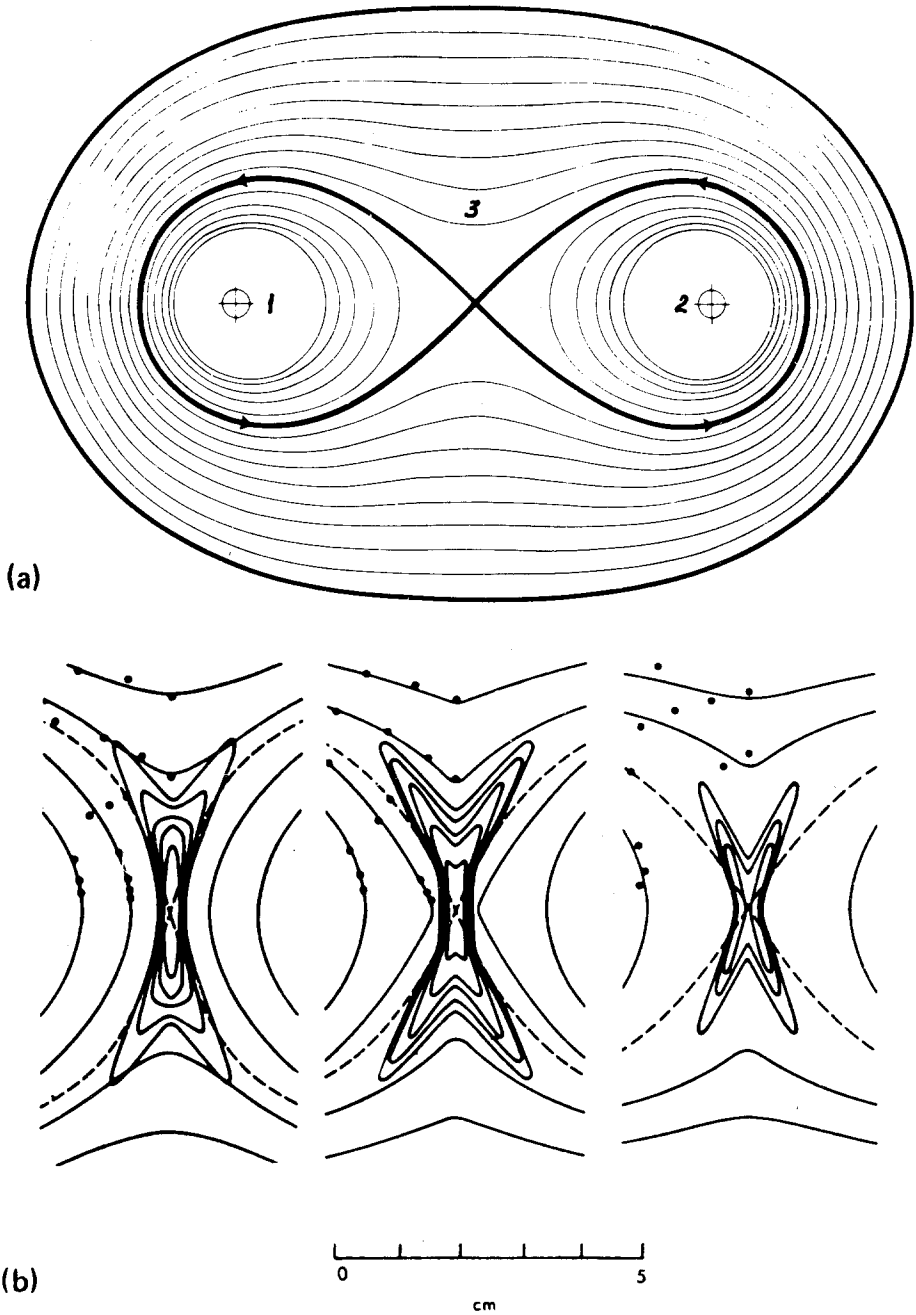

Fig. 5.1. Experiments on the double inverse pinch (Baum and Bratenahl, 1977). (a) The scheme of the installation. The solid lines show the equipotentials of the Z-component of the vector potential produced by a two-current system. The heavy solid line shows the separator (boundary between magnetic fields of two kinds). (b) Current density contours and magnetic field lines at the moments t = 7.0; 7.4; 7.8 ms (from the left to the right).

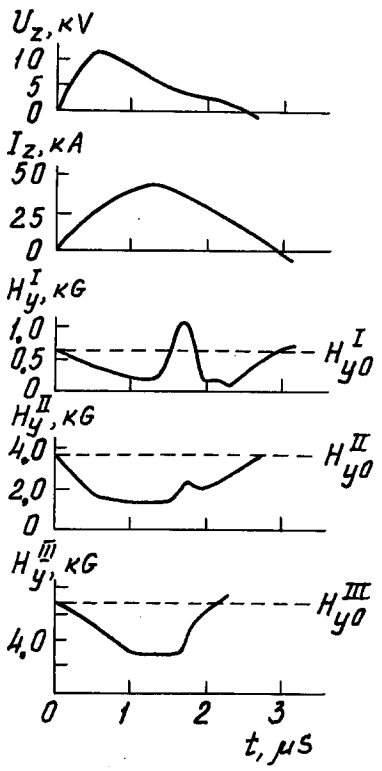

Fig. 5.2. Oscillograms of the electric voltage (U_z) on the plasma interval, of the current intensity (I_z) and of the magnetic field component perpendicular to the current sheet (H_y) obtained at three points spaced along the X-axis: $x_1 = 0.3$ cm; $x_2 = 1.9$ cm; $x_3 = 3.3$ cm. Conditions of the experiment: initial gradient of the magnetic field intensity $h = 2$ kG cm^{-1}; $p = 10^{-2}$ Torr, $E_z^0 = 250$ V cm^{-1}.

has been set in numerical simulation (Ugai and Tsuda, 1977; Tsuda and Ugai, 1977; Hayashi and Sato, 1978; Sato and Hayashi, 1979; Sato, 1979; Brushlinskii *et al.*, 1980; Podgorny and Syrovatsky, 1979; Ugai, 1981). These simulations confirm Petschek's assumption concerning the appearance of a slow shock system. This is of great importance, since the analytical methods are asymptotic and formal ones; using them does not provide any proof for the existence of solution.

In simulation by Sato and Hayashi (1979) and Sato (1979) formation of the shocks was investigated and it was proved that the shock was a slow one. The dependence of the numerical solution on different parameters such as conducitivity, viscosity, boundary conditions, etc. has been studied also. Unfortunately, space and time resolution is not yet sufficient to test the Petschek criterion.

The fast time-dependent reconnection has been studied in papers (Birn, 1980; Birn and Hones, 1981; Forbes and Priest, 1982, 1983). In these papers the tail magnetic field calculated by means of Birn–Schindler's method (see Section 2) has been adopted as an initial magnetic field configuration. Then a finite conductivity has been set up and the further evolution of the system has been investigated numerically. The current sheet

became thinner in the Earthward part and then a neutral line appeared there. Then the reconnection process started, with the formation of shocks and plasma acceleration by the induced electric field. The head fronts of FR-regions were not distinguishable, while parts of shocks near the X-line were clearly seen.

Based on laboratory and numerical simulation, one can make the same conclusions as from the results of theoretical investigation. By now the main regimes of the current sheet have been revealed, but the transitions between them require further studies. To do this it is necessary to carry out simulation at greater magnetic Reynolds numbers, with smaller ratios of gas to magnetic pressure, and to improve the temporal and spatial resolution.

6. Steady-State Solar Wind Flow Around the Magnetosphere

Results of the investigations presented in previous sections show that the field line reconnection can proceed in media with arbitrarily high conductivity and with an arbitrary jump of the magnetic field and plasma parameters at both sides of the reconnection region. The rate of reconnection is proportional to $(\ln \mathrm{Re}_m)^{-1}$; it is thus relatively high and provides sufficiently effective transformation of the magnetic field energy into the kinetic and thermal energy of the plasma. One would believe this circumstance to ensure the validity of the solar wind – magnetosphere interaction models that are based on the assumption of the reconnection of the geomagnetic field with the solar wind magnetic field. However, the problem is much more complicated. Indeed, as we have seen, the electric field providing the transport of the plasma to the merging region and its energization has to exist in the vicinity of the reconnection region in order that the process of reconnection could proceed. However, under steady-state conditions the electric field can by no means be a result of the magnetic field reconnection. Rather, it is an external parameter determined, in particular, by the peculiarities of the flow in the vicinity of the merging region, as well as by those at a significant distance from that region (Vasyliunas, 1975; Pudovkin *et al.*, 1975). Thus, to find the electric field in the vicinity of the reconnection region at the day side magnetopause, one has to know the structure of the plasma flow around the magnetosphere as a whole. At the same time, most of the nowadays-existing 'open' models of the magnetosphere are based on the pure geometrical (vacuum) superposition of the interplanetary and the Earth's magnetic fields, the features of the plasma flow being completely ignored. Then, assuming typical values of the solar wind parameters ($V = 400$ km s^{-1}, $B = 5\gamma$) and for the magnetosphere's diameter ($D_m = 40\ R_E$), the polar cap potential drop ($\Delta\phi$) proves to be of the order of 500 kV (Stern, 1977). However, such a large potential drop across the polar cap has never been observed, and indeed the observed drop seldom exceeds 100 kV; thus, the experimental data are at least 5 times less than the theoretical estimations. In order to have the model agree with the experimental data, some additional assumptions limiting the value of $\Delta\phi$ at the magnetopause are often introduced. For example, Levy *et al.* (1964) assume that only one-fifth of the magnetic field lines impinging on the magnetopause take part in the process of reconnection. The mecha-

nism for such selective behavior of the field lines at the magnetopause is not discussed in that paper. On the other hand, according to papers by Morfill and Scholer (1972), Siscoe and Crooker (1974), and Stern (1975), all the field lines entering the reconnection region are merging. However, these authors assumed that the process of reconnection takes place not over the whole magnetopause but only within a limited longitudinal sector. What the physical mechanism is that limits the length of the reconnection line is not clear; the width of the 'window' is estimated so that the potential drop along that line equals the potential drop across the polar cap. Thus, the physical significance of those models may hardly be estimated.

Second, the steady-state reconnection of the magnetic fields is possible only when the merging rate does not exceed the limit value $V_d = V_a/\ln \mathrm{Re}_m$. On the other hand, the Alfvénic Mach number is known to be of the order of $\mathrm{Ma}_\infty \approx 10$ in the solar wind, and even downstream the bow shock the flow continues to be super-Alfvénic. Whether the Petschek condition may be fulfilled closer to the magnetopause depends on the characteristics of the plasma flow in the magnetosheath, that is, on the peculiarities of the solar wind flow around the magnetosphere.

Thus, before trying to apply the theory of the magnetic field reconnection to the study of the processes of the interaction of the solar wind with the magnetosphere, one has to consider the problem of the MHD flow of the solar wind around the magnetosphere.

6.1. The Flow with an Isolated Stagnation Point

Solution of the system of the MHD equations (A1)–(A5) involves a fair number of difficulties that are insuperable at present. Because of that, while studying the flow of magnetized solar wind around the magnetosphere, researches introduce some simplifications into the system of the MHD equations, and first of all into the equation of motion (A1). This equation may be written in a dimensionless form as:

$$\frac{1}{V_0}\tilde{\rho}\frac{\partial \tilde{\mathbf{v}}}{\partial t} + \tilde{\rho}(\tilde{\mathbf{v}}\cdot\nabla)\tilde{\mathbf{v}} + \frac{P_0}{\rho_0 V_0^2}\nabla\tilde{P} = +\mathrm{Ma}^{-2}[\mathrm{rot}\,\tilde{\mathbf{B}}\times\tilde{\mathbf{B}}], \tag{6.1}$$

where the tilded variables mean dimensionless quantities, and $\mathrm{Ma} = V_d/V_a$ is the Alfvénic Mach number. Since the density of the kinetic energy of the plasma within the solar wind is much higher than the magnetic field energy, hence $\mathrm{Ma}^{-2} \ll 1$, the problem of the solar wind flow around the magnetosphere is often considered approximately by expanding all the variables in series with respect to the small parameter $\varepsilon = \mathrm{Ma}^{-2}$, and by using the linear theory of disturbance. In the zero-order approximation, the whole problem may be split into two separate problems: a pure hydro (gas) dynamic one, in which any influence of the magnetic forces is neglected and hydro(gas) dynamic characteristics of the flow (the plasma density, pressure, velocity) are sought, and a magnetic one, in which the distribution of the magnetic field is calculated on the basis of the known distribution of the plasma velocity and density.

This is the method by which the problem of the solar wind flow around the magnetosphere has been considered by Spreiter *et al.* (1966), Alksne (1967), and Spreiter and

Alksne (1967). However, while numerically integrating equation (A4), Spreiter and Alksne have found that in the case $\sigma \to \infty$ the magnetic field intensity increases infinitely on approaching the magnetopause. Because of that, solution of the problem was obtained only for a region at some distance from the magnetopause (Figure 6.1).

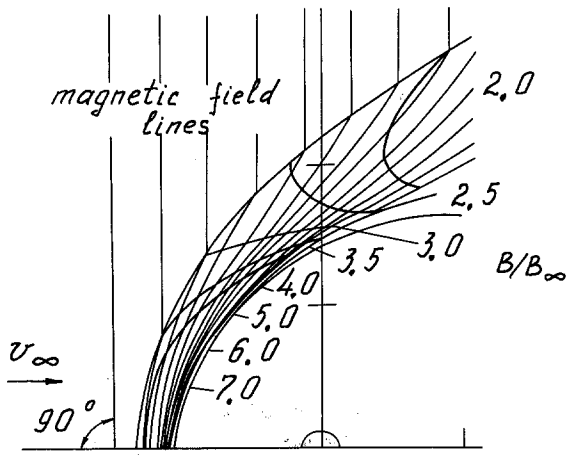

Fig. 6.1. Magnetic field line configuration and isolines of the magnetic field intensity in the magnetosheath (Spreiter *et al.*, 1966).

The physical meaning of such behavior of the magnetic field within the flow was considered by Pudovkin and Semenov (1977a, b), Semenov and Pudovkin (1978), and by Sonnerup (1979). Following them, we shall assume the solar wind plasma to be perfectly conductive. The solar wind magnetic field is assumed to be homogeneous at infinity and perpendicular to the velocity, and the flow of the plasma is assumed to be pure gas dynamic, that is, with a stagnation point at the 'nose' of the magnetopause (Figure 6.2).

The magnetic field intensity variation in a moving plasma is described by equation (A6). In the case $\sigma \to \infty$, this equation is transformed into the equation of the frozen-in magnetic field and may be written in the form:

$$(\mathbf{v} \cdot \nabla) \frac{\mathbf{B}}{\rho} = \left(\frac{\mathbf{B}}{\rho} \cdot \nabla \right) \mathbf{v}. \tag{6.2}$$

One can see from (6.2) that the mean value of (B/ρ) pertaining to some segment of a field line changes in proportion to the length of that segment.

Let us consider a segment AC of a field line situated at a distance r_0 from the stagnation stream line (Figure 6.2.). While moving with the plasma, that segment transforms to $A'C'$, $A''C''$, and so on. By that, the mean value of the (B/ρ) at the segment under consideration increases in accordance with (6.2) in proportion to the length of

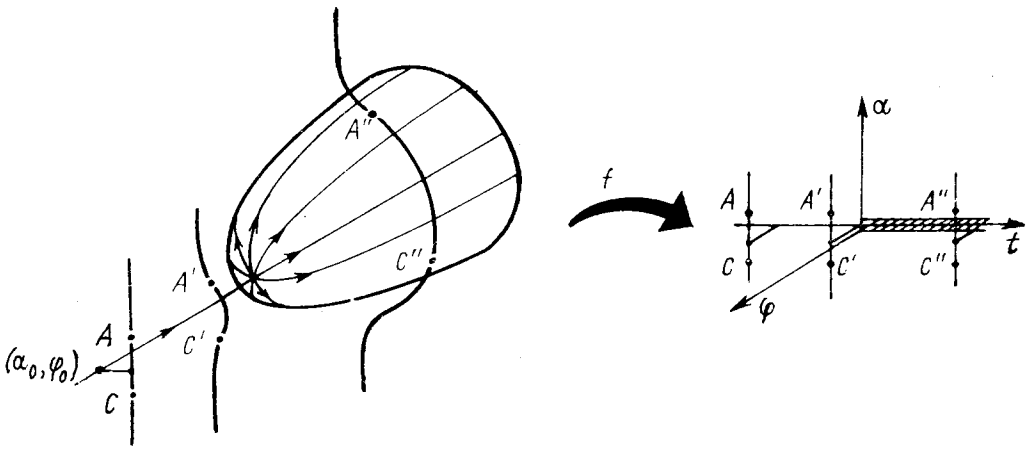

Fig. 6.2. Configuration of the stream lines and of the magnetic field lines in case of the solar wind flow around the magnetosphere with an isolated stagnation point; (a) in the physical space; (b) in the space of the parameters t, α, φ.

the segment:

$$\left(\frac{B}{\rho}\right)_1 = \left(\frac{B}{\rho}\right)_\infty \cdot \frac{A'C'}{(AC)_\infty}; \qquad \left(\frac{B}{\rho}\right)_2 = \left(\frac{B}{\rho}\right)_\infty \cdot \frac{A''C''}{(AC)_\infty} \approx \left(\frac{B}{\rho}\right)_\infty \cdot \frac{D_m}{2r_0}, \tag{6.3}$$

here D_m is the diameter of the magnetosphere at section $A''C''$. It is not difficult to see that at the very surface of the magnetosphere, the value of the 'impact parameter' r_0 of corresponding stream lines tends to zero; as the consequence, the value of (B/ρ) tends to infinity; and that is why Spreiter and Alksne have obtained their inauspicious result.

The relation between the value of (B/ρ) and the length of the field line has been illustrated in a sufficiently explicit form by Parker (1973). As we have already said, that paper contained an investigation of the flow of two encountering streams of a highly conductive incompressible fluid spreading over the plane of contact so that the stream lines were lying in the $(\mathbf{V}_\infty, \mathbf{B}_\infty)$ plane (Figure 6.3). A strict solution of the problem gives $\mathbf{V}(x, z) = k(-x\mathbf{e}_x + z\mathbf{e}_z)$ (see Section 2.2), where k is constant and the Z-axis is directed along the B field. Thus, the length of segment AC of the magnetic field line and, hence, the magnetic field intensity, are proportional to $1/x$.

In the case when the streams spread over the encounter plane in the Y-direction (that is perpendicular to the magnetic field), field lines are not stretched and the magnetic field intensity does not change (Priest and Sonnerup, 1975; Sonnerup and Priest, 1975).

A solution of the problem under consideration (in a kinematic approximation) for a sphere immersed into a stream of a perfectly conductive fluid, with a frozen-in magnetic field transversal with respect to $\mathbf{V}$, was obtained by Bernikov and Semenov (1979). According to that solution, in the case when the flow preserves the peculiarities of a pure hydrodynamic flow, the magnetic field intensity at the surface of the sphere may be

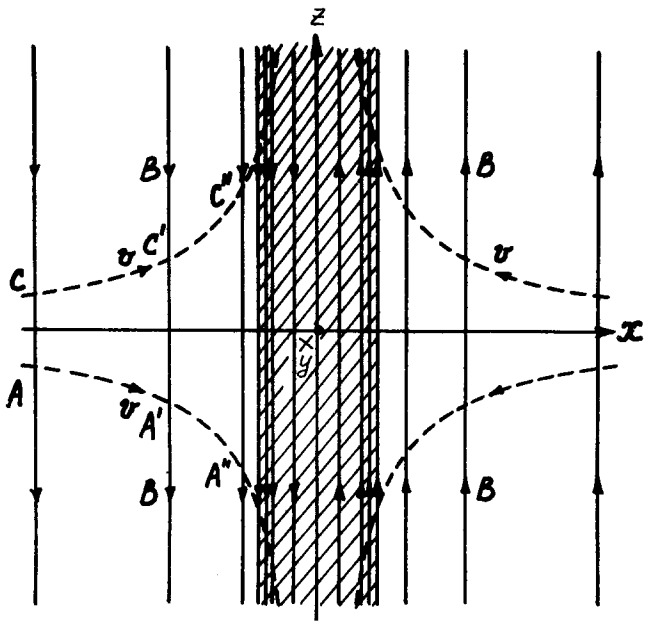

Fig. 6.3. Configuration of the magnetic field lines (solid lines) and of the stream lines (dotted lines) in Parker's (1963) solution.

written as:

$$B_r = \tfrac{2}{3} B_\infty \sqrt{3S}\, \frac{\sin\theta}{1+\cos\theta} \sin\varphi,$$

$$B_\theta = \frac{B_\infty \sin\varphi}{\sqrt{3S}},$$

$$B_\varphi = \frac{B_\infty \cos\varphi}{\sqrt{3S}}. \tag{6.4}$$

Here $s = (r - r_0)/r_0$ is the dimensionless distance from the surface of the body, θ is the angle measured from the polar axis passing through the stagnation point, and φ is the azimuthal angle counted from the meridional plane which is perpendicular to the magnetic field B_∞. Formulas (6.4) show that, indeed, the magnetic field intensity increases infinitely while approaching the surface of the body; this result seems to deprive that solution of a real physical meaning.

The way out of this situation was proposed by Parker (1973). According to the analysis presented in that paper, the increase of the magnetic field intensity takes place only beyond some distance from the body surface. At sufficiently small distances, $x \leqslant \delta = a/(\mathrm{Re}_m)^{-1/2}$ (where 'a' is a characteristic dimension of the problem), the gradient of the magnetic field intensity turns to be so high that the last (diffusion) term

in Equation (A.6) cannot be neglected; as a consequence, the field lines are 'slipping' through this region, and the field intensity is no longer increasing.

Unfortunately, the fact that the solution of (6.4) is valid only outside the boundary layer does not improve the situation in the problem of the solar wind flow around the magnetosphere. Indeed, the width of the boundary layer determined by the value of the magnetic Reynolds number ($\mathrm{Re}_m \approx 10^{10}$ in the case under consideration) is rather small, so that the magnetic field intensity must be significantly high even at the external boundary of that layer. For example, having assumed the value of s in (6.4) to equal $s = \delta/r_0 = 1/\sqrt{\mathrm{Re}_m} \approx 10^{-5}$, one obtains the value of the magnetic field intensity at the outer surface of the boundary layer as $B \approx B_\infty/\sqrt{3s} \approx 200\, B_\infty$.

It is not difficult to see that the results obtained contradict the initial assumption that the Ampère forces are sufficiently small so that the kinematic approximation could be valid. As we have seen, the unequality $\mathrm{Ma}^{-2} \ll 1$ changes its sense well before plasma entering the boundary layer, so that magnetic forces are playing a predominant role in the equation of motion (6.1). In contrast to the gas pressure forces, magnetic forces are strictly perpendicular to the magnetic field, and as a consequence, are greatly anisotropic. In particular, if the magnetic field components in the vicinity of the magnetopause are determined by (6.4), the tangential components of the Ampère forces are:

$$F_\theta = \frac{B_\infty^2}{3r_0 S}(1 - 2\sin^2\varphi)\cdot\frac{\theta}{2},$$

$$F_\varphi = -\frac{B_\infty^2}{3r_0 S}\sin^2\varphi\cdot\frac{\theta}{2}. \tag{6.5}$$

One can see from these formulas that magnetic forces decelerate the plasma motion along the meridian $\varphi = \pm\pi/2$ and accelerate it along the meridian ($\varphi = 0; \pi$), so that the plasma flow around a blunt body tends to be a quasi-two-dimensional. It is worth noting that the flow keeps a quasi-two-dimensional character in a more general case also (Semenov and Bernikov, 1979). Thus the assumption that the flow of a highly conductive plasma around a blunt body preserves the structure of the pure gas dynamic flow in the pressure of a magnetic field also seems to be not only poorly grounded but rather unlikely on the whole.

Influence of the magnetic field on the plasma flow was considered by Lees (1964), Pivovarov and Erkaev (1978) for the case of $\mathbf{B}_\infty \| \mathbf{V}_\infty$, and by Zwan and Wolf (1976) and by Pivovarov and Ekraev (1978) for the case of a magnetic field of arbitrary direction. It has to be noted that in all those studies the plasma flow was supposed to proceed with an isolated stagnation point as it does in pure gas dynamics. As a result, there was shown that the singularity found by Alksne and Spreiter in the magnetic field intensity refers in the general case to the ratio of B/ρ, which agrees with the results by Pudovkin and Semenov (1977a) and by Sonnerup (1979). Thus, a solution for a limited magnetic field intensity may be obtained; however, in such a case, the plasma density at the surface of the body has to tend to zero, as if the magnetic field, increasing as it approaches the body, drives the plasma away from its surface.

From the pure mathematical point of view, such a solution may be satisfactory; however, it seems to be unlikely for physical reasons. Indeed, in a low-density plasma, the electric current density is known to be limited by the value of $j_{cr} \approx C_s ne$, where C_s is the velocity of the ion sound ($C_s \approx \sqrt{kT_e/m_i}$). As a result, a very low density plasma with $n \to 0$ cannot bear the current providing the jump of the magnetic field existing at the magnetopause. Thus, the final result of the calculations – $\rho \to 0$, and hence $j_{cr} \to 0$ – contradicts the initial assumption about the perfect conductivity of the plasma. A quite opposite result was obtained by Shen (1972). Having considered a two-dimensional problem of a cylindrical body flowed by a stream of highly conductive magnetized plasma (with $\mathbf{B}_\infty$ non-parallel to $\mathbf{V}_\infty$), Shen obtained a solution in which the magnetic field intensity at the magnetopause was limited; in spite of that, the plasma density did not vanish and even increased while approaching the magnetopause. However, his result may be explained by his very particular choice of the coordinate system. Because of that coordinate system, he had to exclude the points at the subsolar stream line and near the stagnation point from his numerical computation.

So, as we have seen, most of the existing solutions of the problem bring one to unsatisfactory conclusions: the value of B/ρ has to increase rapidly towards the magnetopause, and, what is more, such an increase has to take place not only in the vicinity of the stagnation point (which would be quite understandable and admissible), but along the whole magnetopause, which seems to disagree with the experimental data.

As was shown above (Figure 6.2), the singularity in the behavior of the function (B/ρ) near the magnetopause arises from the assumed topology of the flow with a stagnation point. At the same time, Figure 6.2 shows that for an acceptable solution to be obtained, the flow has to proceed in such a way that the stream lines enveloping the flanks of the magnetopause do not pass the stagnation point, or that, in accordance with the conclusions by Priest and Sonnerup (1975) and Sonnerup and Priest (1975), the plasma spreads along the magnetopause perpendicularly to the magnetic field. The flow topology meeting those demands was considered by Pudovkin and Semenov (1977a, b) and by Semenov and Pudovkin (1978). As follows from their analysis, a magnetic field, frozen in the solar wind plasma, changes the flow of the latter in such a manner that instead of a stagnation point, there appears at the 'nose' of the magnetopause a whole line of singular points where the stream lines are branching.

The existence of such a branching line was later shown by Erkaev (1981) on the basis of a strict solution of the MHD equations for the case of the stream of a perfectly conductive magnetized plasma flowing around a cone. According to that solution, the magnetic field, the intensity of which increases up to values of the order of $\sim\sqrt{8\pi p_T}$, affects the flow so that stream lines are branching not only at the vertex of the cone, but also at a whole ensemble of points producing a line (Figure 6.4), which agrees with the results by Pudovkin and Semenov (1977a, b) and by Sonnerup (1979).

In a two-dimensional case (for example, in the problem by Parker–Priest–Sonnerup), that branching line (or a separator, according to Sonnerup *et al.*, 1981) turns in to an usual stagnation line ($V = 0$). In a three-dimensional case, the plasma velocity along that line may differ from zero (Semenov and Pudovkin, 1978; Erkaev, 1981). Nevertheless,

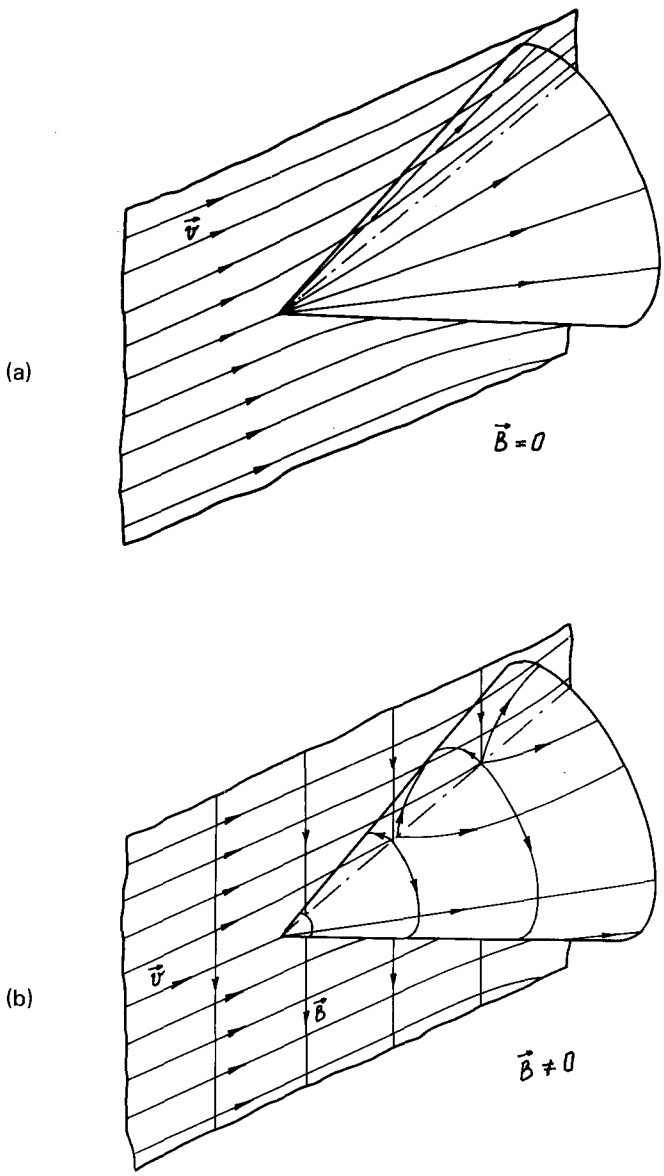

Fig. 6.4. The flow of a perfectly conductive plasma by a conus; (a) in case of $B = 0$; (b) in case of $B \neq 0$, after Erkaev (1981).

taking into account the coincidence of the main pecularities of the flow topology in the two cases and their evolutionary similarity, we shall use the term 'stagnation line' in a three-dimensional case as well (Pudovkin and Semenov, 1977b; Sonnerup 1979).

Now we shall consider characteristics of the flow predicted by the model with a stagnation line.

6.2. THE FLOW WITH A STAGNATION LINE

When the body is axially symmetric, and, at infinity, the magnetic field frozen in the plasma is perpendicular to the velocity, the flow has two planes of symmetry. Consequently, two modes of the flow are possible, corresponding to the cuts lying in the plane $(\mathbf{V}_\infty, \mathbf{B}_\infty)$ or in the plane perpendicular to $\mathbf{B}$.

The first variant (a longitudinal stagnation line) is shown in Figure 6.5 ((a) in the physical space and (b) in the space of parameters t, α, φ (see Appendix)). As is seen from the figure, the stream lines are lying in a plane perpendicular to the magnetic field. The stretching of field lines is finite in this case, hence the mean value of B/ρ at the magnetopause is also limited and equals, as is seen from the figure, $(B/\rho)_m \approx (B/\rho)_\infty \cdot D_m/L_\infty$, where D_m is the diameter of the magnetosphere and L is the distance (in the undisturbed flux) between two extreme stream lines forming the magnetosphere's surface in its meridional section. The intensity of the tangential component of the electric field at the magnetopause and, as a consequence, the potential drop along it, equal zero, which agrees with the results by Sonnerup and Priest (1975) for a transversal flow of the fluid.

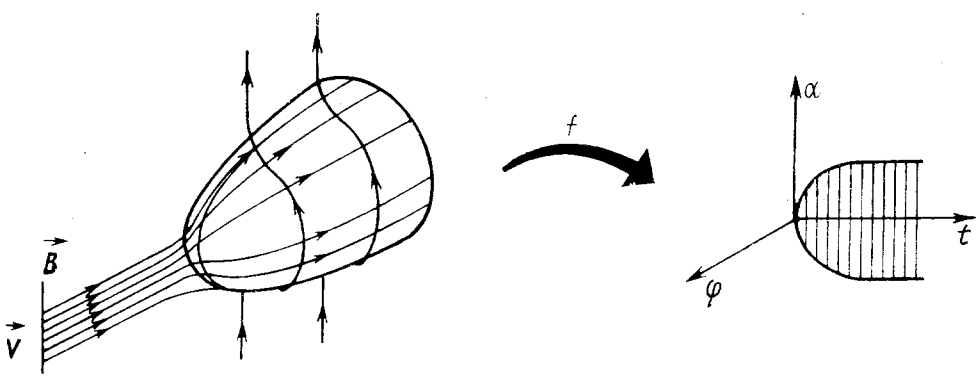

Fig. 6.5. Configuration of the stream lines and of the magnetic field lines in case of the solar wind flow around the magnetosphere with a longitudinal stagnation line. (a) in the physical space; (b) in space of parameters (t, α, φ).

The flow with a transversal stagnation line is shown in Figure 6.6. In this case the flow spreads around the magnetopause mainly along magnetic field lines, the flanks of the magnetosphere being covered by the stream lines passing two tips of the stagnation line instead of a single stagnation point. So, the value of r_0 in Equation (6.3) cannot be less than $L/2$; because of that, the mean value of (B/ρ) at the flanks of the magnetopause is limited and as in the previous case equals

$$(B/\rho)_m \approx (B/\rho)_\infty \frac{D_m}{L_\infty}.$$

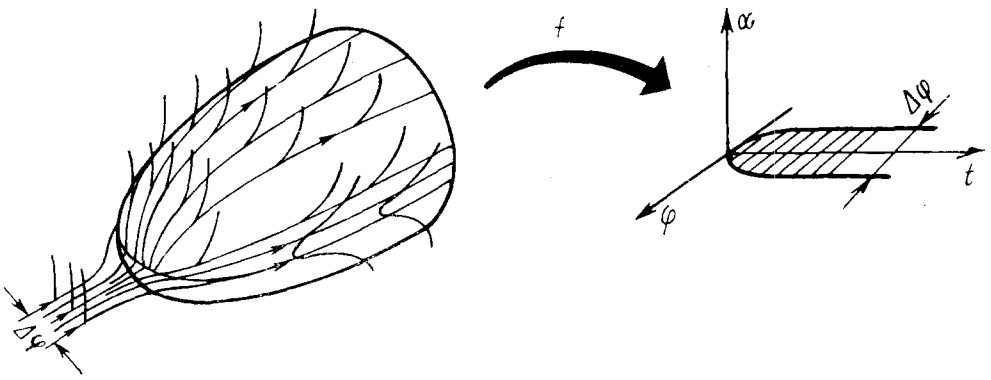

Fig. 6.6. The same as in Figure 6.5 in the case of a flow with a transversal stagnation line.

The behavior of the magnetic field where the stream lines cross the stagnation line is more complicated. Concerning the field line segments moving above and below the plane of the cut, their stretching, and hence the mean value of B/ρ at them, remain finite (see, e.g., the solution obtained by Shen, 1972). At the same time, the field line segments crossing the stagnation line, still exhibit an infinite stretching, and the value of B/ρ should infinitely increase there. However, as we have seen in the case of the Parker flow, this increase is limited by dissipative processes within the boundary layer, which allows one to obtain a finite solution all over the magnetopause. It is of great importance that the configuration of the magnetic field lines be favorable for the process of magnetic field reconnection. In such a case, the magnetic field intensity described in the frame of Petschek's model amounts to a much smaller values than in case of Ohmic dissipation is the Parker model. The concrete value of the ratio (B/ρ) is determined by the pecularities of the plasma flow in the reconnection region, and will be considered later on.

Figure 6.6 shows two more features of the flow with a transversal stagnation line. First, the potential drop at the magnetopause does not vanish and equals

$$\Delta\phi = \frac{1}{c}([\mathbf{v}_\infty \times \mathbf{B}_\infty] \cdot \mathbf{L}_\infty) \tag{6.6}$$

so $\Delta\phi$ depends on the length of the stagnation line which, in its turn, is determined by the parameters of the flow and of the frozen-in magnetic field.

Second, the existence of a tangential component of the electric field under the condition $V_m \neq 0$ suggests the existence of the normal component of the magnetic field at the magnetopause. The rate of the magnetic flux penetration into the magnetosphere is

$$\mathrm{d}F/\mathrm{d}t = B_\infty \cdot V_\infty \cdot L_\infty . \tag{6.7}$$

Thus, the day side magnetopause turns out to be transparent for the magnetosheath's magnetic field.

The penetration of the solar wind magnetic field into the magnetosphere was proved experimentally by Kovner and Feldstein (1973).

Which of those two kinds of flow takes place in reality? As we have seen, in the case with a longitudinal stagnation line, the stretching of the field lines in the vicinity of the stagnation line is rather small, so that the energy loss of the stream flowing around the magnetosphere is minimum. Because of that, one can suppose that in the case of the northward IMF, the flow proceeds with a longitudinal stagnation line.

In the case of the southward interplanetary magnetic field, the picture is much more complicated. The IMF turning to the south causes an increase of the magnetic field jump and, hence, of the current density at the magnetopause. On the other hand, it is not difficult to show that even in the absence of the solar wind magnetic field, the current density at the magnetopause is close to the critical one corresponding to the development of the wave turbulence in the plasma. Indeed, in the absence of the solar wind magnetic field, the jump of the magnetic field across the magnetopause in the vicinity of the subsolar point is equal to

$$\{B\} = B_i = \frac{4\pi}{c} nev_e \cdot \delta, \tag{6.8}$$

where B_i is the magnetospheric magnetic field, δ is the thickness of the current layer, and n and V_e are the number density and current velocity of the electrons in that layer, respectively. According to the experimental data by Sonnerup (1981), the thickness of the current layer near the subsolar point is of the order of some gyroradii of energetic protons in the magnetosheath. The critical value of the electron velocity cannot exceed the value of $C_s = \sqrt{kT_e/m_i}$, so the critical jump of the magnetic field intensity is:

$$\{B^2\}_{\text{cr}} \approx 8\pi n m_i c_s^2 \approx 4\pi p_T, \tag{6.9}$$

where p_T is the thermal plasma pressure. At the same time, the pressure balance at the magnetopause requires that

$$B^2 = 8\pi p_T. \tag{6.10}$$

Having compared expressions (6.10) and (6.9), one can see that the current density at the magnetopause is close to the critical one even in absence of the IMF. The appearance of a southward magnetic field within the solar wind is followed by the increase of the magnetic field's jump at the magnetopause, which results in the development of plasma instabilities in the current sheet, in the violation of the magnetic field screening and in a sporadic beginning of the magnetic field reconnection at the magnetopause. Then the character of the plasma motion in the boundary layer changes significantly and the flow transforms into one with a transversal stagnation line. In its turn, the flow with the transversal stagnation line results in the existence of an electric field directed along that line, which stimulates and promotes the process of reconnection and permits it to proceed in a steady-state regime. The steady-state character of the reconnection is favored by the fact that the enhanced intensity of the magnetic field at the

magnetopause secures the fulfilment of the inequality $V_d \leqslant V_a(\ln \mathrm{Re}_m)^{-1}$ predicted by Petschek's model.

So, it seems reasonable to combine the peculiarities of the flow considered above with the boundary conditions predicted by the reconnection theory. Such an investigation was carried out by Pudovkin *et al.* (1981a, b, c) in the cold plasma approximation. As the result, it proved to be possible to estimate such parameters of the problem as the intensity of the magnetic field in the magnetosheath and in the magnetosphere near the subsolar point at the magnetopause, the intensity of the electric field and the potential drop across the magnetosphere, the geocentric distance of the magnetopause, and the location of the polar cusps relative to the solar wind parameters. The results obtained are confirmed by experimental data.

In spite of the extreme simplification of the model used in that investigation, it contained all the main features of the assumed process of the interaction of the solar wind with the Earth's magnetosphere: the increase of the magnetic field intensity at the magnetopause; the appearance of a stagnation line; the penetration of the magnetosheath's magnetic field into the magnetosphere; and the reconnection of the magnetic fields of the solar wind and of the Earth. The coincidence of the experimental and theoretical data may be considered as confirmation of the basic assumption of the model.

A great advantage of that model is that the dependence of the quantities mentioned on the values of the solar wind parameters may be described analytically, and this permits one to obtain easily these quantities under various conditions. However, the cold plasma approximation does not allow one to obtain the gas dynamic parameters of the solar wind plasma in the magnetosheath.

The interaction of the solar wind with the Earth's magnetosphere, taking the thermal plasma pressure into account, was considered by Pudovkin *et al.* (1982). In accordance with the above, in that analysis it was assumed that:

(1) The magnetic field frozen in the solar wind plasma changes the topology of the flow in the magnetosheath so that instead of an isolated stagnation point a stagnation line appears at the 'nose' part of the magnetopause; its direction is determined by the orientation of the magnetosheath's magnetic field as (Yeh, 1976):

$$\operatorname{tg}\varphi = \frac{-3 \pm \sqrt{9 + 8\operatorname{tg}^2\theta_m}}{2\operatorname{tg}\theta_m} \quad \begin{array}{ll} (+) \text{ if} & 0 \leqslant \theta_m < \pi/2, \\ (-) \text{ if} & \pi/2 < \theta_m \leqslant \pi, \end{array} \tag{6.11}$$

where φ is the angle (in the YZ plane) measured clockwise from the Z-axis of the solar-magnetospheric coordinate system to the stagnation line (Figure 6.7); θ_m is the angle between the Z-axis and the B_m-vector; in the general case, the angle θ_m may differ from θ_∞ in the undisturbed solar wind; index 'm' marks the values of the variables at the magnetopause, and $\mathrm{Ma}_m = 0.1$–0.2 (Petschek, 1964).

(2) Stream lines passing the stagnation line are straight lines parallel to each other all through the sheath. In such a case, Equation (6.2) for the frozen-in magnetic field

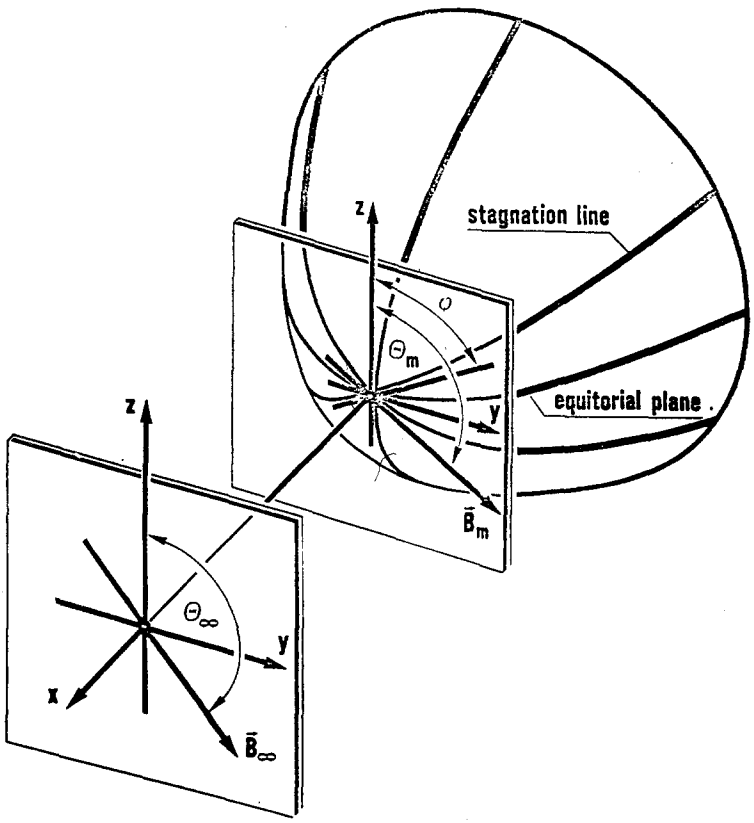

Fig. 6.7. Coordinate systems used for calculations in the case of the IMF of arbitrary orientation.

may be

$$B_{\parallel}/\rho = \text{const.} \tag{6.12}$$

for the magnetic field component parallel to the stagnation line, and

$$B_{\perp} \cdot V = \text{const.} \tag{6.13}$$

for the magnetic field component perpendicular to it.

(3) The boundary condition for the normal component of solar wind velocity at the magnetopause is determined by the Petschek condition:

$$v_m = \text{Ma}_m \frac{B_m \sin(\theta_m - \varphi)}{\sqrt{4\pi\rho_m}}, \tag{6.14}$$

where $\text{Ma}_m = 0.1$–0.2 is the Alfvénic Mach number.

However, even when these assumptions are accepted, solution of the system (A1)–(A5) is a very difficult problem. In this connection, the region of the flow under

consideration was restricted to the immediate vicinity of the stream line passing the subsolar point. Besides, it was assumed, as in the Parker (1973) model, that the flow velocity within the magnetosheath depends linearly on the distance from the magnetopause, and the curvature radius of the magnetic field lines was supposed to equal their geocentric distance.

On these assumptions, the system of Equations (A1)–(A5) can be integrated. Results of the analysis are presented below.

Figure 6.8 shows the variation of the plasma density across the magnetosheath for different directions of the IMF (θ_∞) in the case Ma = 8. As the graphs show, in the case of a predominatingly northward magnetic field ($\theta_\infty < 60°$), the plasma density monotonically increases all through the magnetosheath from the bow shock to the magnetopause. This situation corresponds to the case of a pure gas dynamic flow around a blunt body.

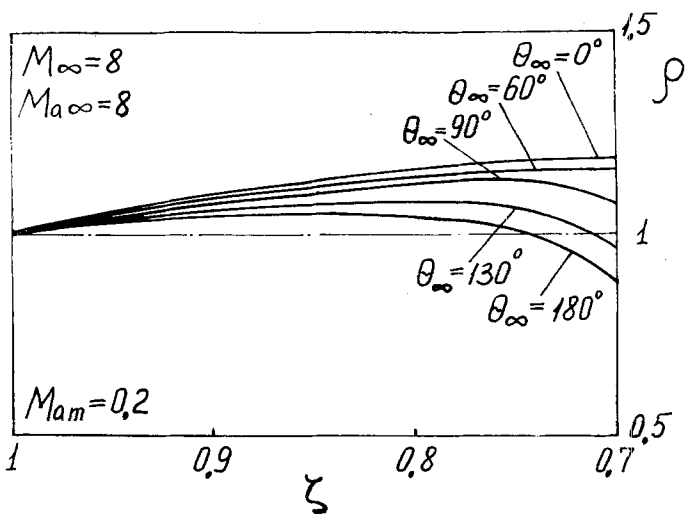

Fig. 6.8. Variation of the plasma density across the magnetosheath for various directions of the IMF.

In the case $\theta_\infty > 60°$, the behavior of the plasma density is rather complicated: first the value of ρ slightly increases; then, while approaching the magnetopause, it rapidly decreases, so that a region of a relatively low density plasma appears at the surface of the flown body. This result perfectly agrees with earlier results by Lees (1964), Zwan and Wolf (1976), Pivovarov and Erkaev (1978). The plasma density does not drop to zero because the flow velocity at the outer boundary of the reconnection region is supposed to be nonzero.

In contrast to the plasma density, the magnetic field intensity is shown to increase all through the magnetosheath irrespective of the IMF direction.

Figure 6.9 shows the normalized values of the plasma density at the magnetopause for $Ma_m = 0.2$ depending on the orientation of the IMF for various values of the

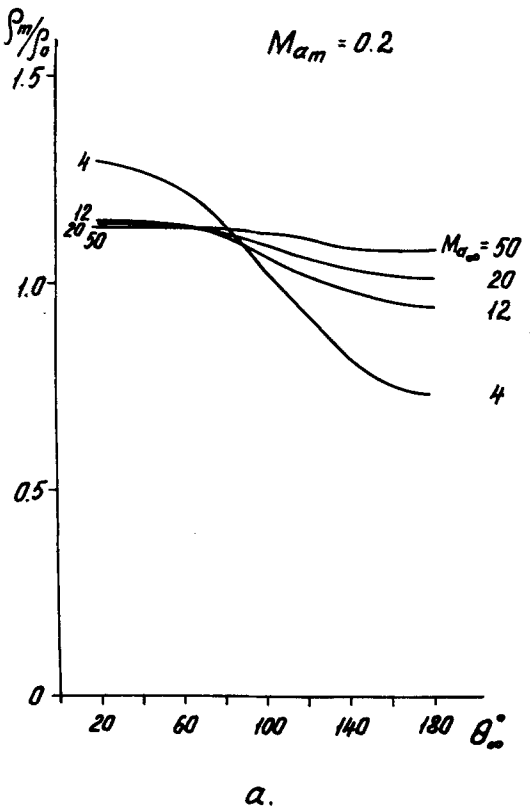

Fig. 6.9. The value of the plasma density normalized to the plasma density at the bow shock in dependence on the IMF orientation (θ_∞) for various Alfvénic Mach numbers Ma in the solar wind; $Ma_m = 0.2$.

Alfvénic Mach number in the solar wind. One can see in the figure that when $\theta_\infty < 60°$, the plasma density at the magnetopause differs insignificantly from that at the bow shock; only in the case of a very intensitive magnetic field ($Ma_\infty = 4$), $(\rho_m/\rho_0) = 1.3$ instead of 1.1 in a pure gas dynamic flow.

For $\theta_\infty > 60°$, the plasma density at the magnetopause decreases with the increase of the angle θ_∞, with the depth of the density depression increasing with the decrease of the Ma_∞ number.

Figure 6.10 presents the normalized intensity of the magnetic field at the magnetopause ($\beta_m = B_m/\sqrt{4\pi\rho_\infty V_\infty^2}$) depending on the θ_∞ angle and on the Ma_∞ number for $Ma_m = 0.2$. One can see that when Ma_∞ is of the order of 10 (which is typical for the solar wind), the intensity of the magnetic field at the magnetopause amounts to the value $B_m \approx (0.4\text{–}0.8)\sqrt{4\pi p_{d,\infty}}$ which is 5–10 times more than in the undisturbed solar wind. This result agrees with the experimental data by Reiff *et al.* (1981) and Crooker *et al.* (1981) concerning the degree of the magnetic field compression in the magnetosheath.

Furthermore, one can see that the magnetic field intensity at the magnetopause depends on the orientation of the IMF, increasing with the increase of the angle θ_∞.

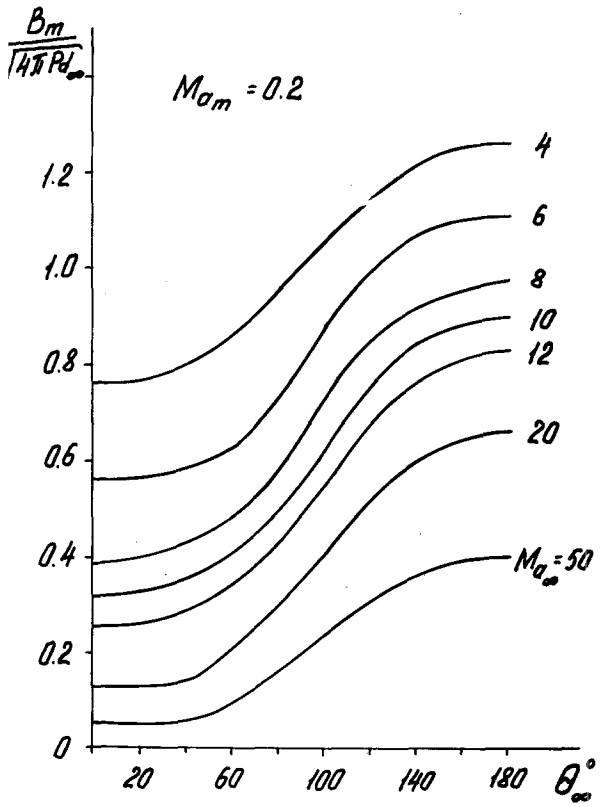

Fig. 6.10. Magnetic field intensity at the magnetopause normalized to the dynamic pressure in the solar wind in dependence on the orientation of the IMF for various Alfvénic Mach numbers Ma_∞ in the solar wind; $Ma_m = 0.2$.

In Figure 6.11 there are given the values of the angles and φ in dependence on the orientation of the IMF (the angle θ_∞) for $Ma_m = 0.2$. As is seen, the direction of the magnetic field at the magnetopause may significantly differ from the direction of the IMF in the undisturbed solar wind. In particular, at $\theta_\infty = 60°-90°$, an interesting phenomenon takes place: the z-component of the magnetic field at the magnetopause proves to be negative, while in the undisturbed solar wind it is positive.

These are the main features of the flow and of the magnetic field in the magnetosheath that are predicted by the model of the flow with a stagnation line. It would be interesting to see if these predictions agree with the experimental data.

6.3. Comparison of the Model with the Experimental Data

(1) As we have already said, the existence of the stagnation line is closely associated with the process of the magnetic field reconnection. However, the very idea on the magnetic field reconnection at the magnetopause has been called in question (Heikkila, 1975). In this connection, the results of observation onboard the satellites ISEE-1 and

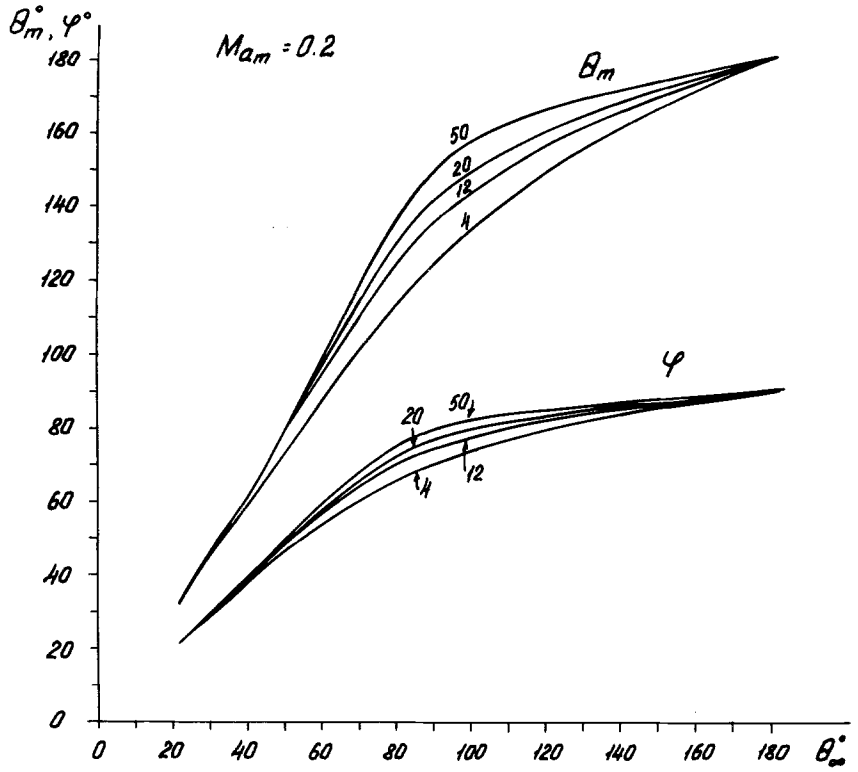

Fig. 6.11. Orientation of the magnetosheath's magnetic field at the magnetopause (θ_m) and that of the stagnation line (φ) depending on the IMF orientation (θ_∞) for various Alfvénic Mach numbers Ma_∞ in the solar wind; $Ma_m = 0.2$.

ISEE-2 seem to be of great importance (Mozer *et al.*, 1979; Paschmann *et al.*, 1979; Sonnerup *et al.*, 1981). These observations show that:

(a) The normal component of the magnetic field at the magnetopause, as a rule, is not zero (the mean value of $B_n \approx 3\gamma$) and is directed to the Earth in the northern hemisphere, and from the Earth in the southern hemisphere.

(b) At the dayside magnetopause, there exists a tangential (with respect to the magnetopause) electric field with the intensity of the order of 1 mV m^{-1}.

(c) In the vicinity of the magnetopause, there are observed intensive fluxes of accelerated particles directed from the low latitudes to the higher ones.

These data give convincing evidence that the magnetic field reconnection does really exist at the magnetopause.

(2) According to Crooker *et al.* (1981), the intensity of the magnetic field at the magnetopause is equal to:

$$B_m^{\exp} = 2^{5/4}\, \mathrm{Ma}_\infty^{-0.5} \sqrt{4\pi p_{d,\infty}}\,. \tag{6.15}$$

This empirical dependence $\beta_m^{\exp}(\mathrm{Ma}_\infty)$ is shown in Figure 6.12 (the upper curve).

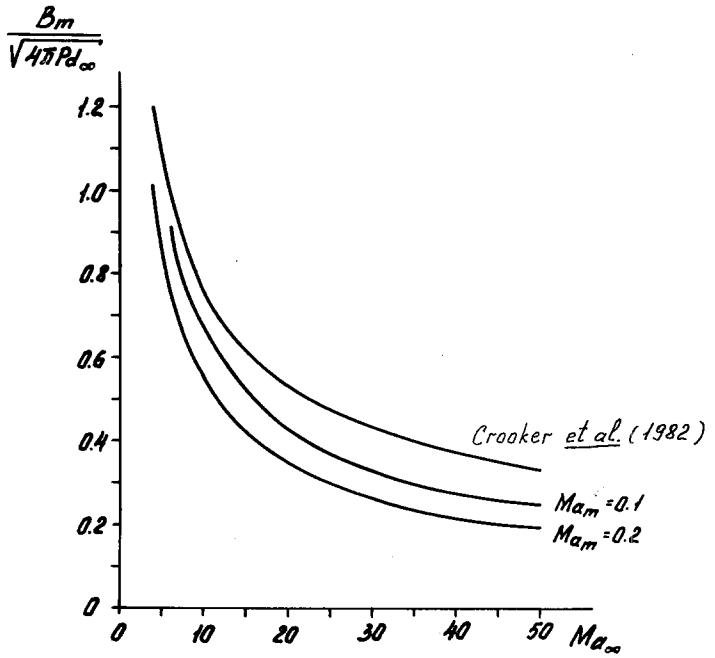

Fig. 6.12. The magnetosheath's magnetic field intensity at the magnetopause in dependence on the Alfvénic Mach number Ma_∞. The upper curve corresponds to the experimental data by Crooker *et al.* (1982); two other curves correspond to calculations by Pudovkin *et al.* (1981d) for $\theta_\infty = 90°$, $Ma_m = 0.1$ and $Ma_m = 0.2$, respectively.

Unfortunately, the IMF orientation is not given in the paper by Crooker *et al.* (1981); because of that, a detailed comparison of the experimental data with the predictions of the model is rather difficult. However, it is known that the solar wind magnetic field is directed on the average along the Parker spirals, so that $|\theta_\infty| \approx \pi/2$. Therefore, in Figure 6.12 there are given also the values of $(\beta_m)_{\theta\infty} = {}_{\pi/2}$ calculated according to the model by Pudovkin *et al.* (1982) for $Ma_m = 0.2$ and $Ma_m = 0.1$, respectively. One can see from the figure that the theoretical curves are sufficiently close to the experimental one. At the same time the absolute values of β_m, calculated for $Ma_m = 0.2$, are 1.5–2 times less than the experimental ones. For $Ma_m = 0.1$, the coincidence of the model and experimental data is better, and for $Ma_\infty < 25$ the discrepancy between those data does not exceed 25%.

(3) Reiff *et al.* (1981) have thoroughly studied the polar cap potential drop ($\Delta\phi^{exp}$) in dependence on the value of the solar wind parameters. In particular, the value of $\Delta\phi^{exp}$ was shown to be independent of the solar wind velocity and proportional to the squared value of the B_∞.

According to the model of the flow with a stagnation line, the potential drop across the magnetosphere equals the voltage along the stagnation line or, in accordance with (6.6):

$$\Delta\phi = \frac{1}{c} v_\infty B_\infty \sin(\theta_\infty - \varphi) \cdot L_m, \tag{6.16}$$

where L_m is the length of the stagnation line. Having assumed $L_m = L_0 = L_\infty$, and determining L_0 from (6.3) as

$$L_0 \approx D_m \frac{(B_0/\rho_0)}{(B_m/\rho_m)}, \tag{6.16a}$$

where B_0 and ρ_0 are the magnetic field intensity and the plasma density at the bow shock, one obtains:

$$\Delta\phi_y = \frac{1}{c} \frac{B^2_{\perp,\infty} D_m}{\beta_m \sqrt{4\pi\rho_m}} \frac{\rho_m}{\rho_0} \cdot \frac{\rho_0}{\rho_\infty} \cdot \sin(\theta_\infty - \varphi) \sin\varphi \, |\sin\varphi|, \tag{6.17}$$

here D_m is the diameter of the magnetosphere ($D_m \approx 30\ R_E \approx 2 \times 10^{10}$ cm), ρ_0/ρ_∞ is the jump of the plasma density at the bow shock; ρ_m/ρ_0 is shown in dependence on Ma_∞ and θ_∞ in Figure 6.9, and β_m is given in Figure 6.10.

The value of $\Delta\phi_y$ corresponds (under some assumption about the configuration of the equipotentials) to the polar cap potential drop along the dawn-dusk line, and it is to be compared with the value of the polar cap potential drop observed by Reiff *et al.* (1981).

Expression (6.17) shows the value of $\Delta\phi_y$ to be independent of the solar wind velocity and to be proportional to $B^2_{\perp,\infty}$, which agrees qualitatively with the results by Reiff *et al.* (1981). Moreover, the relation between $\Delta\phi_y$ and $\Delta\phi^{\mathrm{exp}}$ proves to be not only qualitative but also quantitative. Indeed, in Figure 6.13 the values are shown of $\Delta\phi_y$ calculated according to (6.17) for $\mathrm{Ma}_m = 0.1$ in dependence on the $\Delta\phi^{\mathrm{exp}}$ (the data on $\Delta\phi^{\mathrm{exp}}$ were kindly provided to us by P. H. Reiff). As may be seen, the relation between the two

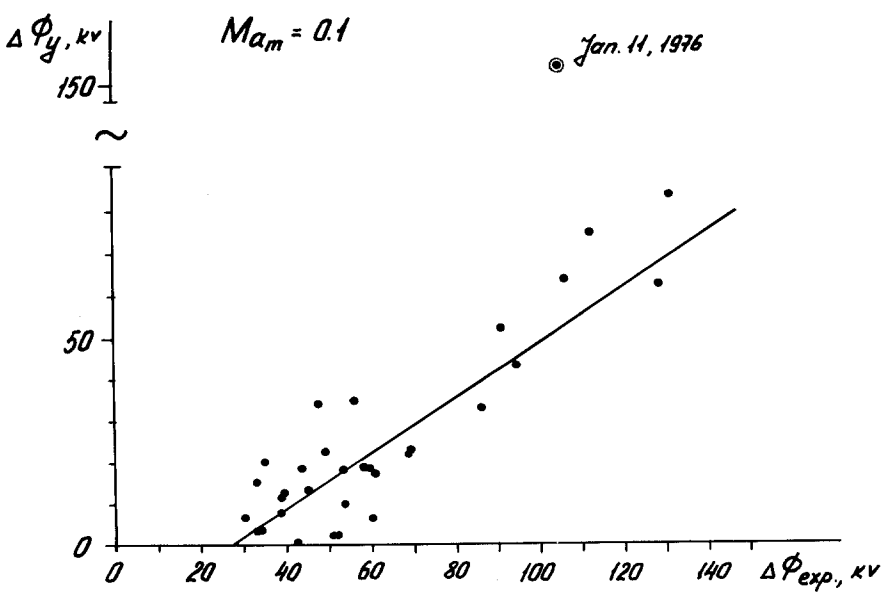

Fig. 6.13. Comparison of the experimental ($\Delta\Phi_{\mathrm{exp}}$) and calculated ($\Delta\Phi_y$) values of the polar cap potential drop.

quantities is linear; the correlation coefficient between them amounts to the value $r = 0.88$, and only one point (corresponding to the polar cap crossing on January 11, 1976) does not fit the general dependence. It has to be noted, however, that the intensity of the z-component of the IMF was greatly variable during that crossing.

The coefficient of regression which determines the dependence of $\Delta\phi_y$ on $\Delta\phi^{\exp}$ proved to be 0.7 instead of 1, which may be due to an improper choice for the value of D_m or to inaccuracy of the equality (6.3).

Apart from that, one can see that all the experimental values exceed the theoretical ones by approximately 30 kV. According to Reiff *et al.* (1981), this discrepancy may be explained by the quasi-viscous interaction of the solar wind with the Earth's magnetosphere.

(4) The enhanced intensity of the solar wind magnetic field at the magnetopause and the penetration of that field into the magnetosphere disturb significantly the pressure balance at the magnetopause and shift the latter earthwards (Kovner and Feldstein, 1973; Kuznetsova and Pudovkin, 1978; Pudovkin *et al.*, 1982). The magnetopause distance calculated in the framework of the discussed model is shown in dependence on the IMF orientation in Figure 6.14. According to the figure, the turn of the IMF southwards causes earthward displacement of the magnetopause; assuming that the mean radius of the latter is of the order of 10 R_E, that displacement amounts to the value

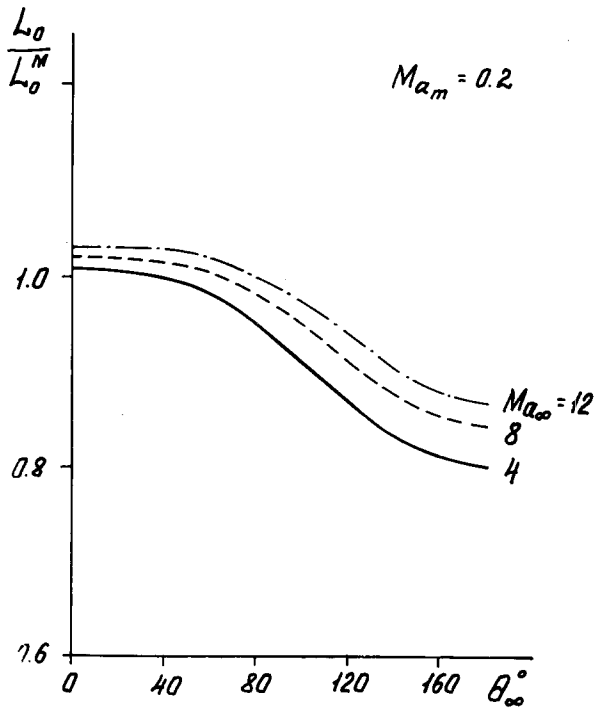

Fig. 6.14. Geocentric distance to the magnetopause (normalized to the magnetopause's radius in Mead's model) in dependence on the IMF orientation (θ_∞).

of about 1.5 R_E, which perfectly agrees with the data by Maezawa (1974), Formissano *et al.* (1979) and by Pudovkin *et al.* (1981c, 1982).

Thus, the available experimental data seems to confirm the conclusions of the model and thereby verify its adequacy.

6.4. The General Scheme of a Steady-State Flow Around the Magnetosphere

The process of a steady-state solar wind flow around the magnetosphere may be presented as follows.

In the case of the northward IMF, the jump of the magnetic field at the magnetopause is relatively small, and the currents which flow in the boundary layer completely screen the magnetosphere from the penetration of the solar wind magnetic field. Under such conditions, there exists at the 'nose' part of the magnetopause a longitudinal (that is parallel to **B**) stagnation line; the plasma density and the magnetic field intensity increase insignificantly across the magnetosheath; the tangential component of the electric field and the normal component of the magnetic field at the magnetopause equal zero; and the magnetopause is in a 'closed' state. However, as was shown by Reiff *et al.* (1981), an electric field may exist in the magnetosphere even in that case due to the quasiviscous interaction of the solar wind with the Earth's magnetosphere.

At the high latitude magnetopause the solar wind magnetic field is antiparallel to the magnetospheric field; thus, the geometry of the field is favorable for the process of the reconnection. However, since the stationary electric field along the magnetopause vanishes in the case under consideration, the process of the reconnection may be realized only as short bursts of a spontaneous reconnection (see Section 4).

Let now the vector of the IMF turn southwards. Then the jump of the magnetic field at the magnetopause increases, which results in the development of plasma instabilities and of the anomalous resistivity and, finally, leads to the field reconnection. When $|\theta_\infty| > |\theta_{cr}|$ (the value of θ_{cr} depending on the value of j_{cr}) the processes of the reconnection become predominant, and the flow changes to one with a transversal stagnation line. This results in the appearance of the quasi-stationary normal component of the magnetic field and of the tangential component of the electric field at the magnetopause; so, the magnetosphere turns to the 'open' state. Parameters of the plasma and of the magnetic field in the magnetosheath are described in that case by formulae (6.11)–(6.15), and are characterized by the decrease of the plasma density and by the increase of the magnetic field intensity at the magnetopause.

At the high latitude magnetopause the geometry of the magnetic field may be still favorable for the process of reconnection. However, the electric field at the high latitude magnetopause is directed now against the electric currents, so that $(\mathbf{E} \cdot \mathbf{j}) < 0$; consequently, the probability of spontaneous reconnection in that region decreases with the increase of the value $|\theta_\infty|$.

Having summarized results of the analysis given above, one can arrive at the conclusion that the physical content of the phenomenon of the solar wind – the Earth's

magnetosphere interaction is determined by two oppositely directed and at the same time closely related processes:

(1) The deceleration of the solar wind flow and the increase of the magnetic field intensity towards the magnetopause.

(2) The reconnection of the magnetic field of the solar wind with the geomagnetic field followed by the acceleration and heating of the plasma.

The first of those processes is followed by the transformation of the kinetic energy of the flow into magnetic energy, while in the course of the second process magnetic energy is released and converted into the kinetic and thermal energy of the plasma. This circumstance allows one to find an analogy between the processes of the solar wind flow around the magnetosphere and the development of magnetospheric substorms. Indeed, the motion of the solar wind through the magnetosheath where the kinetic energy of the plasma transforms into the magnetic energy, corresponds to the initial phase of a substorm. The reconnection of the magnetic fields at the magnetopause is analogous with the expansive phase of a substorm. However, in contrast to the auroral substorm developing in time, the 'substorm' in the magnetosheath, and at the magnetopause in the case of a steady-state flow, develops in space.

The extreme inhomogeneity and variability of the magnetic field and the plasma parameters in the magnetosheath make the process of the reconnection highly non-stationary, thereby increasing the similarity between that process and the magnetospheric substorm phenomenon.

7. Time-Dependent Interaction of the Solar Wind with the Earth's Magnetosphere

7.1. Reconnection at the Day Side Magnetopause

The scheme of the solar wind – the Earth's magnetosphere interaction considered above is based on the Petschek solution of the problem of the steady-state field line reconnection, and hence is not complete. First of all, the high level of fluctuations of the plasma flow and magnetic field parameters within the magnetosheath as well as motions of the magnetopause and of the bow shock make the process of the field line reconnection at the magnetopause greatly irregular and impulsive, a steady-state existing only as a time average. Second, as we have seen, the scheme based on the steady-state solution cannot explain the solar wind – magnetosphere interaction in the case of an utterly northward IMF. So it would be interesting to try to construct a more adequate model on the basis of a solution on the time dependent (spontaneous) field line reconnection. Unfortunately, we have got by now only the simplest solution of that kind and so have to confine ourselves to a qualitative consideration of the problem and to some rough estimates.

Let a front of a southward magnetic field approach the magnetosphere. As we have seen in the previous section, while nearing the magnetopause, magnetic field lines are stretched, and the magnetic field intensity increases; hence, at the magnetopause a current sheet develops and the amount of free energy increase. The field line recon-

nection may start at any point at the day side magnetopause; however, it is most likely that it will set in somewhere near the subsolar point where the field line stretching and hence the magnetopause current intensity are maximum (Figure 7.1).

After reconnection has started, the fronts of the FR-regions move towards the cusps, and the flux of the reconnected magnetic field increases.

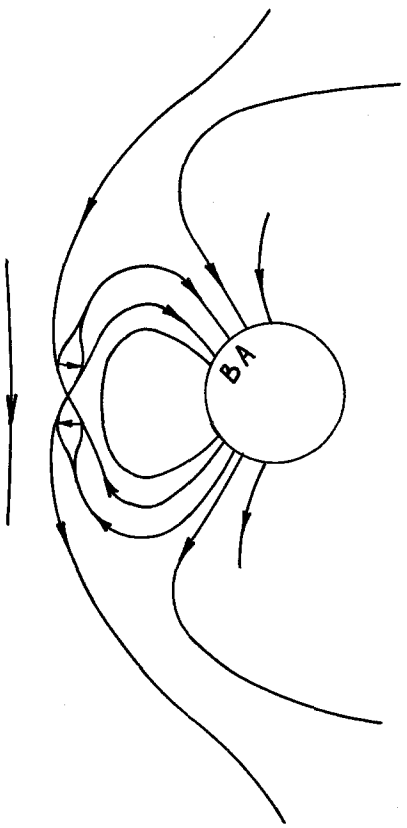

Fig. 7.1. Magnetic field line reconnection at the day side magnetopause in the case of the southward IMF. '*B*' is projection of the diffusion region into the ionosphere; '*A*' is projection of the last reconnected magnetic field line.

Beyond the cusps, the magnetopause currents change their direction, and Ampère forces $F_a = (1/c)\mathbf{j} \times \mathbf{B}_n$ (where $\mathbf{B}_n$ is the magnetic field component normal to the magnetopause) are directed sunwards so that they hinder the plasma motion. This hindrance is compensated by the gradient of the plasma pressure which arises as the result of the plasma acceleration and heating in the course of the field line reconnection.

Thus, at the high latitude magnetopause beyond the cusps, the plasma is moving against the Ampère forces, thus performing some work. As a result, a corresponding amount of the electromagnetic energy is produced which is transported into the magnetosphere's tail in the form of the Poynting vector. The whole chain of the energy

transformation may be presented as: solar wind kinetic energy – magnetic energy (stretching of the field lines) – kinetic and thermal energy (reconnection) – electromagnetic energy (Poynting vector).

So, the character of the interaction of the solar wind with the Earth's magnetosphere is different in different regions of the magnetopause. After the reconnection has started, not only the configuration of the magnetic field changes, but also the plasma flow pattern: the flow with an isolated stagnation point transforms into the flow with a stagnation line where the stream lines are branching and magnetic field lines disrupted. At the spontaneous reconnection, the stagnation line (or lines, if several FR-regions arise simultaneously) is local and extends only for a limited part of the magnetopause. As a result, the configuration of the flow and of the magnetic field at any given moment is very complicated: in one region the reconnection may be just starting, while in another it may be already well developed or even decaying. However, if it is averaged over time, the structure of the flow becomes simpler and may be presented similarly to the steady-state solution as a flow with a single stagnation line. This means that every magnetic field line with the 'impact parameter' r_0 (see Section 6) less than some limit length l_{sp} tears at one of the local stagnation lines corresponding to the spontaneous reconnection. This length (l_{sp}) may be accepted as the effective length of the stagnation line, and when one estimates the electric potential drop at the magnetopause or the reconnected magnetic flux, this length plays the same role as the length of the stagnation line in the case of a steady-state flow.

Thus, having averaged the solar wind plasma and the magnetic field parameters over a time interval longer than the characteristic time of the spontaneous reconnection, for the southward magnetic field we have to obtain results close to those in the steady-state model given in Section 6. As we have seen, in such a case the magnetosphere is open for the magnetic field and closed for the plasma.

In the case of the northward IMF, the situation is quite different. The reconnection is taking place beyond the cusps (Figure 7.2) where the magnetopause current is now the most intensive (Maezawa, 1976; Horwitz and Akasofu, 1979; Quest and Coroniti, 1981). On the day side, the magnetosphere captures magnetic field lines which belonged previously to the solar wind (NN' in Figure 7.2). As the captured magnetic tubes contain some plasma, this process is associated with the plasma flow into the magnetosphere. At the night side of the magnetosphere, an opposed process takes place: the magnetic tubes that belonged to the magnetosphere (NC and $N'N'$ in Figure 7.2) are torn off the magnetopause, and the plasma flows out of the magnetosphere.

At the cusps, the FR-regions are impeded, which results in the increase of the plasma pressure there; the gradients of the pressure drive plasma someway farther sunwards. The whole convection picture obtained by averaging the flow over time is shown in Figure 7.3. Near the cusps, the structure of the flow and of the magnetic field corresponds to the stream line reconnection considered in Section 3.

Thus, in the case of the northward magnetic field the magnetosphere is open for the plasma and closed for the magnetic field.

In the case of the IMF of an intermediate direction, the situation must be more

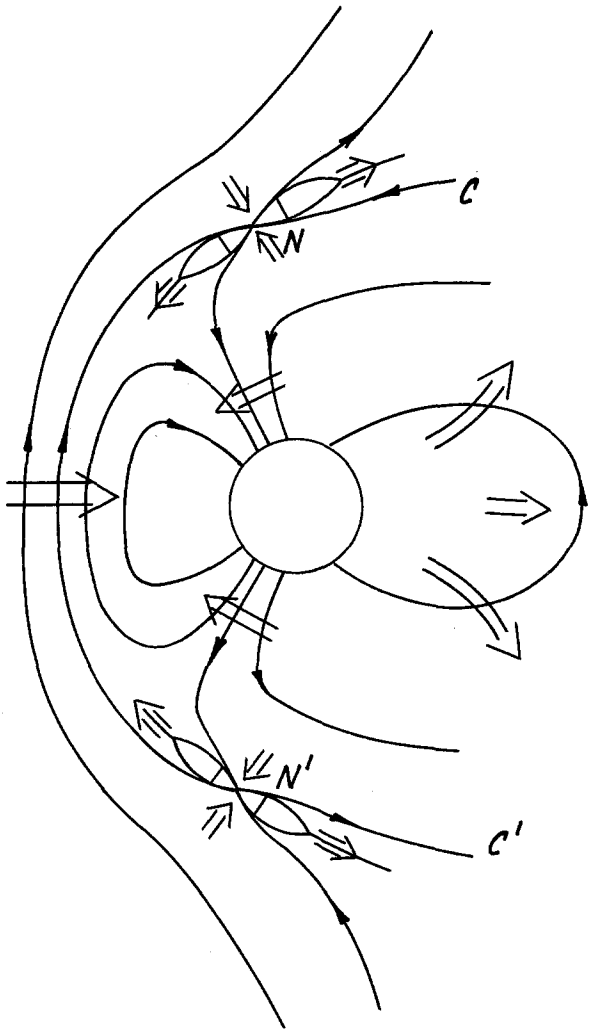

Fig. 7.2. Magnetic field line reconnection in the case of the northward IMF.

complicated, and the magnetosphere seems to be simultaneously open for both the magnetic field and the plasma.

Thus, the physical mechanism of the solar wind – magnetosphere interaction is the same for all the directions of the IMF, and that mechanism is spontaneous reconnection of the magnetic field lines. However, being averaged over time, this process results in very different steady-state models; in particular, the situation with the southward solar wind magnetic field corresponds to the model with the magnetic field reconnection, while that with the northward IMF corresponds to the model with the stream line reconnection. Unfortunately, the last process is studied insufficiently as yet, which makes any quantitative consideration of the problem impossible. Nevertheless, we believe that this process has to be taken into consideration in future investigations.

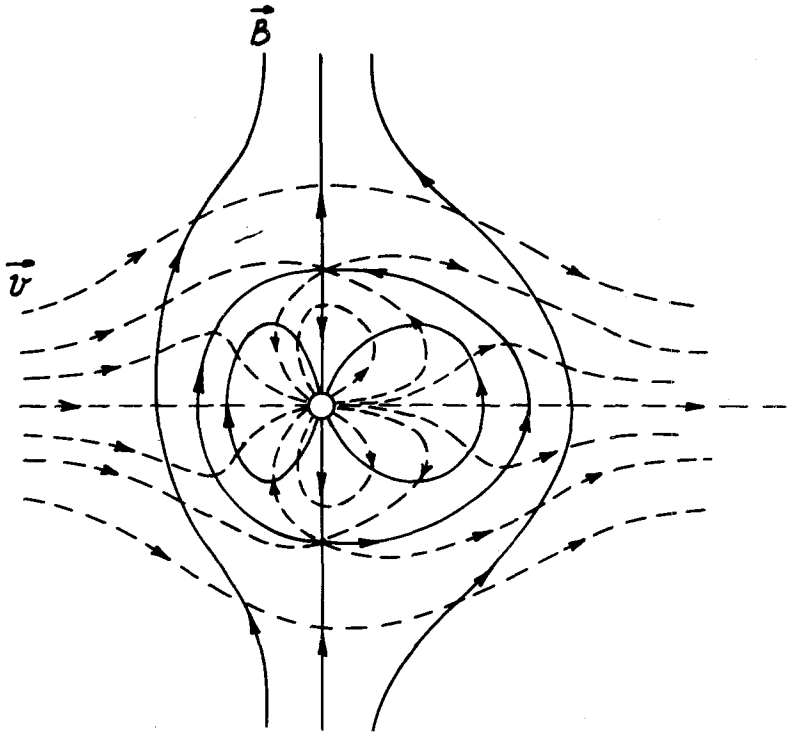

Fig. 7.3. The pattern of the magnetospheric plasma convection in the case of the northward IMF. The magnetosphere is closed for the magnetic field and open for the plasma.

7.2. The Initial Phase of the Substorm

Now we shall consider (though very briefly) the problem of magnetospheric substorms. First of all, it has to be noted that a single entrance of the magnetic flux into the magnetosphere (in the case of the southward IMF) is not sufficient for the necessary amount of magnetic energy to be accumulated there. Indeed, the field line reconnection results in the appearance of a normal component of the magnetic field B_n at the day side magnetopause. The mean value of B_n may be estimated from the experimental data for the electric potential drop across the polar cap:

$$B_n = \frac{\Delta\Phi}{V_{sw}L}, \tag{7.1}$$

where L is the characteristic dimension of the magnetosphere. Assuming that $\Delta\Phi = 60$ kV, $V_{sw} = 400$ km s^{-1}, $L = 30\,R_E$, one obtains $B_n = 0.5\,nT$. As a consequence, an additional magnetic field appears in the magnetosphere with approximately the same intensity (the inner sources of the magnetic field in the magnetosphere are assumed to be unchanged). In such a case, the total magnetic field energy within the magnetosphere increases by an amount which is insufficient for a substorm, and for the

energy to be accumulated, a current sheet has to develop in the magnetotail (see Section 2).

Basic features of the initial phase of a substorm, such as the increase of the magnetic flux in the magnetotail's lobes, expansion of the auroral oval, intensification of the plasma sheet currents, and decrease of the Z-component of the magnetic field in the tail (McPherron, 1970; Pudovkin *et al.*, 1970a; Sergeev and Tsyganenko, 1980) allow one to identify this phase with the process of the magnetic energy accumulation.

As was shown in Section 4, a current sheet may effectively accumulate magnetic energy if three basic dimensionless parameters of the problem are small: $\mathrm{Re}_m^{-1} \ll 1$; $\mathrm{Ma} \ll 1$, and $\beta \ll 1$. As regards the first inequality, it is surely fulfilled in the magnetotail ($\mathrm{Re}_m \gg 1$). However, the other two are not valid everywhere. In particular $\mathrm{Ma} = 1$ within the plasma mantle, and $\beta = 1$ in the central regions of the plasma sheet. So, from the theoretical considerations, it is not clear if the magnetic energy must be stored in the tail lobes. At the same time, analysis of experimental data shows (Semenov and Sergeev, 1981) that a greater (though it is not clear exactly how much) part of the electromagnetic energy entering the tail's lobes during the initial phase of a substorm really is stored there. A very rough estimate of the energy amount accumulated in the magnetotail may be obtained in the Syrovatsky approximation. In this approximation, the component of magnetic field normal to the current sheet equals zero: $(B_{\mathrm{cr}})_n = 0$. Hence, the current sheet, like the bottom of a vessel, gathers the magnetic flux entering the magnetotail.

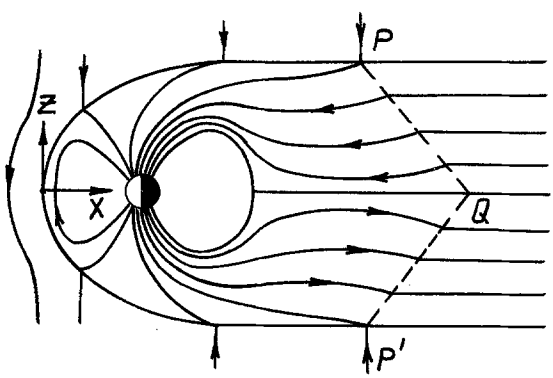

Fig. 7.4. Free energy accumulation in the magnetotail in Syrovatsky's approximation. PQ and PQ' show the fronts of the fast magnetoacoustic wave.

Let us assume that the front of a southward magnetic field is approaching the magnetosphere (Figure 7.4). For simplicity, we shall assume that the reconnection proceeds at the day side magnetopause in a steady-state regime, so that the magnetic flux entering the magnetopause is given by equality (7.1). Then the magnetic field intensity in the tail may be calculated by adding the magnetic flux, that has entered by a moment t to that existing there previously:

$$B(x, t) = B_0(x) + \Delta B(x, t),$$

$$\Delta B(x, t) = \frac{2c\Delta\Phi}{\pi R_T^2}\left[\frac{V_{sw} \cdot t + (x - x_0)}{V_{sw}}\right]\theta(V_{sw} \cdot t + x - x_0), \tag{7.2}$$

where θ is the Heaviside function, R_T is the radius of the magnetosphere's cross section, and x_0 is the geocentric distance to the subsolar point at the magnetopause. The values of ΔB calculated for $\Delta\Phi = 50$ kV, $V_{sw} = 300$ km s^{-1}, are shown in Figure 7.5. As may be seen from the figure, for an initial phase 30 min long, the magnetic field intensity increases at $x = 10\ R_E$ by 5 nT, that is 10 times more than in the case when the current sheet is absent. And what is especially important, all those 5 nT contribute to the free energy which is necessary for the reconnection. Indeed, as we have earlier seen (Section 2), at the phase of energy accumulation, the electric field is small ($E_{cs} \ll E_0$) in the vicinity of the current sheet or it even vanishes ($E_{cs} = 0$), as in the Syrovatsky approximation. Thus, $(\mathbf{I}_{cs} \cdot \mathbf{E}_{cs}) = 0$ (where $\mathbf{I}_{cs}$ is the current density), and the total energy entering the magnetotail is transformed into magnetic energy.

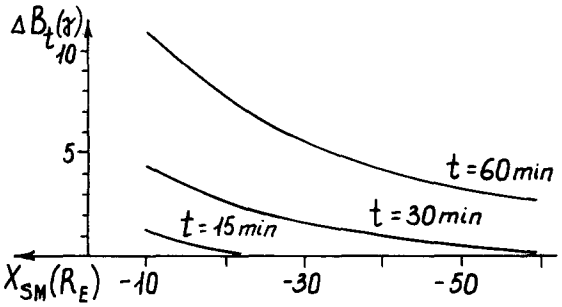

Fig. 7.5. Magnetic field intensity in the magnetotail's lobes at moments 15, 30, and 60 min after the disturbance front approached the magnetopause.

Thus, Equation (7.2) presents the estimate of the maximum value of the magnetotail's magnetic energy during the initial phase of the substorm.

7.3. THE MAGNETOSPHERIC SUBSTORMS

According to Equation (7.2), the extreme values of the current sheet parameters which may 'switch on' the reconnection process are reached at the inner edge of the sheet: the current density there is maximum, and the sheet's thickness is minimum; besides, significant gradients of the electric field intensity exist there. This is why the reconnection may be expected to start in that region (Hones, 1973; Schindler, 1979; Akasofu, 1977; Vasyliunas, 1976).

Taking into account the known MHD solution, the expansion phase of the substorm may be connected to the spontaneous reconnection of the magnetic field lines (see Section 4). According to the experimental data (Sergeev and Tsyganenko, 1980; Sergeev, 1981), a substorm ~ 15 min long consists of a sequence of microsubstorms 5–7 min long, each in their turn consisting of a series of activations with a characteristic duration of about 2 min. Every individual burst of reconnection is associated with the development of FR-regions (Figure 7.6), with the left-hand one moving earthwards and the right-hand one tailwards.

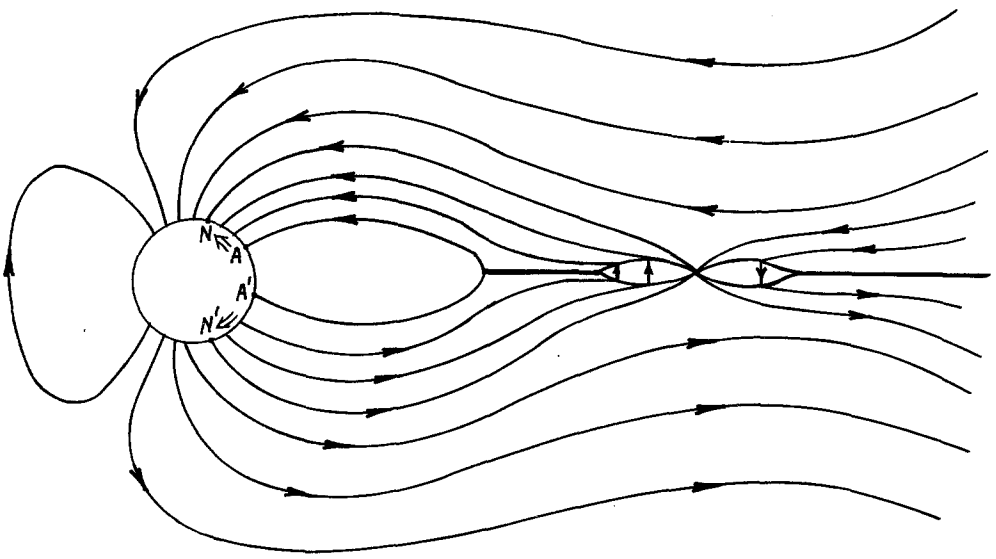

Fig. 7.6. An elementary act of reconnection in the magnetotail: development phase. Projections of the inner edge of the plasma sheet onto the inosophere (points A and A') are motionless while the projections of the diffusion zone (points N and N') are moving polewards.

Bearing in mind the theoretical results of Section 4, let us now discuss some effects which may be observed in the magnetosphere.

(1) The plasma flows accelerated up to the Alfvén speed $V_a = (0.5\text{–}1.5) \times 10^3$ km s^{-1} have to be observed in the magnetospheric tail (see the data by Frank, 1971; Nishida *et al.*, 1981).

(2) If a spacecraft is situated in the right-hand FR-region (see Figure 7.6), a plasma flow directed away from the Earth and a southward magnetic field component are to be expected; an opposite case is that with a spacecraft in the left-hand FR-region (Sergeev *et al.*, 1985).

(3) After the reconnections have started, an expansion of the plasma sheet is to be expected since the FR-region should pass by a spacecraft. A plasma sheet expansion speed can be estimated as εV_a, where $\varepsilon = b/B_0$, and b is the reconnected magnetic field. As $\varepsilon = 0.1\text{–}0.2$, then $\varepsilon V_a = 100\text{–}200$ km s^{-1}. It should be emphasized that this is a fictitious movement. The real plasma velocity in the direction of the Z_{GSM} axis should be much less (Forbes *et al.*, 1981; Andrews *et al.*, 1981; Sergeev *et al.*, 1985).

(4) The reconnection process leads to generation of an induced electric field of the order of $E_r = c^{-1}\varepsilon V_a B_T$ (see formula (4.24)). Taking $\varepsilon = 0.2$, $B_T = 25$ nT, $V_a = 10^8$ cm s^{-1}, we have $E = 5$ mV m^{-1}, which exceeds by more than one order of magnitude the value for the stationary convection electric field under $\Delta\Phi = 60$ kV. Direct observation in the magnetospheric tail indicated the impulsive electric field of the intensity up to 80 mV m^{-1} (Cattell *et al.*, 1982).

(5) The impulsive electric field seems to be responsible for the fast particle acceler-

ation in the diffusion region (Bulanov *et al.*, 1979; Zeleny *et al.*, 1982); the energetic protons and α-particles are observed at the dawn side of the plasma sheet while electrons appear at the dusk side. The acceleration of α-particles must be more effective than that of protons (Sergeev *et al.*, 1985).

We considered the features of the spontaneous reconnection in the magnetospheric tail and proceed now to some ionospheric effects.

(6) The presence of a strong dawn-dusk electric field in the diffusion region should result in a strong auroral electron precipitation (bright auroral arc – see calculations by Tsyganenko and Zaitseva (1979)) slightly equatorwards of the ionospheric projection of the X-line. Therefore, the bright poleward edge of the expanding auroral bulge is supposed to delineate the X-line projection into the ionosphere. Since the reconnected magnetic flux increases during the reconnection process, this projection has to move polewards (points N and N' in Figure 7.6) providing the expanding auroral bulge. The area of the auroral bulge characterizes the amount of reconnected magnetic flux.

(7) After the current system of the Alfvén wave I_A has reached the edge of the current sheet in the magnetospheric tail, the interaction of the systems I_0 and I_A (see Section 2.1) seems to be stopped. Then the Alfvén wave has to propagate along the magnetic field lines into the ionosphere, resulting in a formation of the Birkeland current system loop (see Figure 7.7), which is now adopted as the most essential element of the substorm expansive phase (Atkinson, 1967; Akasofu, 1972, 1977).

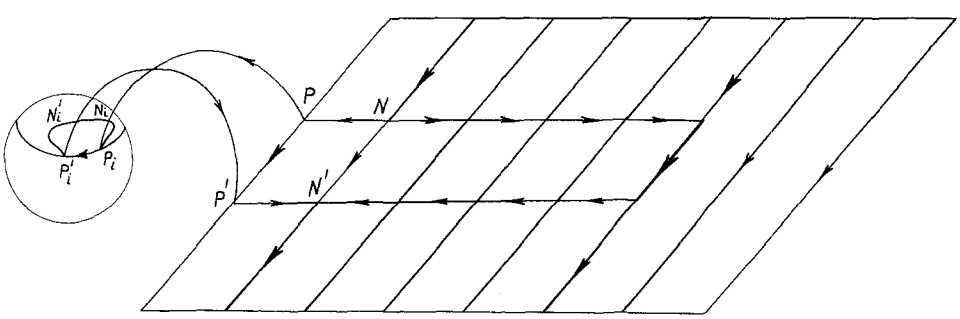

Fig. 7.7. Formation of the Birkeland current loop in the magnetotail.

(8) The incident Alfvén wave (see point 7) appears to be reflected at the ionosphere. It does not come back into the diffusion region since the reconnected magnetic flux increases, and, hence, this wave is located now inside the internal magnetosphere and propagates along the closed field lines. Furthermore, another Alfvén wave can be generated a little earlier due to an increase of the ionospheric conductivity caused by the intense electron precipitation (see point (6)) (Lyatsky and Maltsev, 1983). Both these waves seem to be able to produce a train of the Pi-2 pulsations, which are one of the most typical features of a substorm (Saito *et al.*, 1976; Akasofu, 1977; Sergeev and Tsyganenko, 1980).

Thus, the spontaneous reconnection model is able to explain some important features (points (1)–(8)) of a substorm. Having no opportunity to discuss the problem in a more detail, let us yet carry out some estimations. We begin with the estimation of the electric field using the ionospheric data (Semenov and Sergeev, 1981). Let us construct the surface of field lines emanating from the X-line (delineating the edge of the auroral bulge) for each moment of the expansion. As the magnetic flux across this surface is zero, by neglecting the field-aligned 'potential difference' we have:

$$(E_w + c^{-1}U \cdot B_i)l = E_y \Delta Y, \tag{7.3}$$

where E_y and E_w are the values of the azimuthal component of the electric field in the diffusion region and in projection into the ionosphere, ΔY and l are the lengths of the X-line (NN' in Figure 7.7) and its projection in the ionosphere ($N_i N_i'$ in Figure 7.7), respectively; and U is the speed of poleward auroral expansion. As $Y/l \approx 20$ (Sergeev and Tsyganenko, 1980) we obtain:

$$E_y = \frac{1}{20}\left(E_w + \frac{1}{c}UB_i\right). \tag{7.4}$$

Taking $E_w = 10$–20 mV m^{-1}, $U = 1$ km s^{-1}, we have: $E_y = 3$ mV m^{-1}. The maximum observed expansion speed of $U = 3$ km s^{-1} (Hirasawa and Nagata, 1972) will result in the values $E_y = 10$ mV m^{-1}, which is in agreement with the values obtained in point (4). Formula (7.4) allows us to reconstruct the reconnection process if we have ionospheric data with a high temporal resolution, since the electric field in the diffusion region as a function of time determines the solution of the reconnection problem (see (4.24)). Therefore the speed of poleward auroral expansion taken as a function of time is the most important characteristic of the reconnection process. Unfortunately, we have no data with the appropriate time resolution.

To estimate the energy released in the reconnection process, the following values can be accepted as pertinent to the expansive phase of a magnetospheric substorm (Sergeev, 1981): $t_0 = 10^2$ s, $n = 0.1$ cm^{-1}, $B_0 = 25$ nT, $\varepsilon = 0.1$ ($b = 2.5$ nT), $l = 2 \times 10^9$ cm. Then expression (4.27) gives $W = 2 \times 10^{20}$ erg. The total energy of a substorm is a sum of energies of the subsequent individual acts of the reconnection, and amounts to the value of 10^{22} erg.

The important question as to what plasma instabilities may initiate the reconnection will not be discussed (see the corresponding reviews in Kindel and Kennel, 1971; Smith, 1977; Papadopoulos, 1977; Galeev and Zeleny, 1978; Syrovatsky, 1981; Zeleny *et al.*, 1982; Liperovsky and Pudovkin, 1983). However, we shall breafly consider the externally induced reconnection. It is known from the experimental data (Pudovkin *et al.*, 1970b; Dmitrieva and Sergeev, 1983) that southward reversals of the IMF do not initiate substorms, whereas northward reversals do. This effect can be explained in the following way. The jumps of the IMF in the solar wind are transformed into the fast magnetoacoustic waves inside the tail lobes. If the IMF turns southwards, the current at the wave front is parallel to the current in the plasma sheet (see Figure 7.4); i.e., the

wave has parallel current polarization. As we have seen in Section 3, such a wave makes the reconnection threshold increase, and thus hinders the reconnection. On the other hand, if the IMF turns northwards, the fast magnetoacoustic wave has antiparallel current polarization and, therefore, stimulates the reconnection process.

Once the reconnection process is complete, the left-hand FR-region dissipates in the inner magnetosphere, while the right-hand FR-regions runs into the magnetotail. At the steady state the right-hand FR-regions are carrying away magnetic flux equal to that entering the magnetosphere from reconnection at the day side magnetopause. Once it has been averaged over a time interval longer than the initial phase duration, the whole picture (Figure 7.8) is close to the classical scheme of the magnetospheric convection (Dungey, 1961).

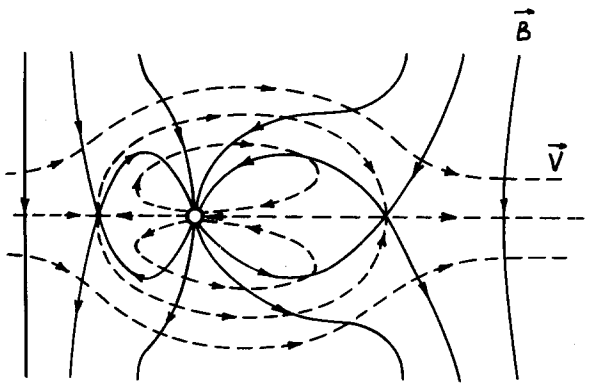

Fig. 7.8. Time-averaged configuration of the magnetic field (solid lines) and of the flow (dotted lines) in the case of the southward IMF.

Now we shall consider a delicate question on the initial (growth) phase of the substorms. The basic features of the solution of the spontaneous reconnection problem having been taken into account, considering the initial phase of the substorm may be unnecessary. Indeed, as we have seen, in the framework of the Petschek model, the reconnection is impossible only in the current-free magnetic field. At the same time, according to experimental data, a current sheet with spare magnetic energy always exists in the magnetotail, so that the reconnection may start there as soon as the necessary conditions arise in the current sheet (for example, due to a rapid change of the solar wind parameters).

On the other hand, intensive substorms are associated with the accumulation of a great amount of the free energy in the magnetotail's lobes, with the process of accumulation being most effective in the case of a southward IMF. And this exact process is the initial phase of the substorm.

Thus, we believe that in a long and, in our opinion, sufficiently fruitful argument on the initial phase of the substorm, both sides proved to be right. In particular, the conclusion by McPherron (1970), Pudovkin *et al.* (1970a), Aubry *et al.* (1970), that every

substorm has the initial phase may be correct on principle, as we have just seen, since the process of reconnection. requires some free energy, and the process of energy accumulation is the initial phase. Besides, every isolated and sufficiently intensive substorm really has its initial phase.

On the other hand, the current sheet always exists in the magnetotail in a sufficiently developed form; therefore many substorms start without any preliminary variation of the magnetotail parameters. Thus, Akasofu and his colleagues (see Akasofu, 1977), who assumed the initial phase to be unnecessary, are also right.

8. Conclusion

On presenting this review, the authors have intended to clear up to what extent the theories existing nowdays can explain qualitatively and describe quantitatively the process of the interaction of the solar wind with the geomagnetic field, and in particular, the process by which the solar wind energy enters the magnetosphere. Taking into account that within the solar wind the energy exists mainly in the form of the kinetic energy of the moving plasma, while it enters the magnetosphere in the form of electromagnetic energy, it is necessary also to find out the mechanism of the solar energy conversion within the magnetosheath and in the boundary layer at the magnetopause.

The analysis of experimental and theoretical data carried out above allows us to formulate the following general conception of the interaction of a highly conducting plasma with a magnetic field within the systems characterized by $\mathrm{Re}_m \gg 1$. At the initial stage of evolution of such systems, the magnetic field as a rule may be considered as frozen into the plasma. In the case of an inhomogeneous flow, a stretching of the field lines may take place, the last effect being the most drastic near singular points of the type of $V = 0$ and $B = 0$. Those points are the 'weak' places in the plasma, and the processes developing at them determine totally the following evolution of the system. At the sites of singularities current sheets appear; these develop and intensify, and finally the threshold of some plasma instability is reached; then there begins the process of the field line reconnection associated with the generation of running shock waves (the process described by Petschek).

Concerning the plasma motion, the singularities $\mathbf{B} = 0$ and $\mathbf{V} = 0$ may be considered as some barriers, and the magnetic field lines have to tear while passing them; it is the process of the field line reconnection that provides the field line disruption.

The field line reconnection is a global process embracing a significant part of the system; at the same time, it is initiated and is determined mainly by local characteristics of the plasma in the diffusion region, such as the plasma density, temperature, and conductivity, as well as by the electric and the magnetic field intensities. As regards the magnetosphere, all those characteristics are determined by peculiarities of the solar wind flow around the magnetosphere. Thus, the whole problem of the solar wind interaction with the Earth's magnetosphere, though it is in essence the problem of the field line reconnection at the magnetopause, may be solved only in common with the problem of the solar wind flow around the magnetosphere.

The first attempts to solve that problem for an idealized steady-state flow are given in this review. Unfortunately, that solution is applicable only to the low-latitude regions of the magnetopause; the processes developing at the high-latitude magnetopause seem to be non-stationary, and another approach is required to describe them.

The processes developing inside the magnetosphere are considered only very briefly in our review. This has happened because many processes important for the development of the magnetospheric disturbances, such as the energy accumulation and dissipation processes, are mainly determined by the configuration and intensity of the current systems and of the electric fields in the magnetosphere. At the same time, both theoretical and experimental data concerning this point are rather poor as yet, and the search for the configuration of the three-dimensional current systems and for their sources is one of the basic problems of magnetospheric physics.

Acknowledgements

The authors are greatly indebted to V. A. Sergeev, S. A. Zaitseva, N. A. Tsyganenko, I. V. Kubyshkin, and M. F. Heyn for fruitful discussions, and to M. V. Holeva and L. L. Nemtseva for their help in preparing the paper.

APPENDIX

A.1. The MHD-system of equations

The MHD-system of equations can be written as follows:

$$\rho \frac{\partial \mathbf{V}}{\partial t} + \rho(\mathbf{V}\nabla)\mathbf{V} = -\nabla\left(p + \frac{B^2}{8\pi}\right) + \frac{1}{4\pi}(\mathbf{B}\nabla)\mathbf{B}, \tag{A1}$$

$$\frac{\partial \rho}{\partial t} + \operatorname{div} \rho\mathbf{V} = 0, \tag{A2}$$

$$\operatorname{div} \mathbf{B} = 0, \tag{A3}$$

$$\frac{\partial \mathbf{B}}{\partial t} = \operatorname{rot}[\mathbf{V} \times \mathbf{B}], \tag{A4}$$

$$\frac{\mathrm{d}}{\mathrm{d}t}\frac{p}{\rho^{\gamma}} = 0, \tag{A5}$$

where ρ, p, and $\mathbf{V}$ are plasma density, pressure, and velocity, respectively. $\mathbf{B}$ is magnetic field, and γ is the ratio of specific heats.

When the plasma conductivity σ is finite, Equation (A4) should be replaced by:

$$\frac{\partial \mathbf{B}}{\partial t} = \operatorname{rot}[\mathbf{V} \times \mathbf{B}] + \frac{c^2}{4\pi\sigma}\Delta\mathbf{B}. \tag{A6}$$

In magnetohydrodynamics the following conditions must be satisfied at any discontinuity surface:

$$\{B_n\} = 0; \qquad B_n\{\mathbf{V}_l\} = m\left\{\frac{\mathbf{B}_l}{\rho}\right\}; \qquad \{m\} = 0, \tag{A7}$$

$$m\left\{\frac{p}{(\gamma-1)\rho} + \frac{V^2}{2} + \frac{p}{\rho} - \frac{mD_n}{\rho} + \frac{B_0^2}{4\pi\rho}\right\} - \frac{B_n}{4\pi}\{\mathbf{B}_l \cdot \mathbf{V}_l\} = 0, \tag{A8}$$

$$\left\{p + \frac{B^2}{8\pi} + \frac{m^2}{\rho}\right\} = 0, \tag{A9}$$

$$\left\{m\mathbf{V}_l - \frac{1}{4\pi}B_n \cdot \mathbf{B}_l\right\} = 0, \tag{A10}$$

where $m = \rho(V_n - D_n)$, $\mathbf{D}$ is the velocity of the discontinuity, and suffices l and n refer to the components that are tangential and normal to the surface of the discontinuity (Baranov and Krasnobaev, 1977).

A.2. Frozen-in coordinate system

Some problems of ideal magnetohydrodynamics can be solved by use of a special coordinate system, so-called frozen-in coordinates. The main idea of their introduction is as follows. Let there be two vector fields $\mathbf{a}(\mathbf{r})$ and $\mathbf{b}(\mathbf{r})$. It is required to construct such a coordinate system in which vector lines of $\mathbf{a}$ and $\mathbf{b}$ were coordinate lines simultaneously whereas both $\mathbf{a}$ or $\mathbf{b}$ were covariant base vectors. As is shown in general theory (Misner *et al.*, 1973; Dubrovin *et al.*, 1979), this may be done only when the following condition is fulfilled:

$$(\mathbf{a}\nabla)\mathbf{b} = (\mathbf{b}\nabla)\mathbf{a}, \tag{A11}$$

which means that the Lie derivative of the two vector fields $\mathbf{a}$ and $\mathbf{b}$ equals zero.

In the ideal magnetohydrodynamics, magnetic field lines are frozen in the flow. The mathematical formulation of this fact is (Landau and Lifshitz, 1959b):

$$\frac{\partial}{\partial t}\frac{\mathbf{B}}{\rho} + (\mathbf{V}\nabla)\frac{\mathbf{B}}{\rho} = \left(\frac{\mathbf{B}}{\rho}\nabla\right)\mathbf{V}. \tag{A12}$$

It results immediately from (A12) that in a stationary case, the vectors $\mathbf{V}$ and $\mathbf{B}/\rho$ satisfy the condition (A11), and hence, a frozen-in coordinate system can indeed be introduced. And what is more, having interpreted (A12) as a condition in the four-dimensional Minkovsky space, one may construct a frozen-in coordinate system in that space also, which allows one to proceed to the time-dependent case.

For simplicity, only a non-relativistic case will be considered. Let us introduce the coordinates $x^0 = ct$, $x^1 = x$, $x^2 = y$, $x^3 = z$, and two four-vectors: $V_{(4)} = (c, \mathbf{V})$, and $B_{(4)} = (0, \mathbf{B})$. For $V_{(4)}$ and $B_{(4)}/\rho$, Equation (A12) coincides with (A11); therefore there

exist such coordinates τ and α, that:

$$\frac{dx^i}{d\tau} = V^i_{(4)}; \qquad \frac{dx^i}{d\alpha} = \frac{B^i_{(4)}}{\rho}. \tag{A13}$$

Let us add two other coordinates ψ, ζ to τ and α, such that the Jacobian of transformation from (x^0, x^1, x^2, x^3) to $(\tau, \alpha, \psi, \zeta)$ does not equals zero. To simplify the notation of the MHD-equation, we may choose the arbitrary coordinates ψ, ζ in some special way. On this purpose, let us write the first pair of the Maxwell equations in coordinates $(\tau, \alpha, \psi, \zeta)$. The simplest way to do this is by using the technique of differential forms (see for example Flanders, 1963; Misner *et al.*, 1973):

$$\omega_F = \tfrac{1}{2} F_{ik}\, dx^i \wedge dx^k, \qquad d\omega_F = 0, \qquad F_{ik} = \begin{Vmatrix} 0 & E_x & E_y & E_z \\ -E_x & 0 & -B_z & B_y \\ -E_y & B_z & 0 & -B_x \\ -E_z & -B_y & B_x & 0 \end{Vmatrix}, \tag{A14}$$

where ω_F and F_{ik} are two-form and tensor of the electromagnetic field, respectively. In new variables $(\tau, \alpha, \psi, \zeta)$, and using (A13), $\omega_F = -\rho\sqrt{-g}\, d\psi \wedge d\zeta$; then from equation $d\omega_F = 0$ we obtain the first pair of the Maxwell equations in the form:

$$\frac{\partial \rho\sqrt{-g}}{\partial \tau} = \frac{\partial \rho\sqrt{-g}}{\partial \alpha} = 0,$$

where $\sqrt{-g}$ is the Jacobian. Thus, $\rho\sqrt{-g}$ depends only on ψ and ζ. The arbitrary coordinates ψ and ζ may be chosen so that

$$\rho\sqrt{-g} = 1. \tag{A15}$$

The matrix of transformation from (t, x, y, z) to $(\tau, \alpha, \psi, \zeta)$ will be:

$$A = \begin{Vmatrix} 1 & 0 & 0 & 0 \\ V_x & B_x/\rho & x_\psi & x_\zeta \\ V_y & B_y/\rho & y_\psi & y_\zeta \\ V_z & B_z/\rho & z_\psi & z_\zeta \end{Vmatrix}. \tag{A16}$$

It would be noticed that some arbitrariness in choosing coordinates ψ, ζ preserves. Namely, transformations $t' = t + f(\psi, \zeta)$; $\alpha' = \alpha + h(\psi, \zeta)$; $\zeta' = \zeta'(\psi, \zeta)$; $\psi' = \psi'(\psi, \zeta)$ with Jacobian equal to unity are possible. This can be useful in some cases.

Coordinates $(\tau, \alpha, \psi, \zeta)$ are called frozen-in ones since they can be constructed only when frozen-in condition (A12) is fulfilled. Frozen-in coordinates are studied in detail by Pudovkin and Semenov (1977a), Semenov and Pudovkin (1978), Semenov (1979).

Of course, the frozen-in coordinates are unknown a priori, and the problem consists of finding the functions $t = \tau$, $x = x(\tau, \alpha, \psi, \zeta)$, $y = y(\tau, \alpha, \psi, \zeta)$, $z = z(\tau, \alpha, \psi, \zeta)$, i.e. of mapping f on the physical space into the parameter space: f: $(t, x, y, z) \to (\tau, \alpha, \psi, \zeta)$. After the mapping of f has been carried out, the unknowns **V**, **B**, and ρ are found from (A13) and (A15), and then the remaining unknowns may be easily determined. Such an

approach turns out to be more convenient in some MHD problems than is solving the system of the system of equations (A1)–(A5).

The image of the physical space in the frozen-in coordinate space will be called *F*-manifold.

Different subsets of *F*-manifold have a simple physical sense. First of all, τ and α-coordinate lines are the images of the trajectories and magnetic field lines, respectively. Let us pass from $(\tau, \alpha, \psi, \zeta)$ to (t, x, y, z) in the following forms:

$$d\tau \wedge d\zeta \wedge d\psi = B_z\, dt \wedge dx \wedge dy + B_y\, dt \wedge dz \wedge dx + \\ + B_x\, dt \wedge dy \wedge dz, \tag{A17}$$

$$d\zeta \wedge d\alpha \wedge d\psi = \rho\, dx \wedge dy \wedge dz - \rho V_x\, dt \wedge dy \wedge dz - \\ - \rho V_y\, dt \wedge dz \wedge dx - \rho V_z\, dt \wedge dx \wedge dy, \tag{A18}$$

$$d\tau \wedge d\alpha \wedge d\psi \wedge d\zeta = \rho\, dt \wedge dx \wedge dy \wedge dz, \tag{A19}$$

(A17) means that the area of a section of the hypersurface $\alpha = \text{const.}$ equals the magnetic flux through the corresponding surface in the physical space integrated over time $\int B_n\, dS\, dt$;

(A18) means that the area of a section of the hypersurface $\tau = \text{const.}$ equals the mass of the plasma in the corresponding volume in the physical space;

(A19) means that a volume in the frozen-in coordinate space equals the mass of the plasma integrated over time in the physical space $\int \rho\, dV\, dt$.

In the stationary case $\partial/\partial\tau = \partial/\partial\zeta$; i.e., all the functions depend on $(\tau + \zeta)$. Using a new variable $t = \tau + \zeta$ (t – time along stream line), one can obtain for elementary displacement:

$$d\mathbf{r} = \mathbf{V}\, dt + \frac{\mathbf{B}}{\rho} d\alpha + \mathbf{r}_\varphi\, d\varphi, \tag{A20}$$

where the φ symbol is used instead of ψ since φ, as will be shown below, is in essence an electric potential. On this purpose we recall the relation between a covariant $\mathbf{e}_i$ and a contravariant $\mathbf{e}^i$ basic vectors (Korn and Korn, 1961)

$$\mathbf{e}_i = \sqrt{g}\, \mathbf{e}^k \times \mathbf{e}^j; \qquad \mathbf{e}^i = \frac{1}{\sqrt{g}} \mathbf{e}_k \times \mathbf{e}_j, \tag{A21}$$

where symbols i, j, k are circular permutations of symbols t, α, φ, and $\sqrt{g}$ is Jacobian. By means of (A21), grad φ will be:

$$\nabla\varphi = \mathbf{e}^\varphi \cdot \frac{\partial}{\partial\varphi} \cdot \varphi = \mathbf{e}^\varphi = \mathbf{V} \times \mathbf{B}.$$

Since $\mathbf{E} = -(1/c)[\mathbf{V} \times \mathbf{B}]$, φ/c is really an electric potential. Analogously, the following formulas can be deduced:

$$\rho\mathbf{V} = \nabla\alpha \times \nabla\varphi; \qquad \mathbf{B} = \nabla\varphi \times \nabla t; \qquad \rho\mathbf{r}_\varphi = \nabla t \times \nabla\alpha. \tag{A22}$$

One can see from (A22) that functions $\alpha(\mathbf{r})$, $t(\mathbf{r})$, and $\varphi(\mathbf{r})$ are Euler potentials (see also Erkaev, 1981). In a two-dimensional case, $\alpha(\mathbf{r})$ is the stream function, whereas $-t(\mathbf{r})$ is the z-component of the magnetic vector potential.

Let us consider similarly to (A17)–(A19) the following forms:

$$\mathrm{d}t \wedge \mathrm{d}\varphi = B_z\,\mathrm{d}x \wedge \wedge \mathrm{d}y + B_y\,\mathrm{d}z \wedge \mathrm{d}x + B_x\,\mathrm{d}y \wedge \mathrm{d}z, \tag{A23}$$

$$\mathrm{d}\varphi \wedge \mathrm{d}\alpha = \rho V_z\,\mathrm{d}x \wedge \mathrm{d}y + \rho V_y\,\mathrm{d}z \wedge \mathrm{d}x + \rho V_x\,\mathrm{d}y \wedge \mathrm{d}z, \tag{A24}$$

$$\mathrm{d}t \wedge \mathrm{d}\alpha \wedge \mathrm{d}\varphi = \rho\,\mathrm{d}x \wedge \mathrm{d}y \wedge \mathrm{d}z. \tag{A25}$$

(A23) implies that the area of a section of the plane t = const. equals the magnetic flux through the corresponding surface in the physical space;

(A24) implies that the area of a section of the plane t = const. equals the plasma mass flux through the corresponding surface in the physical space;

(A25) implies that a volume in the frozen-in coordinate space equals the mass of the plasma in the corresponding volume in the physical space.

The simplest way to write the MHD system of equations in frozen-in coordinates is to use the variation principle (Polovin and Akhiezer, 1959) which reduced in our case to a variation of the Lagrangian:

$$L = \int \left(\tfrac{1}{2}\rho V^2 - \rho W - \frac{B^2}{8\pi}\right) \mathrm{d}v\,\mathrm{d}t \tag{A26}$$

with additional condition (A15), the total pressure $P = p + (B^2/8\pi)$ being the Lagrangian multiplier. In (A26), W is the internal energy, $x(r)$, $y(r)$, and ρ are variated in two-dimensional case. The spreaded Lagrangian L' will be:

$$L' = \int \left\{\frac{\varepsilon^2}{2}(x_\tau^2 + y_\tau^2) - w - \frac{\rho}{2}(x_\alpha^2 + y_\alpha^2) + P(x_\zeta y_\alpha - x_\alpha y_\zeta) - \frac{P}{\rho}\right\} \mathrm{d}\tau\,\mathrm{d}\zeta\,\mathrm{d}\alpha.$$

Having variated L', the following system of equations in the frozen-in coordinates is obtained:

$$\varepsilon^2 x_{\tau\tau} - (\rho x_\alpha)_\alpha = -P_\zeta y_\alpha + P_\alpha \cdot y_\zeta, \tag{A27}$$

$$\varepsilon^2 y_{\tau\tau} - (\rho y_\alpha)_\alpha = -P_\alpha x_\zeta + P_\zeta x_\alpha, \tag{A28}$$

$$\rho(x_\zeta y_\alpha - x_\alpha y_\zeta) = 1, \tag{A29}$$

$$P = \tfrac{1}{2}[p + \rho^2(x_\alpha^2 + y_\alpha^2)], \tag{A30}$$

$$p = \beta \cdot \rho^\gamma, \tag{A31}$$

where $\varepsilon = V/V_a$ is the Alfvénic Mach number, $\beta = 8\pi p_0/B_0^2$ is the ratio of the magnetic to the gas pressures.

Let us now consider the conditions to the satisfied at MHD discontinuity, the only case of an incompressible plasma being studied. Let the equation of discontinuity be $\alpha = f(r, \zeta)$; then the discontinuity will be defined in the physical space in parametric

way: $x = x(\tau, f(\tau, \zeta), \zeta)$; $y = y(\tau, f(\tau, \zeta), \zeta)$. Using formulas of differential geometyry, one can find the tangential to discontinuity vector **l**, the normal vector **n**, and the discontinuity speed **D**:

$$\mathbf{l} = \frac{1}{a}(x_\zeta + x_\alpha \cdot f_\zeta; y_\zeta + y_\alpha \cdot f_\zeta),$$

$$\mathbf{n} = \frac{1}{a}(-(y_\zeta + y_\alpha \cdot f_\zeta); x_\zeta + x_\alpha \cdot f_\zeta),$$

$$a^2 = (x_\zeta + x_\alpha \cdot f_\zeta)^2 + (y_\zeta + y_\alpha \cdot f_\zeta)^2,$$

$$\mathbf{D} = (x_\tau + x_\alpha \cdot f_\tau; y_\tau + y_\alpha \cdot f_\tau). \tag{A32}$$

(A32) yields:

$$B_n = \frac{1}{a}: \qquad V_n - D_n = -\frac{1}{a} f_\tau. \tag{A33}$$

When the plasma is incompressible, $\varepsilon(V_n - D_n) = \pm B_n$, and equation of the discontinuity will be:

$$\pm \alpha = \tau + q(\zeta), \tag{A34}$$

where $q(\zeta)$ is an arbitrary function. In a stationary case the equation of discontinuity is $\pm \varepsilon\alpha = \tau$.

In the case of incompressible plasma all the conditions at the discontinuity (apart from those at the tangential discontinuity) reduce to the following:

$$\{x\} = \{y\} = \{P\} = 0. \tag{A35}$$

For simplicity we shall prove that if (A35) is fulfilled, (A7)–(A10) are fulfilled also. In the space of (τ, α, ζ), the discontinuity is a two-dimensional surface with tangential vector $\mathbf{L} = (1, f_\tau, 0)$. Since the functions $x(\tau, \alpha, \zeta)$ and $y(\tau, \alpha, \zeta)$ are continuous at the discontinuity, the tangential derivatives of these functions have to be continuous also:

$$\{\varepsilon x_\tau + x_\alpha\} = 0, \qquad \{\varepsilon y_\tau + y_\alpha\} = 0. \tag{A36}$$

It can be easily shown that together with $\{P\} = 0$ (A33), (A34), and (A35) fulfill all the discontinuity conditionàs (A7), (A9), and (A10) (condition (A8) cannot be taken into account in an incompressible plasma).

For a tangential discontinuity the mapping of f, generally speaking, will not be continuous.

In the case of a compressible plasma the mapping of f is continuous at discontinuity too, but all the discontinuity conditions do not reduce to (A35) (Semenov *et al.*, 1983a).

References

Akasofu, S.-I.: 1972, in E. R. Dyer (ed.), *Solar Terrestrial Physics*, D. Reidel Publ. Co., Dordrecht, Holland.

Akasofu, S.-I.: 1977, *Physics of Magnetospheric Substorms*, D. Reidel Publ. Co., Dordrecht, Holland.

Akasofu, S.-I. and Chapman, S.: 1972, *Solar-terrestrial Physics*, Clarendon Press, Oxford.

Akhiezer, A. I., Akhiezer, I. A., Polovin, R. V., Sitenko, A. G., and Stepanov, K. N.: 1975, *Plasma Electrodynamics*, Pergamon Press, Oxford.

Alfvén, H.: 1976, *J. Geophys. Res.* **81**, 4019.

Alfvén, H.: 1977, *Rev. Geophys. Space Phys.* **15**, 271.

Alksne, A. Y.: 1967, *Planet. Space Sci.* **15**, 239.

Alksne, A. Y.: 1970, *Planet. Space Sci.* **18**, 1203.

Andrews, M. U., Keppler, E., and Daly, P. W.: 1981, *J. Geophys. Res.* **86**, 7543.

Atkinson, G.: 1967, *J. Geophys. Res.* **72**, 5373.

Aubry, M. P., Russell, C. T., and Kivelson, M. G.: 1970, *J. Geophys. Res.* **75**, 7018.

Baranov, V. B. and Krasnobaev, K. V.: 1977, *Hydrodynamic Theory of Space Plasma*, Moscow (in Russian).

Baum, P. J. and Bratenahl, A.: 1974a, *J. Plasma Phys.* **11**, 93.

Baum, P. J. and Bratenahl, A.: 1974b, *Phys. Fluids* **17**, 1232.

Baum, P. J. and Bratenahl, A.: 1977, *J. Plasma Phys.* **18**, 257.

Bernikov, L. V. and Semenov, V. S.: 1979, *Geomagn. Aeronomy* **19**, 671 (in Russian).

Birn, J.: 1979, *J. Geophys. Res.* **84**, 5143.

Birn, J.: 1980, *J. Geophys. Res.* **85**, 1214.

Birn, J. and Hones, E. W.: 1981, *J. Geophys. Res.* **86**, 6802.

Birn, J., Sommer, R. R., and Schindler, K.: 1977, *J. Geophys. Res.* **82**, 141.

Bogdanov, S. Yu., Markov, V. S., Syrovatsky, S. I., Frank, A. G., and Hodzhaev, A. Z.: 1980, *Izv. AN SSSR, Phys. Ser.* **44**, 2469 (in Russian).

Brushlinskii, K. V., Zaborov, A. M., and Syrovatsky, S. I.: 1980, *Soviet Plasma Phys.* **6**, 297 (in Russian).

Bulanov, S. V. and Sasorov, P. V.: 1978, *Soviet Phys. Plasma* **4**, 746 (in Russian).

Bulanov, S. V., Sasorov, P. V., and Syrovatsky, S. I.: 1979, Paper presented at *XI Leningrad Symposium on Space Physics.*

Cattell, C. A., Kim, M., Lin, R. P., and Mozer, F. S.: 1982, *Geophys. Res. Letters* **9**, 539.

Cowley, S. W. H.: 1974a, *J. Plasma Phys.* **12**, 319.

Cowley, S. W. H.: 1974b, *J. Plasma Phys.* **12**, 341.

Cowley, S. W. H.: 1975, *J. Plasma Phys.* **14**, 475.

Crooker, N. U., Siscoe, G. L., Mullen, P. R., Russell, C. T., and Smith, E. J.: 1982, *J. Geophys. Res.* **87**, 10407.

Dmittrieva, N. P. and Sergeev, V. A.: 1983, *Geomagn. Aeronomy* **23**, 518 (in Russian).

Dubrovin, B. A., Novikov, S. P., and Fomenko, A. T.: 1979, *Modern Geometry*, Nauka, Moscow (in Russian).

Dungey, J. W.: 1961, *Phys. Rev. Letters* **6**, 47.

Erkaev, N. V.: 1981, Dep. VINITI No. 3253 Dep. 55 pp. (in Russian).

Fairfield, D. H. and Mead, G. D.: 1975, *J. Geophys. Res.* **80**, 535.

Flanders, H.: 1963, *Differential Forms with Applications to the Physical Sciences*, Academic Press, New York.

Forbes, T. G., Hones, Jr., B. W., and Bame, S. J., *et al.*: 1981, *J. Geophys. Res.* **86**, 3459.

Forbes, T. G. and Priest, E. R.: 1982, *Solar Phys.* **81**, 303.

Forbes, T. C. and Priest, E. R.: 1983, *J. Geophys. Res.* **88**, 863.

Formisano, V., Domingo, V., and Wensel, K. P.: 1979, *Planet. Space Sci.* **27**, 1137.

Frank, A. G.: 1974, in *Neutral Current Sheet in Plasma*, Trudy FIAN, Nauka, p. 108 (in Russian).

Frank, L. A.: 1971, *J. Geophys. Res.* **76**, 5202.

Galeev, A. A.: 1978, Report M.6.4. at *STP Symposium*, Insbruck, Austria.

Galeev, A. A. and Zeleny, L. M.: 1978, in *Theoretical and Computational Plasma Physics*, International Atomic Energy Agency, Vienna, Austria.

Gekelman, W. and Stenzel, R. L.: 1981, *J. Geophys. Res.* **86**, 659.

Hayashi, T. and Sato, T.: 1978, *J. Geophys. Res.* **83**, 217.

Heikkila, W. J.: 1975, *Geophys. Res. Letters* **12**, 154.

Hirasawa, T. and Nagata, T.: 1972, JARE Sci. Rept. A., No. 10, 28 pp.

Hones, E. W.: 1973, *Radio Sci.* **8**, 979.

Horwitz, J. L. and Akasofu, S.-I.: 1979, *J. Geophys. Res.* **184**, 2567.

Kindel, J. M. and Kennel, C. F.: 1971, *J. Geophys. Res.* **76**, 3055.
Kirii, N. P., Markov, V. S., and Syrovatsky, S. I.: 1979, in *Flare Process in Plasma*, Trudy FIAN, Vol. 110, Nauka, p. 121 (in Russian).
Korn, G. A. and Korn, T. M.: 1961, *Mathematical Handbook for Scientists and Engineers*, McGraw-Hill Book Co. Inc., New York, Toronto, London.
Kovner, M. S. and Feldstein, Ya. I.: 1973, *Planet. Space Sci.* **21**, 1191.
Kuznetsova, T. V. and Pudovkin, M. I.: 1978, *Planet. Space Sci.* **26**, 229.
Landau, L. D. and Lifshitz, E. M.: 1959a, *Fluid Mechanics*, Pergamon Press, New York.
Landau, L. D. and Lifshitz, E. M.: 1959b, *Fluid Electrodynamics*, Addison-Wesley Publ. Co. Inc., Reading, Mass.
Lees, L.: 1964, *AIAA J.* **2**, 1576.
Levy, R. H., Petschek, H. E., and Siscoe, G. L.: 1964, *AIAA J.* **2**, 2065.
Lyatsky, V. B. and Maltsev, Yu. P.: 1983, *Magnetosphere-Ionosphere Interaction*, M., Nauka (in Russian).
Liperovsky, V. A. and Pudovkin, M. I.: 1983, *Anomalous Resistivity and Double Layers in the Magnetospheric Plasma*, M., Nauka (in Russian).
Maezawa, K.: 1974, *Planet. Space Sci.* **22**, 1443.
Maezawa, K.: 1976, *J. Geophys. Res.* **81**, 2289.
McPherron, R. L.: 1970, *J. Geophys. Res.* **75**, 5592.
Misner, C. W., Thorne, K. S., and Wheeler, J. A.: 1973, *Gravitation*, W. H. Freeman and Co., San Francisco, Vol. 1.
Mitchell, H. G. and Kan, J. R.: 1978, *Plasma Phys.* **20**, 31.
Morfill, G. and Scholer, M.: 1972, *J. Geophys. Res.* **77**, 4021.
Mozer, F. S., Cattel, C. A., and Temerin, M. *et al.*: 1979, *J. Geophys. Res.* **84**, 5875.
Nishida, A., Hayakawa, H., and Hones, Jr., E. W.: 1981, *J. Geophys. Res.* **86**, 1422.
Ohyabu, N. and Kawashima, N.: 1972, *J. Phys. Soc. Japan* **35**, 496.
Papadopoulos, U. A.: 1977, *Rev. Geophys. Space Phys.* **15**, 113.
Parker, E. N.: 1963, *Astrophys. J. Suppl. Ser.* **8**, 177.
Parker, E. N.: 1973, *Plasma Phys.* **9**, 49.
Paschmann, G., Sonnerup, B. U. Ö., and Papamastorakis *et al.*: 1979, *Nature* **282**, 243.
Petschek, H. E.: 1964, *AAS-NASA Symposium on the Physics of Solar Flares*, NASA Spec. Publ., SP–50, 425 pp.
Pivovarov, V. G. and Erkaev, N. V.: 1978, *Interaction of Solar Wind with the Earth's Magnetosphere*, Novosibirsk, Nauka (in Russian).
Podgorny, A. I. and Syrovatsky, S. L.: 1979, in *Flare Process in Plasma*, Trudy FIAN, Vol. 110, Nauka, p. 33 (in Russian).
Podgorny, I. M. and Sagdeev, R. Z.: 1969, *U.F.N.* **98**, 409 (in Russian).
Polovin, R. V. and Akhiezer, I. A.: 1959, *Ukr. Phys. J.* **4**, 677 (in Russian).
Prandtl, L.: 1904, *Verhand. d III Internat. Mathem. Kongr.*, Heidelberg.
Priest, E. R.: 1981, in E. R. Priest (ed.), *Solar Flares Magnetohydrodynamics*, Gordon and Breach, New York, p. 139.
Priest, E. R. and Raadu, M. A.: 1975, *Solar Phys.* **43**, 177.
Priest, E. R. and Sonnerup, B. U. Ö.: 1975, *Geophys. J. Roy. Astron. Soc.* **41**, 405.
Pudovkin, M. I., Isaev, S. I., and Zaitseva, S. A.: 1970a, *Ann. Geophys.* **26**, 761.
Pudovkin, M. I., Raspopov, O. M., and Dmitrieva, L. A., *et al.*: 1970b, *Ann. Geophys.* **26**, 389.
Pudovkin, M. I., Raspopov, O. M., and Kleimenova, N. G.: 1975, *Geomagnetic Field Disturbances*. Leningrad Univ. Press, Leningrad, Vol. 1.
Pudovkin, M. I. and Semenov, V. S.: 1977a, *Ann. Geophys.* **33**, 429.
Pudovkin, M. I. and Semenov, V. S.: 1977b, *Ann. Geophys.* **33**, 423.
Pudovkin, M. I., Zaitseva, S. A., and Kuznetsova, T. V.: 1981a, Preprint IZMIRAN No. 14 (in Russian).
Pudovkin, M. I., Zaitseva, S. A., and Kuznetsova, T. V.: 1981b, Preprint IZMIRAN No. 15 (in Russian).
Pudovkin, M. I., Zaitseva, S. A., and Kuznetsova, T. V.: 1981c, Preprint IZMIRAN No. 24 (in Russian).
Pudovkin, M. I., Heyn, M. F., and Lebedeva, V. V.: 1982, *J. Geophys. Res.* **87**, 8131.
Reiff, P. H., Spiro, R. W., and Hill, T. W.: 1981, *J. Geophys. Res.* **86**, 7639.
Quest, K. B. and Coroniti, F. V.: 1981, *J. Geophys. Res.* **86**, 3289.
Saito, T., Sakurai, K., and Koyama, Y.: 1976, *J. Atmos. Terr. Phys.* **38**, 1265.
Sato, T.: 1979, *J. Geophys. Res.* **84**, 7177.
Sato, T. and Hayashi, T.: 1979, *Phys. Fluids* **22**, 1189.

Sato, T., Matsumoto, H., and Nagai, K.: 1981, *J. Geophys. Res.* **87**, 6089.
Schindler, K. and Birn, J.: 1982, *J. Geophys. Res.* **87**, 2263.
Schindler, K.: 1979, *Space Sci. Rev.* **23**, 365.
Sedov, L. I.: 1973, *Fluid Mechanics*, Vol. 1, Nauka, Moscow (in Russian).
Semenov, V. S.: 1979, *Geomagnetic Res.* **24**, 32 (in Russian).
Semenov, V. S. and Bernikov, L. V.: 1979, *Geomagnetic Res.* **26**, 40 (in Russian).
Semenov, V. S. and Kubyshkin, I. V.: 1981, Paper presented at *4th IAGA Sci. Assembly*, Edinburgh.
Semenov, V. S. and Kubyshkin, I. V.: 1984, *Geomagn. Aeronomy* **24**, 766 (in Russian).
Semenov, V. S. and Pudovkin, M. I.: 1978, *Geomagnetic Res.* **23**, 66 (in Russian).
Semenov, V. S. and Sergeev, V. A.: 1981, *Planet. Space Sci.* **24**, 271.
Semenov, V. S., Kubyshkin, I. V., and Heyn, M. F.: 1983a, *J. Plasma Phys.* **30**, 303.
Semenov, V. S., Kubyshkin, I. V., Heyn, M. F., and Biernat, H. K.: 1983b, *J. Plasma Phys.* **30**, 321.
Semenov, V. S., Heyn, M. F., and Kubyshkin, I. V.: 1983c, *Soviet Astron. J.* **60**, 1138 (in Russian).
Semenov, V. S., Vasilyev, E. P., and Pudovkin, A. I.: 1984, *Geomagn. Aeronomy* **24**, 448 (in Russian).
Sergeev, V. A.: 1981, *J. Geophysics* **49**, 176.
Sergeev, V. A. and Tsyganenko, N. A.: 1980, *The Earth's Magnetosphere*, Nauka, Moscow (in Russian).
Sergeev, V. A., Bösinger, T., and Lui, A. T. Y.: 1985, *J. Geophysics*, in press.
Shen, W. W.: 1972, *Cosmic Electrodynamics* **2**, 381.
Siscoe, G. and Crooker, N. A.: 1974, *Geophys. Res. Letters* **1**, 17.
Smith, D. F.: 1977, *J. Geophys. Res.* **82**, 704.
Somov, B. V. and Syrovatsky, S. I.: 1974, in 'Neutral Current Sheets in Plasma', *Trudy FIAN* **74**, 14 (in Russian).
Sonnerup, B. U. Ö.: 1970, *J. Plasma Phys.* **4**, 161.
Sonnerup, B. U. Ö: 1979, in S.-I. Akasofu (ed.), *Transport Mechanisms of the Magnetosphere*, D. Reidel Publ. Co., Dordrecht, Holland, p. 77.
Sonnerup, B. U. Ö. and Priest, E. R.: 1975, *J. Plasma Phys.* **14**, 283.
Sonnerup, B. U. Ö., Paschmann, G., and Papamastorakis, I., *et al.*: 1981, *J. Geophys. Res.* **86**, 10049.
Soward, A. M.: 1982, *J. Plasma Phys.* **28**, 415.
Soward, A. M. and Priest, E. R.: 1977, *Phil. Trans. Roy. Soc. London* **A284**, 369.
Soward, A. M. and Priest, E. R.: 1982, *J. Plasma Phys.* **28**, 355.
Spreiter, J. R. and Alksne, A. Y.: 1967, *Rev. Geophys.* **7**, 11.
Spreiter, J. R., Summers, A. L., and Alksne, A. Y.: 1966, *Planet. Space Sci.* **14**, 223.
Stenzel, R. L., and Gekelman, W.: 1981, *J. Geophys. Res.* **86**, 649.
Stenzel, R. L., Gekelman, W., and Wild, N.: 1982, *J. Geophys. Res.* **87**, 111.
Stern, D. P.: 1975, Prepr. X-602–75–17, Goddard Space Flight Center.
Stern, D. P.: 1977, *Rev. Geophys. Space Phys.* **15**, 156.
Sweet, P. A.: 1958, in B. Lehnert (ed.), *Electrodynamic Phenomena in Cosmical Physics*, Cambridge Univ. Press, London, p. 123.
Syrovatsky, S. I.: 1971, *ZETF* **33**, 933 (in Russian).
Syrovatsky, S. I.: 1979a, *Izv. AN SSSR, Phys. Ser.* **43**, 695 (in Russian).
Syrovatsky, S. I.: 1979b, in 'Flare Process in Plasma', *Trudy FIAN* **110**, 5 (in Russian).
Syrovatsky, S. I.: 1981, *Ann. Rev. Astron. Astrophys.* **19**, 163.
Tsuda, T. and Ugai, M.: 1977, *J. Plasma Phys.* **18**, 451.
Tsyganenko, N. A. and Zaitseva, S. A.: 1979, *Geomagnetic Res.* **25**, 61 (in Russian).
Tur, T. Y. and Priest, E. R.: 1976, *Solar Phys.* **48**, 89.
Ugai, M.: 1981, *J. Plasma Phys.* **25**, 89.
Ugai, M. and Tsuda, T.: 1977, *J. Plasma Phys.* **17**, 337.
Vasyliunas, V. M.: 1975, *Rev. Geophys. Space Phys.* **13**, 303.
Vasyliunas, V. M.: 1976, in B. M. McCormac (ed.), *Magnetospheric Particles and Fields*, D. Reidel Publ. Co., Dordrecht, Holland, p. 99.
Yang, C. K. and Sonnerup, B. U. Ö.: 1976, *Astrophys. J.* **206**, 570.
Yang, C. K. and Sonnerup, B. U. Ö.: 1977, *J. Geophys. Res.* **82**, 699.
Yeh, T.: 1976, *J. Geophys. Res.* **81**, 2140.
Yeh, T. and Axford, W. I.: 1970, *J. Plasma Phys.* **4**, 207.
Yeh, T. and Dryer, H.: 1973, *Astrophys. J.* **182**, 301.
Zeleny, L. M., Lipatov, A. S., Lominadze, D. G., and Taktakishvili, A. L.: 1982, Preprint 697, Space Res. Inst., Moscow.
Zwan, B. J. and Wolf, R. A.: 1976, *J. Geophys. Res.* **81**, 1636.